MORTON THIOKOL INC.

Space Operations

Assembly Test Article (ATA)
Final Test Report

February 1988

Prepared by:

Gle A Rufz (2/19/88)

Test Planning and Reports

Approved by:

Michael Williams

Test Planning and Reports Supervisor

D R Sauvageau

f. Space Systems Engineering Manager

D R Sauvageau

Systems Test and Support Manager

Jack R. Kapp

Space Engineering Design Manager

2/19/88

Project Engineer

J. H. Keller

Program Manager

Certification Planning

System Safety

H. H. Dittmer

Reliability

P C Tydeck 2/22/88

Data Management

REVISION ___

88942-10.1

DOC NO. TWR-16829 | VOL

SEC | PAGE

Major contributing authors to this report are listed below, with the appropriate section and their acceptance signatures.

Fred Baugh
Insulation Design

John Furgeson
Structural Applications

Ron Bell
Instrumentation

Lynn Abrahamson
Propellant and Adhesive Structures

Don Ferney
GSE Structures

ABSTRACT

The assembly test article (ATA) consisted of two live loaded redesigned solid rocket motor (RSRM) segments which were assembled and disassembled to simulate the actual flight segment stacking process. The test assembly joint was flight RSRM design, which included the J-joint insulation design and metal capture feature.

The ATA test was performed mid-November through 24 Dec 1987, at Kennedy Space Center (KSC), Florida. The purpose of the test was 1) certification that vertical RSRM segment mating and separation could be accomplisehd without any damage, 2) verification and modification of the procedures in the segment stacking/destacking documents, and 3) certification of various GSE to be used for flight segment assembly and inspection.

A live loaded aft segment was fastened to the mobile launch platform (MLP) in the vehicle assembly building (VAB). Two partial mates and two full mate/demate sequences were performed with loaded aft and aft center segments to evaluate the RSRM joint configuration. The insulation J-joint contact area and metal parts fit were evaluated during these segment assembly/disassembly processes, as well as the performance of various (GSE). Profile measurements and nondestructive evaluation (NDE) inspections were also performed on the segments.

RSRM vertical segment assembly/disassembly is possible without any damage to the insulation, metal parts, or seals. The insulation J-joint contact area was very close to the predicted values. Numerous deviations and changes to the planning documents were made to ensure the flight segments are effectively and correctly stacked. Various GSE was also certified for use on flight segments, and are discussed in detail in the body of this report.

CONTENTS

CONTENTS (Cont)

CONTENTS (Cont)

FIGURES

FIGURES (Cont)

TABLES

TABLES (Cont)

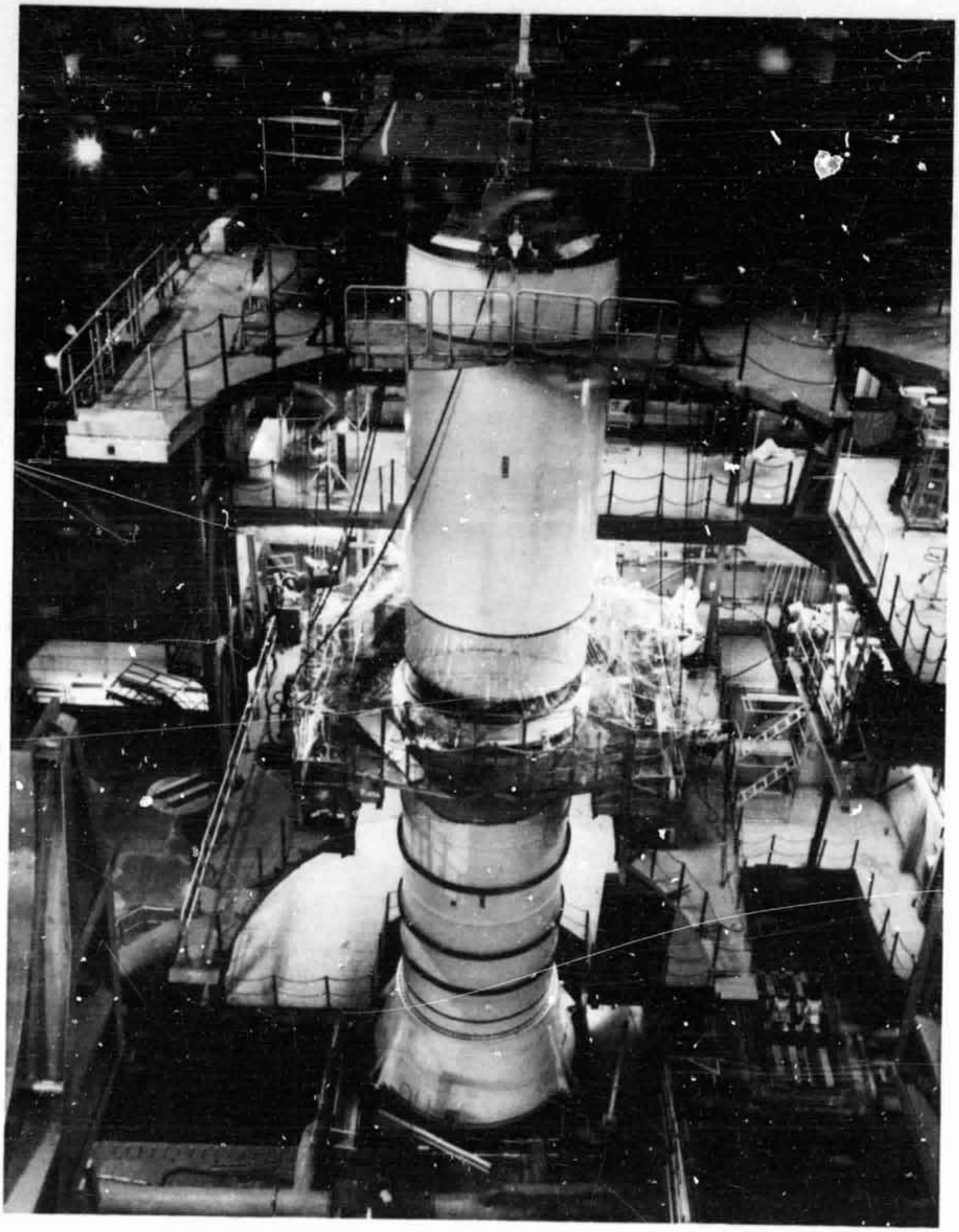

Two live-motor segments are prepared for mate during the Assembly Test Article (ATA) operations. This test, performed at Kennedy Space Center, Florida, simulated the actual flight segment stacking procedures.

1
INTRODUCTION

1.1 HISTORICAL BACKGROUND

As part of the overall redesign effort of the space shuttle, significant changes have been made in the joint configurations of the solid rocket boosters (SRBs). These changes effect the SRB assembly stacking process which occurs on the mobile launch platform (MLP) as the shuttle is being assembled. New and/or modified GSE and operational procedures are required to support the SRB stacking operation, as well as revised crew training and timeline establishment. These procedural modifications and equipment verifications were established and certified during the ATA test. The majority of the test was performed in December 1987.

1.2 TEST ARTICLE DESCRIPTION

The ATA test article was assembled on MLP No. 3, which was located in high Bay No. 1 of the VAB at KSC, Florida. The entire ATA assembly (Figure 1-1) was supported by a high performance motor (HPM) aft skirt which was fastened to four MLP holddown posts. The post studs were instrumented by Grumman Aerospace with strain gages to evaluate the holddown post load distribution. The live loaded aft segment, which was attached to the aft skirt, consisted of an HPM aft dome, two standard weight HPM stiffener segments, and an RSRM lightweight attach cylinder. The stiffener rings, supplied by KSC, were the same ones previously assembled on the STS-61G hardware. The external tank attach (ETA) ring, supplied by United Space Boosters Inc. (USBI), was a right hand RSRM 360-deg configuration. The aft segment was closed on the aft end with a cover plate and HPM nozzle fixed housing, as no RSRM nozzle parts were included. The aft center segment consisted of two lightweight RSRM cylinders joined together. These cylinders were insulated, and the entire segment was live loaded. No systems tunnel was present on either of the ATA segments. No joint heater, protection system, or complete joint closeout was used during the ATA test.

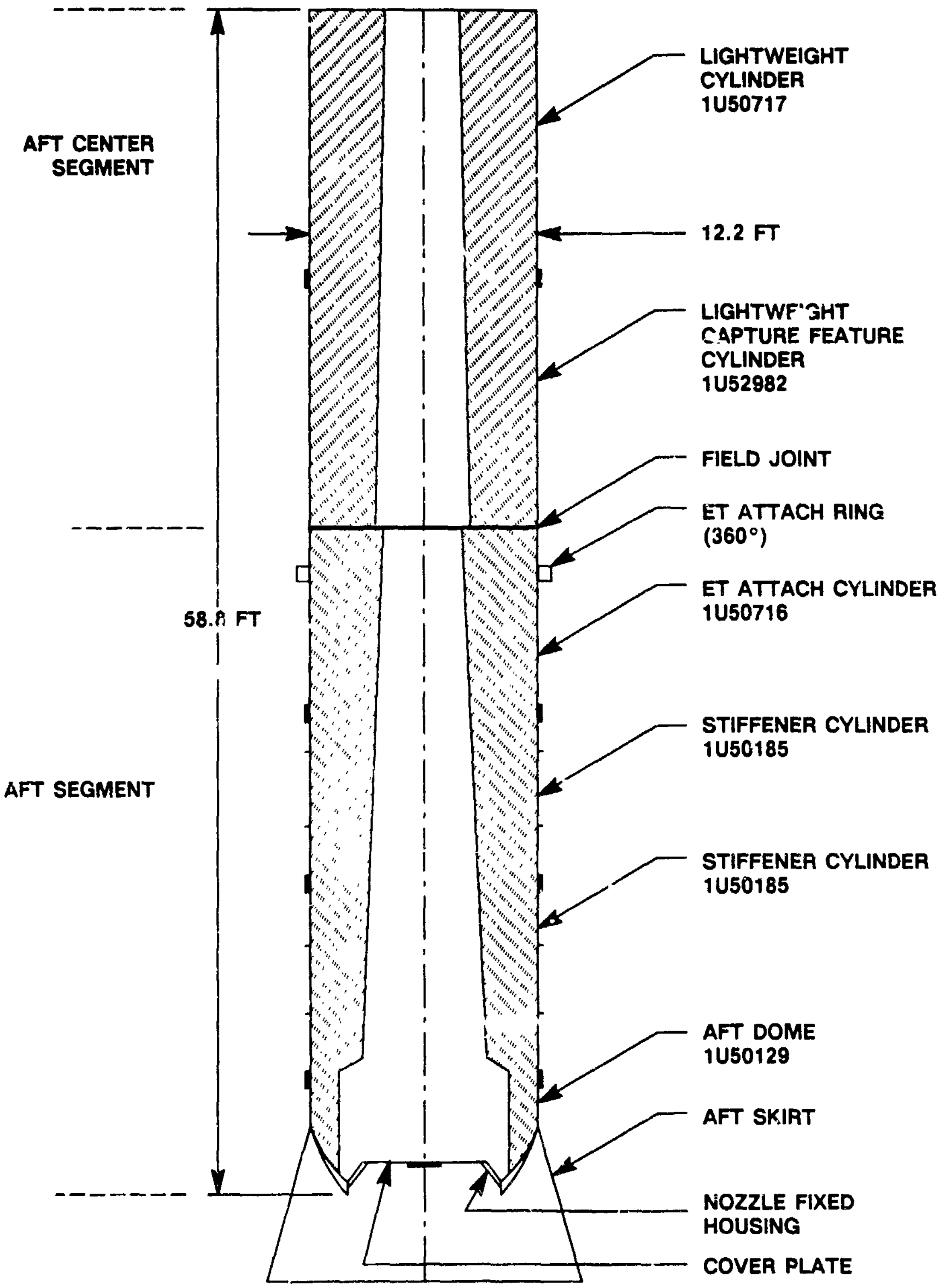

Figure 1-1. Assembly Test Article

The metal parts and insulation design on the test joint were RSRM DM-9/ flight configuration. This included the lightweight capture feature and J-joint insulation profile. An illustration of the test joint features can be found in Figure 1-2.

The aft center segment was moved from the transfer aisle to the high bay test area with the VAB crane. Fine segment movement control was completed with the 250-ton hydraset, suspended directly below the crane block. Beneath the hydraset was the modified 4-point lifting beam, which suspended the segment at four locations 90 deg apart. An illustration and evaluation of this lifting equipment is in Section 7.1.3.

1.3 TEST PROCESS DESCRIPTION

The ATA testing sequence consisted of two partial mates and two full mate/ demate sequences. The partial mates allowed instrumentation measurements on the segments (tang and clevis) and the GSE that otherwise would not have been possible during the full mates. The full mates allowed complete evaluation of the assembly process, including insulation J-seal and capture feature performance. Also included in the test were various segment inspections and measurements. The entire test sequence description, including the deviations from the test plan (CTP-0008 Rev C), is discussed in Section 4.

A010527a R4

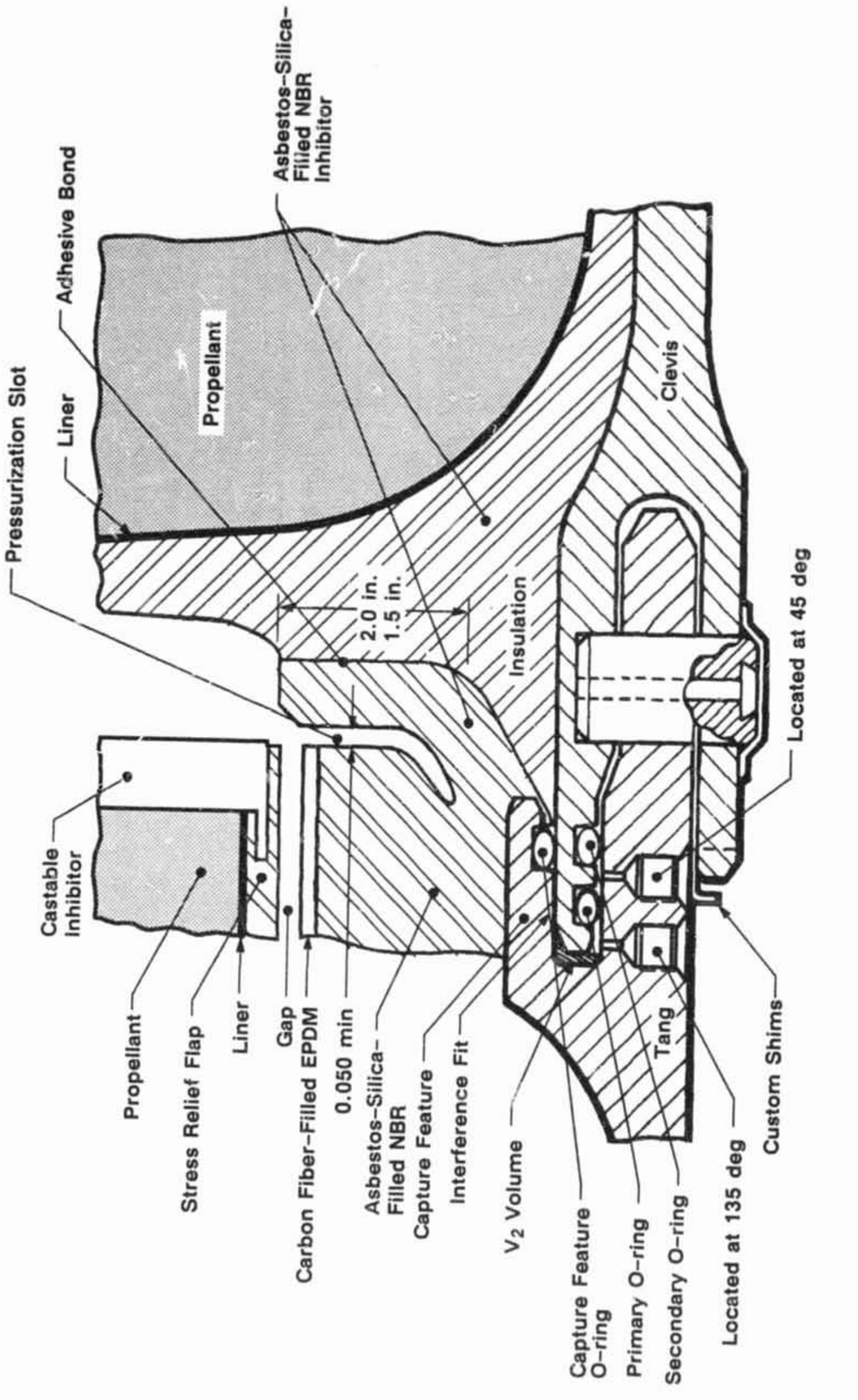

Figure 1-2. ATA Test Joint Configuration

2

OBJECTIVES

The ATA test objectives, as listed in the Development and Verification (D&V) Plan (TWR-15723) are listed below. These objectives, as well as the CEI Specification paragraphs referenced within, are also listed and evaluated in Section 3.2.

2.1 QUALIFICATION OBJECTIVES

a. Certify assembly and disassembly of RSRM segments is possible in the vertical position in accordance with Assembly/Disassembly of Segments as listed in CPW1-3600, Para 3.2.5.1 and Para 3.2.5.2.f.

b. Certify the case has a pin retention device in accordance with Case, CPW1-3600, Para 3.2.1.3.g.

c. Certify existing spares storage and maintenance facilities are used to the maximum extent possible in accordance with Facilities and Facility Equipment, CPW1-3600, Para 3.4.3.

d. Certify that the design has considered tasks to be accomplished by operating, test, and maintenance personnel including considerations for safety, accessibility, critical tasks, complexity, and necessity for training.

e. Certify use and operating procedures of the following GSE:

	Equipment	Model No.	Configuration
1.	Pin Retaining Wedge Kit	A77-0424	8U75930
2.	Alignment Pin Kit	H77-0438	8U52624
3.	Field Joint Assembly Fixture	H77-0442	7U75170
4.	Joint Measuring Fixture	A77-0448	8U75901
5.	Vertical Disassembly (separation) Fixture	H77-0451	7U52919
6.	Leak Check System	C77-0457	8U75902
7.	Auxiliary Shaping Tool	C77-0470	8U75900

	Equipment	Model No.	Configuration
8.	Mechanical Case-to-Insulation Bondline Inspection Kit	C77-0475	2U129799
9.	Comparator	A77-0477	8U75903
10.	Ultrasonic Case-to-Insulation Bondline Inspection Kit	C77-0479	2U129431
11.	Joint Insulation Profile Measuring Kit	C77-0481	2U129541
12.	J-seal Terminus Inspection System	C77-0485	2U129541
13.	J-seal Bondline Inspection Tool	C77-0484	8U76225
14.	Assembly Instrumentation		
	Temposonics	C77-0487	8U75919
	4-point Beam	H77-U0384	
15.	Slump Measuring Tool	C77-0488	8U75923

f. Certify that the leak test method is compatible with the field joint insulation to verify joint seals.

g. Certify that the field joint insulation configuration will ensure that system performance and structural integrity is maintained during the assembly process.

h. Certify that the field joint insulation does not shed fibrous or particulate matter during assembly which could prevent sealing.

i. Certify that the field joint insulation will permit preflight demating. This shall preclude insulation damage.

j. Certify that contamination is controlled to assure system safety, performance, and reliability.

2.2 DEVELOPMENTAL OBJECTIVES

k. Determine mate/demate loads on hardware and GSE (including bondline stress)

l. Evaluate baseline joint configuration fit during and after mate.

m. Gather actual data for analytical comparison.

n. Provide for crew training.

o. Establish timelines for maintenance/replacement functions of case segments.

p. Validate procedures for RSRM assembly/disassembly and handling.

3

SUMMARY, CONCLUSIONS, AND RECOMMENDATIONS

The ATA test objectives can be classified into three general categories: 1) certification of vertical RSRM segment stacking, 2) verification of the procedures in the segment stacking documents, and, 3) certification of the GSE used during ATA for flight segment stacking. This section contains: 1) a brief overview of the test results, 2) an evaluation of the certification conclusions reached as they relate to the test objectives and CEI Specifications, 3) and a listing of the significant recommendations made from the results and conclusions drawn. Complete detailed evaluations of the procedures and equipment are contained in other sections of the report and are referenced, where possible, in the summary below.

3.1 SUMMARY

3.1.1 Vertical Segment Stacking

Two vertical segment mates were performed during the ATA test; one with joint insulation contact transfer medium (dry mate), and one with joint insulation adhesive (wet mate). Two partial mates were also performed. Specifics of all ATA operations are discussed in Section 4. Post-test inspections confirmed that RSRM segments can be vertically assembled and disassembled without damage to the insulation, seals, and metal parts.

3.1.1.1 Mate/Demate Loads. Segment mate/demate loads were determined from the hydraset (placed directly below the crane block) and the load pins in the 4-point lifting beam arms. Actual measurements between the hydraset and beam load pins varied greatly throughout the ATA mating/demating operations. No bondline stress data were gathered during the ATA test due to instrumentation deletions. Details of the mate/demate sequence loads, as well as an evaluation of the metal parts hardware, is in Section 7.2.

3.1.1.2 Segment Shaping. The post-demate inspection with joint adhesive showed joint insulation contact full circumference, with a maximum, minimum, and average contact width of 0.30, 0.13, and 0.19 in. respectively. Analysis predictions were 0.27 in. maximum and 0.13 minimum at 75°F. No fibrous or particulate contamination attributed to the insulation itself was found.

3.1.1.3 Insulation Inspection. The assembled joint was visually inspected by the "man in the bore" method during the first full (dry) mate. The insulation contact profile and overall joint contamination results were very favorable. Case-to-insulation bondline inspections were also performed during the ATA test.

3.1.1.4 Environment Enclosure. An environment enclosure was used during the ATA test to control contamination during joint assembly/disassembly operations. Although area cleanliness was greatly improved over past operations, additional improvements must be made. A complete evaluation of the insulation performance, bondline inspections, and the environment enclosure is given in Section 7.3.

3.1.2 Procedures Verification

Procedures for the RSRM segment handling and assembly/disassembly as specified in TWA-791 were validated during ATA. Numerous deviations and problems were encountered with the operating tasks as specified in the Operational Maintenance Instructions (OMI) throughout the ATA test. These requirements were corrected, edited, or deleted. The specifics of these procedural changes are discussed in the applicable sections, and the ATA procedures are discussion in Section 4.

3.1.2.1 Segment Mating Criteria. Segment mating criteria for flight stacking was determined from the ATA results. Changes were incorporated into the planning documents through the "ATA Lessons Learned" revision change notice (RCN-MB7878). This includes:

a. Premate Segment Relative Axis Position (centering)--To be as close as possible, but vary no more than 0.065 in. in any direction.

b. Segment Concentricity (shape)--To be as close as possible, but vary no more than 0.125 in. radially.

c. Segment Parallelism (levelness)--Prior to tang/FJAF insertion, the two segments (tang and clevis) will be within 0.035 in. of each other. During the mating sequence, insertion will be as smooth and continuous as possible, as stopping and starting adversely affects segment parallelism. Lurching, which is defined as a sudden lowering movement of the segment, is permissible as long as the applicable out-of-parallelism limits are not exceeded. An illustration of the required parallelism verses position is in Figure 3-1. During initial engagement and until the segments are within 2.6 in. from the fully-mated position, the out-of-parallelism value will not exceed 0.5 inch. The out-of-parallelism limit reduces to 0.125 in. during the interval when the tang is between 2.6 and 0.72 in. from full mate. The value is then relaxed to 0.25 in during the last 0.72 in. of tang insertion.

d. Segment Insertion Rate Verses Position--Insertion rate as a function of position is shown in Figure 3-2. An insertion rate of 0.200 in./min is allowed while the tang is between 4.0 and 2.0 in. from the mated position. A maximum insertion rate of 0.060 in./min will again be applied for the final 2.0 in. of tang engagement.

3.1.2.2 Personnel Tasks. It was also shown during ATA that the RSRM segment and joint design adequately considered operating, test, and maintenance personnel tasks. Crew training was also provided. An overview of all ATA operations is given in Section 4, and areas where additional training is required are discussed in the applicable sections.

3.1.3 GSE Evaluation

The other key purpose of the ATA test was certification of the GSE to be used for flight segment inspection and stacking. Whereas this section briefly highlights the results, detailed GSE evaluation is in Section 7.1.

3.1.3.1 Assembly/Alignment GSE.

a. Alignment Pin Kit (H77-0438)--The alignment pins were used for the first full mate. Prior to joint separation, one pin could not be reinserted at 0 deg. After a 0.0005 in. pin diameter reduction, the 8U52624 pin kit is certified for use on flight segments.

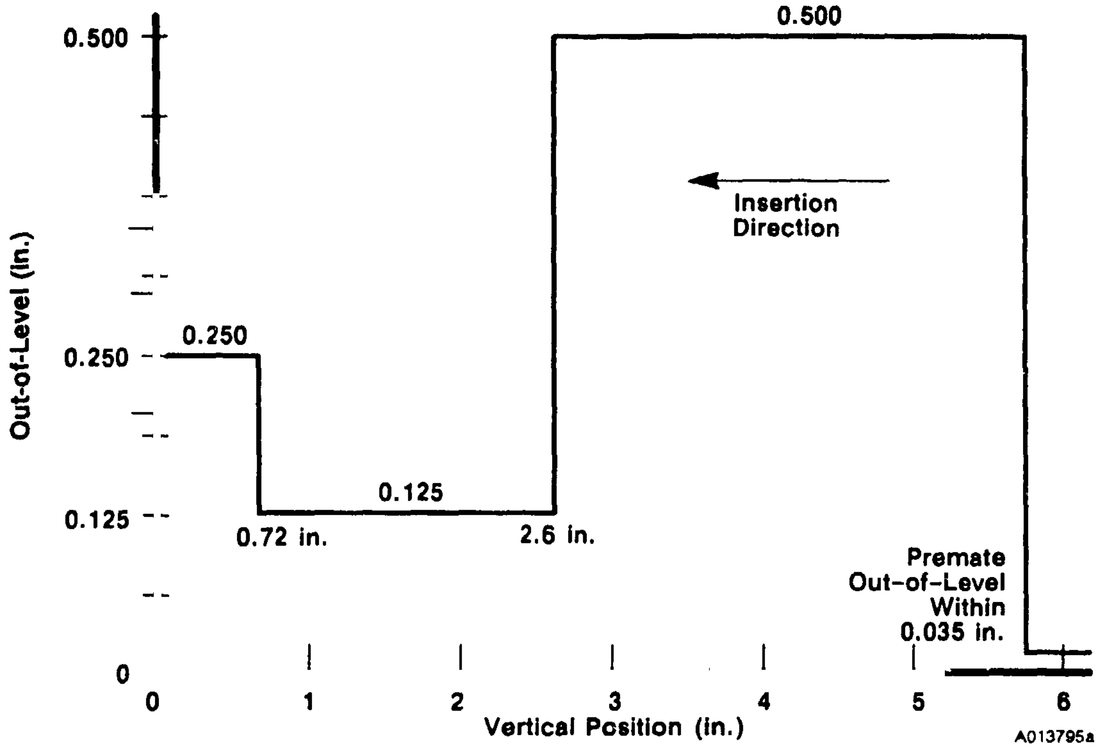

Figure 3-1. Flight Segment Parallelism (levelness) Versus Position

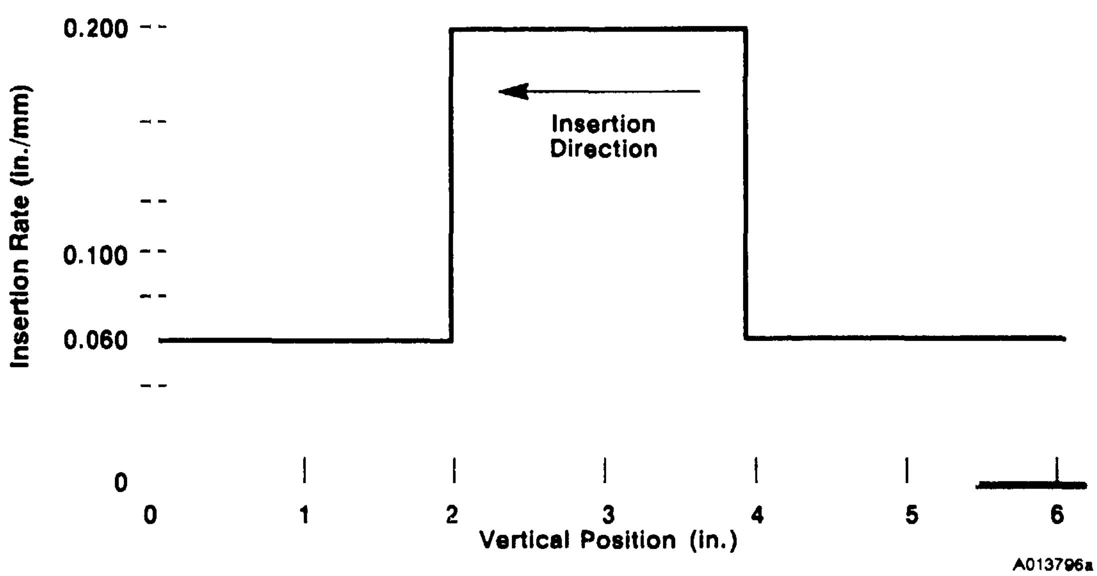

Figure 3-2. Flight Segment Insertion Rate Versus Position

b. Field Joint Assembly Fixture (H77-0442 FJAF)--The ATA tests verified the FJAF joint shim thicknesses were sufficient to compensate for the ratcheting effects of the tang and clevis. Shim thickness calculations were also completed for the STS-26 stacking. Continued evaluation is being done on this FJAF shim calculation process, and is documented in TWR-18067. The 7U75170 FJAF is certified for use on flight segments.

c. Joint Measuring Fixture (A77-0448 sine bar)--This GSE was used extensively to determine segment shape. All changes in segment snape, due to load variation on the aft center segment, were readily apparent. Use of the 8U75901 tool during the test certify it for use on flight segments.

d. Vertical Separation Fixture (H77-0451)--This fixture was used to separate the segments after the dry mate. Separation was erratic and uneven primarily due to lack of operator training. Due to risk of segment damage, no joint separation should be attempted without the VSF. Improvements to the fixture are being made prior to use on any flight contingency destacking operation. With these changes, the 7U52818 VSF is certified for use on flight segments.

e. Leak Test System (C77-0457)--A leak check was performed on the segment joint during the dry mate to verify both the leak check procedure and equipment use. No insulation incompatibility with the leak test method was found. Although hardware and software problems with the equipment were discovered, they were resolved and the joint seals passed the test with ample margin. The 8U75902 system is certified for flight segment use.

f. Assembly Instrumentation (C77-0487)--The assembly instrumentation evaluated during ATA consists of four temposonic height gages, the 4-point lifting beam, and the hydraset. The 8U75919 temposonic gages, located 90 deg apart on the motor, were used to determine segment relative position and out-of-parallelism. Real-time display of this information was extremely beneficial during mate/demate operations.

Fine segment movement control was accomplished by using the hydraset rather than movement of the crane block. Segment beamload distribution load was adjusted with the 4-point lifting beam. More shaping tests are needed, however, before a complete understanding of the shaping phenomena is understood and confidence can be placed in a shaping analysis model. Segment shaping is discussed in Section 7.1.

3.1.3.2 Nondestructive Evaluation (NDE) GSE

a. Mechanical Case-to-Insulation Bondline Inspection Kit (C77-0475)--An air load inspection was performed on the aft center segment clevis. T' tool was not used on any tang surface during ATA, but was used on segment tangs. The 2U129799 tool is qualified for use on flight s s.

b. Ultrasonic Case-to-Insulation Bondline Inspection Kit (C77-0479)--Ultrasonic inspections were performed on the segment tang and clevis ends during ATA. No calibration standard was available for the tang inspection (one has since been obtained). Kit use during ATA, as well as on DM-9 segments, qualify the 2U129431 tool for use on flight segments.

c. Joint Insulation Profile Measuring Kit (C77-0481 J-seal profile)--The required inspection time averaged about 18 hr, with two tools being used. Some areas of improvement were identified although no significant inspection time reduction is foreseen. The 2U129541 tool is certified for flight segments.

d. J-seal Terminus Inspection System (C77-0485)--The 2U129578 tool was used on the aft center segment tang insulation and is certified for use on flight segments.

e. Slump Measuring Tool (C77-0488)--Slump measurements were taken prior to and after the ATA test. A greater than expected propellant modulus was calculated based on the measured ATA slump results. Complete propellant evaluation is contained in Section 7.4. The 8U75?23 tool was certified for use on flight segments.

3.1.3.3 GSE Not Certified During ATA

a. Pin Retaining Wedge Kit (A77-0424)

b. Auxiliary Shaping Tool (C77-0451)

c. Comparator (A77-0477)

d. J-seal Bondline Inspection Tool (C77-0484)

3.2 CONCLUSIONS

A summary of conclusions, as they relate to the D&V Plan (TWR-15723) objectives and the Contract End Item Specifications (CEI Specifications, CPW1-3600A, dated 3 August 1987), is stated below. The section where the results are discussed in detail is also listed.

OBJECTIVE/CEI SPECIFICATION

Qualification Objectives:

Objective A--Certify assembly/disassembly of RSRM segments is possible in the vertical position in accordance with Assembly/Disassembly of Segments, as specified in CPW1-3600 Para 3.2.5.1 and Para 3.2.5.2.f.	Certified--RSRM segment assembly/disassembly is possible in the vertical position. Section 4.
Paragraph 3.2.5.1 Assembly/Disassembly of segments.	Certified--The segment alignment criteria of document USBI-10183-0022 was met.
Para 3.2.5.2.f	Certified
Objective B--Certify the case has a pin retention device in accordance with Case Para 3.2.1.3.g of CPW1-3600	Not Certified--No case pin retention device was used during the ATA test.
Para 3.2.1.3.g	Not Certified
Objective C--Certify existing spares storage and maintenance facilities are used to the maximum extent possible in accordance with Facilities and Facility Equipment Para 3.4.3 of CPW1-3600	Partially Cerified--No spares storage of segments was done during ATA. All maintenance functions were performed using the existing facilities. Section 4.
Para 3.4.3	Partially Certified
Objective D--Certify that the design has considered tasks to be accomplished by operating, test, and maintenance personnel including considerations for safety, accessibility, critical tasks, complexity, and necessity for training.	Certified--The ATA design considered all applicable personnel tasks. Section 4.

Objective E--Certify use and operating procedures of the following GSE:	
a. Pin Retaining Wedge Kit (A77-0424/8U75930)	Not Certified--Section 7.1.3 a
b. Alignment Pin Kit (H77-0438/8U52624)	Certified--Section 7.1.3 b
c. Field Joint Assembly Fixture (H77-0442/7U75170)	Certified--Section 7.1.3 c
d. Joint Measuring Fixture (sine bar) (A77-0448/8U75901)	Certified--Section 7.1.3 d
e. Vertical Disassembly (Separation) Fixture (VSF) (H77-0451/7U52919)	Certified--Section 7.1.3 e
f. Leak Check System (C77-0457/8U75902)	Certified--Section 7.1.3 f
g. Auxiliary Shaping Tool (H77-0451/8U75900)	Not Certified--Section 7.1.3 g
h. Mechanical Case-to-Insulation Bondline Inspection Kit (C77-0475/2U129799)	Certified--Section 7.1.3 h
i. Comparator (A77-0477/8U75903)	Not Certified--Section 7.1.3 i
j. Ultrasonic Case-to Insulation Bondline Inspection Kit (C77-0479/2U129431)	Certified--Section 7.1.3 j
k. Joint Insulation Profile Measuring Kit (C77-0481/2U129541)	Certified--Section 7.1.3 k
l. J-seal Terminus Inspection System (C77-0485/2U129528)	Certified--Section 7.1.3 l
m. J-seal Bondline Inspection Tool (C77-0484/8U76225)	Not Certified--Section 7.1.3 m
n. Assembly Instrumentation (C77-0487/8U75923)	Certified--Section 7.1.3 n
o. Slump Measuring Tool (C77-0488)	Certified--Section 7.1.3 o
Objective F--Certify that the leak test method is compatible with the field joint seals. Para 3.2.1.8.1.1.b)	Certified--Section 7.1.3 f and Section 7.3.
Para 3.2.1.8.1.1.b	Certified
Objective G--Certify that the field joint insulation configuration will ensure that system performance and structural integrity is maintained during the assembly process. (Para 3.2.1.8.1.1.c)	Certified--Post-test inspections verified structural integrity was maintained. Section 7.3.3.

Para 3.2.1.8.1.1.c	Certified
Objectives H--Certify that the field joint insulation does not shed fibrous or particulate matter during assembly which could prevent sealing. (Para 3.2.1.8.1.1.f)	Certified--No fibrous or particulate matter (from the insulation) was detected. Section 7.3.3.
Para 3.2.1.8.1.1.f	Certified
Objective I--Certify that the field joint insulation will permit preflight demating. This shall not preclude insulation damage. (Para 3.2.1.8.1.1.h)	Certified--Segment demating caused no insulation damage. Section 7.3.3.
Para 3.2.1.8.1.1.h	Certified
Objective J--Certify that contamination is controlled to assure system safety, performance, and reliability. (Para 3.3.9)	Partially Certified--The environmental contamination enclosure worked partially, but additional improvements must be made. Section 7.3.3.6.
Para 3.3.9	Partially Certified
DEVELOPMENTAL OBJECTIVES	
Objective K--Determine mate/demate loads on hardware and GSE (including bondline stress) (Para 3.3.6.1.1.2.b)	Partially Completed--More evaluation is required on the ATA determined loads. No bondline stress was measured. Section 7.2.3.2.
Para 3.3.6.1.1.2.b	Partially Certified
Objective L--Evaluate baseline joint configuration fit during and after mate.	Partially Completed--Insulation evaluation was very close to predicted analysis. Section 7.3.3. Tang and clevis measurements were only taken during the full mate. Section 7.2.3.6.
Objective M--Gather actual data for analytical comparison.	Partially Completed--Data for was gathered for both the case hardware (Section 7.2) and GSE (Section 7.1). No bondline stress loads were measured.
Objective N--Provide for crew training.	Partially Completed--Crew training was provided, however, additional crew training must be provided to fully satisfy this objective. Section 4.

Objective O--Establish timelines for maintenance/replacement functions of case segments.	Partially Completed--Some maintenance functions were established. No replacement functions were performed. Section 4.
Objective P--Validate procedures for RSRM assembly/disassembly and handling.	Completed--The RSRM assembly/disassembly and handling procedures actually used during ATA were validated. Section 4.

3.3 RECOMMENDATIONS

Numerous improvements to the equipment and procedural changes were recommended as a result of the ATA test. They are outlined below, classified according to section.

3.3.1 GSE Recommendations

Details of the GSE evaluation are discussed in Section 7.1 the recommendation from that section are summarized below.

3.3.1.1 Alignment Pin Kit.

a. The alignment index pin diameters should be reduced 0.0005 inch.

b. An alignment pin tolerance study should be performed to determine why the 0-deg pin could not be inserted during the dry mate.

c. The short index alignment pins should be deleted.

3.3.1.2 Field Joint Assembly Fixture (FJAF).

a. A premate bearhug evaluation should be performed on each joint during the STS-26 stacking. Similar bearhugging measurements should also be performed the first time the 8U5686 FJAF is used for flight segment stacking.

b. The 7U75170 FJAF should be lightly sanded to eliminate any teflon peeling due to overspray, and all exposed surfaces coated with HD-2 grease to avoid corrosion while not in use.

c. The point edge by the tang should be feathered to avoid adverse interference during paint/FJAF guide block engagement.

Recommended changes to be made on the 8U75686 FJAF, which will replace the 7U include:

d. Increased FJAF back thickness dimensions: minimum dimension 0.377 to 0.407 in., maximum 0.440 to 0.460 inch.

e. Joint shim tolerance changed from ±0.010 to ±0.001 inch.

f. FJAF pinhole size changed from 1.50 in. to 1.25 inch.

g. A third set of handles be added to allow a third person help with the section handling.

3.3.1.3 Vertical Separation Fixture (VSF). Additional training for the VSF operation is needed, as it is felt lack of operator training was the primary cause for the erratic separation during the first full (dry) mate. No segment separation or demate should be attempted without the use of the VSF to insure no damage to the segment. In addition to crew training, other recommended changes are:

a. Hydraulic cart size reduction to improve work platform level accessibility.

b. Hydraulic hose lengthening for operational ease.

c. Main control valve sensitivity reduction, to reduce the chance of operator error.

d. Elimination of the LVDTs on the VSF cylinders.

e. The main pressure gage readout scale should be replaced with one that is scaled for easy readability in the sensitive operating range.

3.3.1.4 Joint Measuring Fixture (sine bar). Recommended improvements are:

a. The guide fingers should be modified to more readily insure proper placement during use.

b. An audible alarm to alert the operator if an LVDT reading goes out of range should be included.

c. Additional operator training, including general personal computer familiarity and specifics relating to the sine bar software.

d. A copy of all future plots and/or printouts made are to be included in the OMI during segment stacking.

3.3.1.5 Assembly Instrumentation (temposonics, hydraset, 4-point lifting beam).

a. Additional operator training on the hydraset is recommended, to improve awareness of the low movement rates required for mate/demate operations.

b. The 4-point lifting beam load pin data should be incorporated into the same data acquisition system as the temposonics. The feasibility of including the hydraset data as well should also be assessed.

c. More investigation into segment mate/demate loads should be accomplished. Good correlation between hydraset, load pin, and segment relative position should be established in order to more fully understand critical areas.

3.3.1.6 Segment Shaping Tests.

a. It is strongly recommended more segment shaping data be analyzed during flight stacking, to enlarge the data base and aid in refinement of the segment shaping model.

3.3.1.7 Leak Test System. Recommended improvements made to the system are:

a. A torque limiting ratchet type valve handle will be used to avoid overtightening.

b. Flex lines will replace the currently used hard tubing, if it is verified the flex line volumes do not change with pressurization (adversely effecting leak rate calculations).

c. Software changes to allow the operator to start and end the various test sequences are being made, allowing verification of proper equipment functionality prior to measurement. Updates are also being made to display measured values as they are acquired, and when the leak check process is complete, a final summary will be printed for review.

d. Additional procedural training in the leak check solution application technique, to avoid solution contamination and corrosion of the metal parts is needed.

e. An evaluation of the leak check sequence and timing is being performed to eliminate the negative leak results. This is currently under consideration; all approved changes will be incorporated into the applicable paperwork.

3.3.1.8 Mechanical Case-to-Insulation Bondline Inspection Kit (air load test). Procedural and physical changes recommended are:

a. An intercom system between operators should be used during operation (excessive air flow noise prevents normal talking).

b. Support should be added to the video and air lines to prevent torquing of the probe guide block.

c. Any grease left on the inner clevis leg must be cleaned prior to tool use. If not, grease will be blown into the unbond, and created significant grease removal and unbond repair problem.

3.3.1.9 Ultrasonic Case-to-Insulation Bondline Inspection Kit. Recommendations are:

a. A second magnetic track should be procured to significantly reduce inspection operation time.

b. The test system is delicate and should not be moved more than absolutely necessary. A permanent location should be selected where the equipment can be kept, then moved only when necessary.

3.3.1.10 Joint Insulation Profile Measuring Kit (J-seal profile). Tool operation time is lengthy and difficult and could possibly be improved with the use of another tool. Improvements to be made on the tool include:

a. Attachment to each end of the propellant slump tool.

b. Use of glass scales and LVDTs.

c. Long-range planning is also in effect for an auto-laser profile tool.

3.3.1.11 J-seal Terminus Inspection System (fiber optics). Recommended improvements are:

a. Reduce the current wand width to allow easier lateral movement within the J-seal.

b. Dead end the fiber optic cable to camera connection to prevent rotation.

c. Offline computer enhancement and characterization should be used to further evaluate future inspection results. If this cannot be done, a leader should be produced on the inspection tape to explain the images.

3.3.1.12 Propellant Slump Measuring Tool. Improved tool use could be implemented by:

a. Incorporation of a computer data system in place of the data logger.

b. A lighter but stiffer beam (as the current beam weighs about 150 lb).

c. All data printouts in the future will be included immediately in the OMI.

3.3.2 Structural Recommendations

Recommendations from the structures section not included in the above GSE section are:

a. O-ring packaging improvements should be made to ensure O-ring integrity upon arrival and installation on flight segments. This includes detailed inspection at Space Operations, double bagging and hard packaging, and only a grease inspection at KSC prior to installation.

b. Improved measurement techniques should be determined for interference fit calculations, as the ATA segments were not measured using the new baseline precision measuring device (PMD).

3.3.3 Insulation Recommendations

Insulation design recommendations were made following evaluation of the ATA test and review of the procedures as contained in the OMI. Recommendations relating to specification and OMI changes are not listed below, but are included in Section 7.3.

Other recommendations are:

a. No tape be applied to the J-joint critical bonding surface.

b. An inspection for tape residues be performed and residues removed prior to any joint abrasion operation.

c. The J-joint surface be inspected for proturbances (especially the tang ID tip where the mold tool sprue holes are located) prior to any abrasion process. Note these areas and inspect again after the abrasion to verify removal.

d. Thoroughly clean all transfer powder off of the segment joint and inhibitor surfaces following any dry fit operation.

e. Inspect for minute abrasion products following any abrasion and cleaning process, to confirm no adhesive or joint contamination.

f. Establish a uniform and accurate case insulation unbond inspection and documentation method.

g. Improve the environment enclosure as discussed in Section 7.3.

h. Blacklight inspection and grease removal from the J-joint surfaces be accomplished prior to adhesive application.

i. The joint assembly sequence as discussed in Section 7.3 should be used for flight segment assembly.

3.3.4 Propellant and Adhesive Structures Recommendations

More propellant slump measurements, on live segments should be made in order to broaden the data base and further refine the modulus analysis model.

4

TEST PROCESS DESCRIPTION

4.1 PREMATE PREPARATIONS

Both ATA segments were shipped to KSC by rail in early November 1987. On 11 Nov 1987, the aft segment was broken over and mated to the aft skirt in the rotational processing and surge facility (RPSF), the last pin being installed about 0900 hr. Stiffener ring installation was completed during the next two days. Out-of-level problems with the ETA ring were encountered during ring installation on the 13 Nov 1987. The ring lugs were relocated and the turnbuckles were readjusted in order to improve ring weight balance. Ring installation continued and was completed early on the 14 Nov 1987. The strain gage readings on the ETA ring during installation were recorded and evaluated by USBI. No significant ring strains were measured during the installation process. Sine bar, or roundness measurements were also made on the aft segment at this time. The aft segment was found to be very round. Possible reasons for this roundness include use of a 360-deg ETA ring, and use of a fixed cover plate instead of an actual nozzle. A complete evaluation of the sine bar performance during the ATA test is discussed in Section 7.1.3.

On 16 Nov 1987 the aft segment was softmated to the MLP holddown posts. After evaluating the load distribution from the holddown post strain gages, it was determined there was at least a 20 percent difference in the load distribution on the four posts. The segment was removed, and the posts were then reshimmed to more evenly distribute the segment load. The next day, when the aft segment was reset on the posts, erroneous strain outputs (negative X-axis readouts) were still present. Final evaluation results of the holddown post loads during the ATA mating tests were inconclusive.

During the next few days numerous ultrasonic inspections, propellant slump readings, pi tape measurements, and insulation repair and profile evaluations were made on both segments. While the MLP posts were being reshimmed, measurements were performed on the aft center segment in the RPSF. After aft segment reinstallation and holddown post torquing, insulation repair work was done on the aft segment where some internal instrumentation (bondline stress) had been removed prior to shipment from Space Operations. Clevis profile data were also gathered at this time. The results of these inspections, and evaluation of the GSE equipment used during these inspections is discussed in Sections 7.3 and 7.1, respectively.

After the aft center segment was moved to the VAB transfer aisle on 21 Nov 1987, simultaneous instrumentation installation commenced on both segments. Various problems were encountered during the instrumentation installation process. Details of the overall instrumentation performance and gage problems and deletions are documented in Section 5. Instrumentation installation for both segments was completed 24 Nov 1987.

The 7U75170 FJAF was installed on the aft segment clevis on 30 Nov 1987. During the next four days a total of three FJAF bearhugs were performed to evaluate the clevis leg movements during FJAF torquing, verify the instrumentation sensitivity, evaluate the calculated FJAF shim thicknesses, and prepare for the first partial mate. A complete evaluation of the 7U75170 FJAF performance during the ATA test, and the recommended improvements for the 8U75686 FJAF, are contained in Section 7.1.3.

While the above mentioned FJAF evaluations were being accomplished on the aft segment clevis, the aft center segment tang was being shaped while suspended in the transfer aisle. Segment reshaping is done by redistribution of the load of the 4-point lifting beam. An evaluation of the segment shaping results from the ATA test, as well as the recommendations for segment shaping during fli ht stacking, is contained in Section 7.1.3. It is noted here that with this particular aft center segment, the closest shape match to the aft segment was attained with a 2-point loading profile, or when the segment weight was almost entirely suspended from the 90- to 270-deg axis points.

4.2 FIRST PARTIAL MATE

The first partial mate was started 3 Dec 1987 at approximately 2000 hr. According to sine bar data, the greatest out-of-round variation between the tang and clevis was 0.055 in. at any radial point prior to mating. An overlay of the tang and clevis shapes prior to the first partial mate can be seen in Figure 4-1. The lowering rate and segment out-of-parallelism for this mating sequence can be seen in Figures 4-2 and 4-3. Between Points A and B in both plots, the segment was lowered at an approximate rate of 0.08 in./min. At Point B, at the 4.4-in. position, initial tang engagement with tne FJAF guide blocks occurred. At Point C, the 90-deg location lagged the 270-deg location insertion position by 0.19 in., the maximum out-of-parallelism value reached during this part mating sequence. At Point D, the entire tang edge had moved below the FJAF guide block ramps, and the segment had reoriented itself to a near level position. Segment insertion was delayed between Points D and E for about 6 min. The final 0.45 in. of insertion for the partial mate occurred between Points E and F.

The FJAF was detorqued and the temposonics were then removed. The segment was lifted by the crane about 12 in. above the clevis at approximately 2330 hr.

4.3 SECOND PARTIAL MATE

On 4 Dec 1987, the aft center segment beam load was redistributed to make the aft center segment more out-of-round. A shape mismatch between the tang and clevis was desirable in order to evaluate the FJAF performance during a worst case partial mating situation. A comparison of the tang and clevis shapes prior to the second partial mate can be seen in Figure 4-4. It should be noted the OMRSD requirement of less than 0.125 in. radial deviation was exceeded at this time.

The second partial mate was initiated on 5 Dec 1987, at about 1345 hr. Figures 4-5 and 4-6 show the lowering rate and segment out-of-parallelism for this second partial mating sequence. At Point A in Figures 4-5 and 4-6, the tang is about 0.06 in. from FJAF guide block contact. As the tang

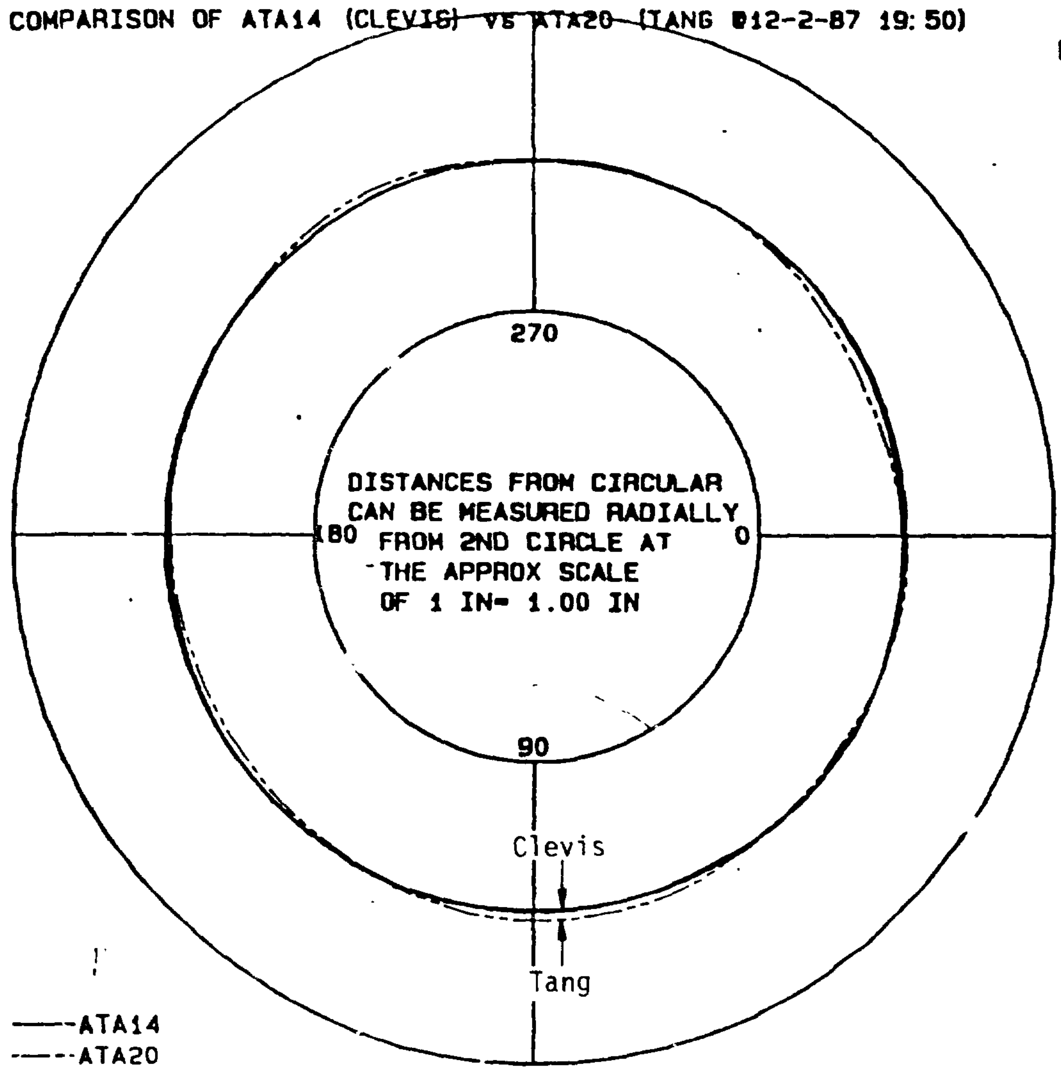

DIFF IN DELTAS FROM CIRC

ANGLE	DIFF	ANGLE	DIFF
0	-0.025	320	0.038
10	-0.032	330	0.055
20	-0.006	340	0.049
30	0.025	350	0.013
40	0.029		
50	-0.003		
60	-0.040		
70	-0.054		
80	-0.049		
90	-0.046		
100	-0.034		
110	-0.003		
120	0.028		
130	0.044		
140	0.048		
150	0.047		
160	0.040		
170	0.022		
180	0.003		
190	0.000		
200	0.006		
210	-0.001		
220	-0.023		
230	-0.047		
240	-0.055		
250	-0.040		
260	-0.015		
270	0.004		
280	0.005		
290	-0.003		
300	0.000		
310	0.016		

Figure 4-1. Tang and Clevis Shape Comparison Prior to First Partial Mate

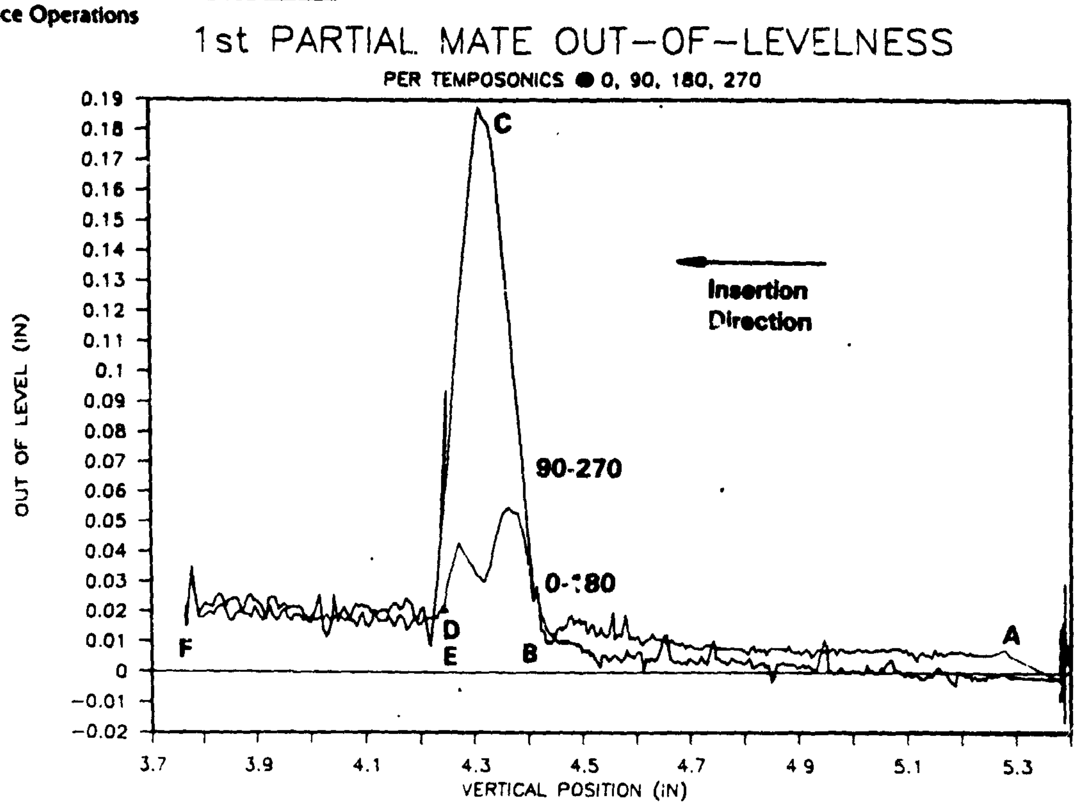

Figure 4-2. First Partial Mate Out-of-Levelness Versus Vertical Position

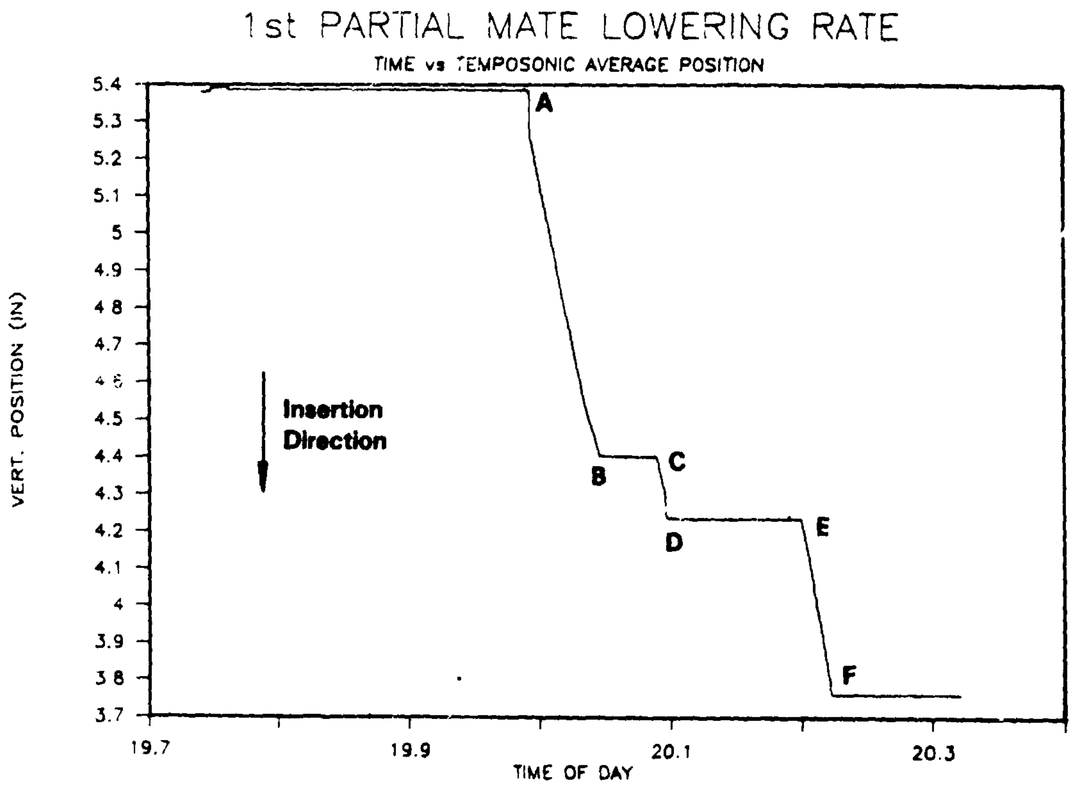

Figure 4-3. First Partial Mate Vertical Positions Versus Time

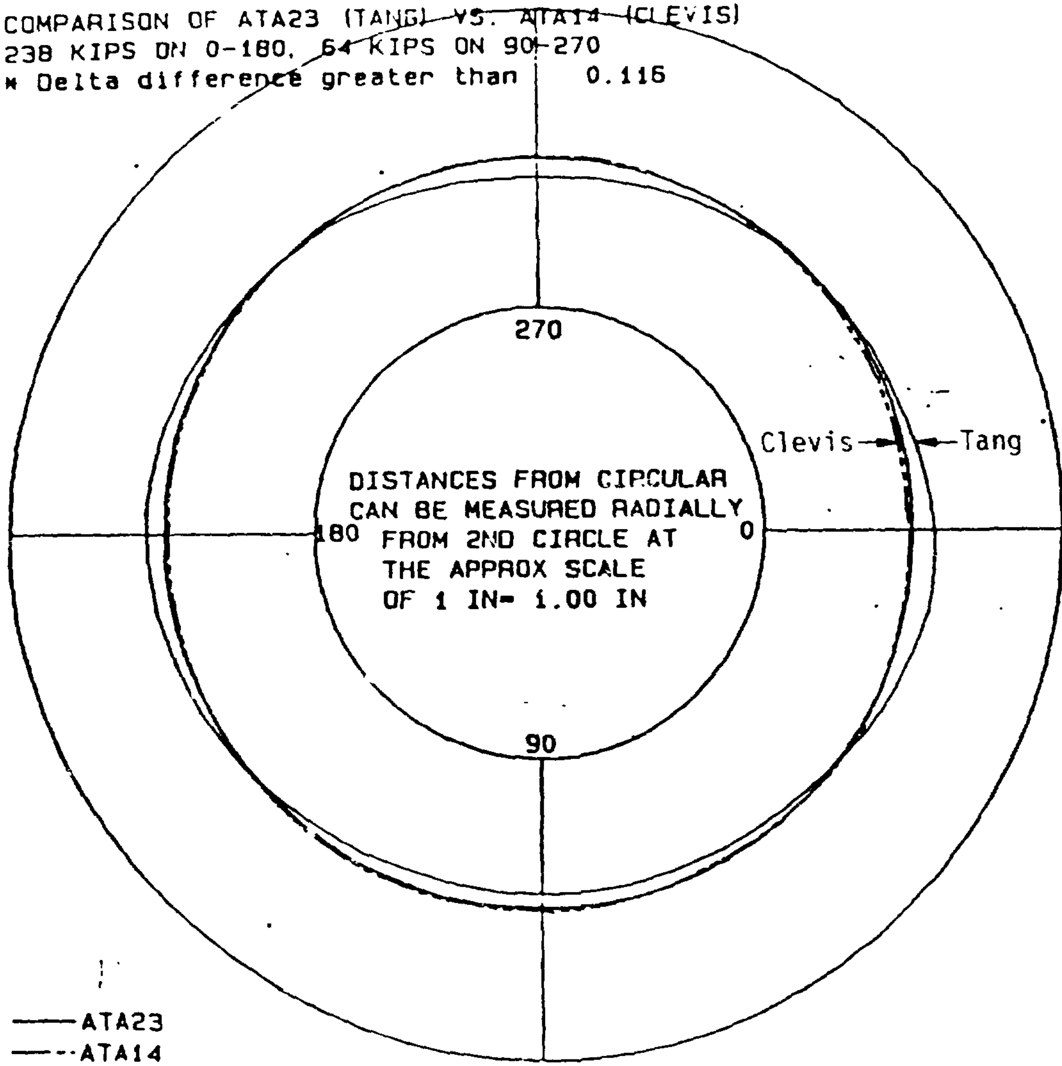

DIFF IN DELTAS FROM CIRC

ANGLE	DIFF	ANGLE	DIFF
* 0	0.167	320	0.014
* 10	0.166	330	0.040
20	0.115	340	0.075
30	0.043	*350	0.124
40	-0.017		
50	-0.044		
60	-0.059		
70	-0.083		
80	-0.109		
90	-0.116		
100	-0.111		
110	-0.108		
120	-0.091		
130	-0.050		
140	0.002		
150	0.051		
160	0.092		
*170	0.125		
*180	0.143		
*190	0.132		
200	0.097		
210	0.060		
220	0.028		
230	-0.002		
240	-0.040		
250	-0.086		
*260	-0.127		
*270	-0.145		
*280	-0.130		
290	-0.091		
300	-0.050		
310	-0.016		

Figure 4-4. Tang and Clevis Shape Comparison Prior to Second Partial Mate

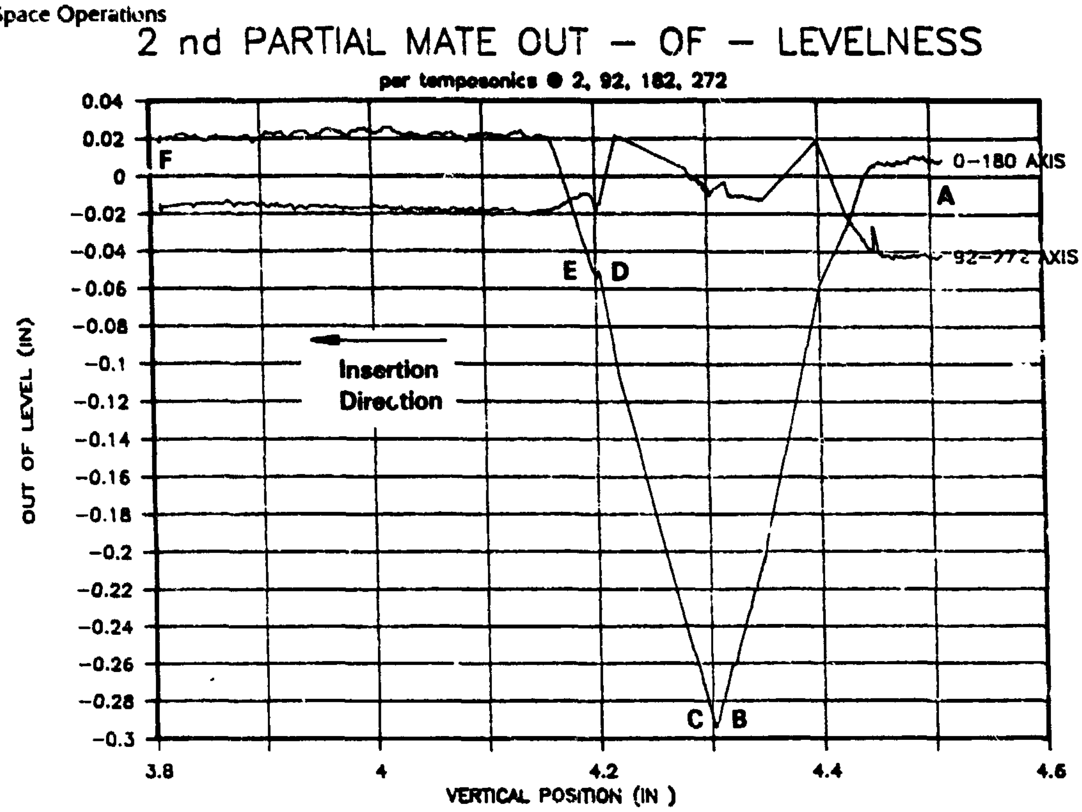

Figure 4-5. Second Partial Mate Out-of-Levelness

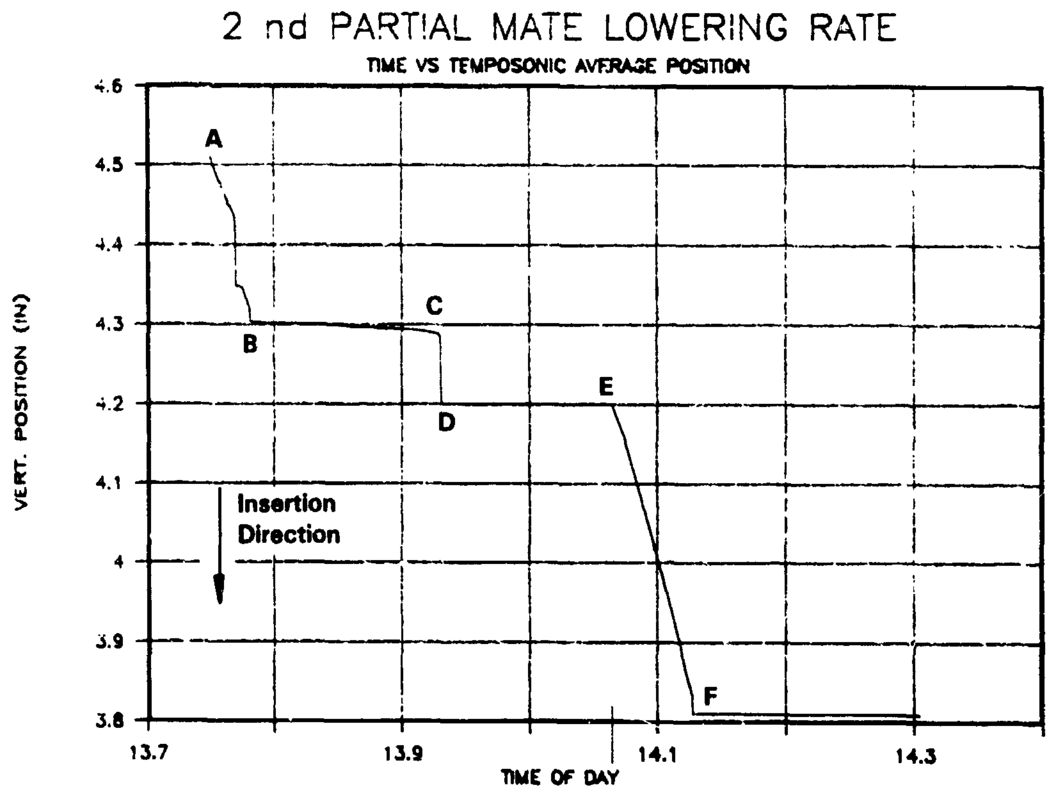

Figure 4-6. Second Partial Mate Lowering Rate

segment was lowered, the 0-deg location hung up on the edge of the FJAF guide blocks while the 180-deg tang location continued to drop. Recall from the shape comparison in Figure 4-4 the tang 0- to 180-deg axis was the long axis due to the oval segment shape, so maximum interference was expected at either the 0- to 180-deg location. The lowering operation was stopped when the out-of-parallelism limit of 0.25 in. was exceeded, as indicated at Point B in Figures 4-5 and 4-6. For the next 8 min., between Points B and C, there was very little vertical segment movement. Due to the new load distribution on the tang, however, the aft center segment slowly reshaped until the 0-deg location slipped down into the FJAF guide block bore. This sudden movement can be seen between Points C and D, and resulted in a final near-level position. After another small delay, tang insertion was reinitiated, and the final 0.38 in. of travel was completed in about 4 min. (as seen between Points E and F).

It was noted at this time there was a maximum separation of 0.015 in. between the FJAF contact band and outer clevis leg from 2 to 18 deg. (Again, recall this is on the axis of maximum interference, due to the oval aft center segment shape). After the required measurements had been taken, the temposonics and FJAF were removed, and the aft center segment was lifted to the transfer aisle.

The activities of the next few days consisted of installation of the environment enclosure top and the reshaping of the aft center segment in the transfer aisle back to more closely match the aft segment. A comparison of the tang and clevis shape prior to the first full (dry) mate can be seen in Figure 4-7. Once the upper segment had been lifted to the D level, the environment enclosure was completed. An evaluation of the enclosure performance during ATA, and the recommended improvements are found in Section 7.3.3. Joint preparation steps were taken next, which included application of the joint contact transfer medium and O-ring installation. Some delays were encountered due to O-ring contamination caused by unpackaging errors, which were resolved by using a second set of O-rings.

COMPARISON OF THE TANG SUSPENDED OVER CLEVIS PRIOR TO 1st DRY MATE ON 12-10-87 (ATA28 12-7-87 @0411 ATA29 12-9-87 @ 2350)

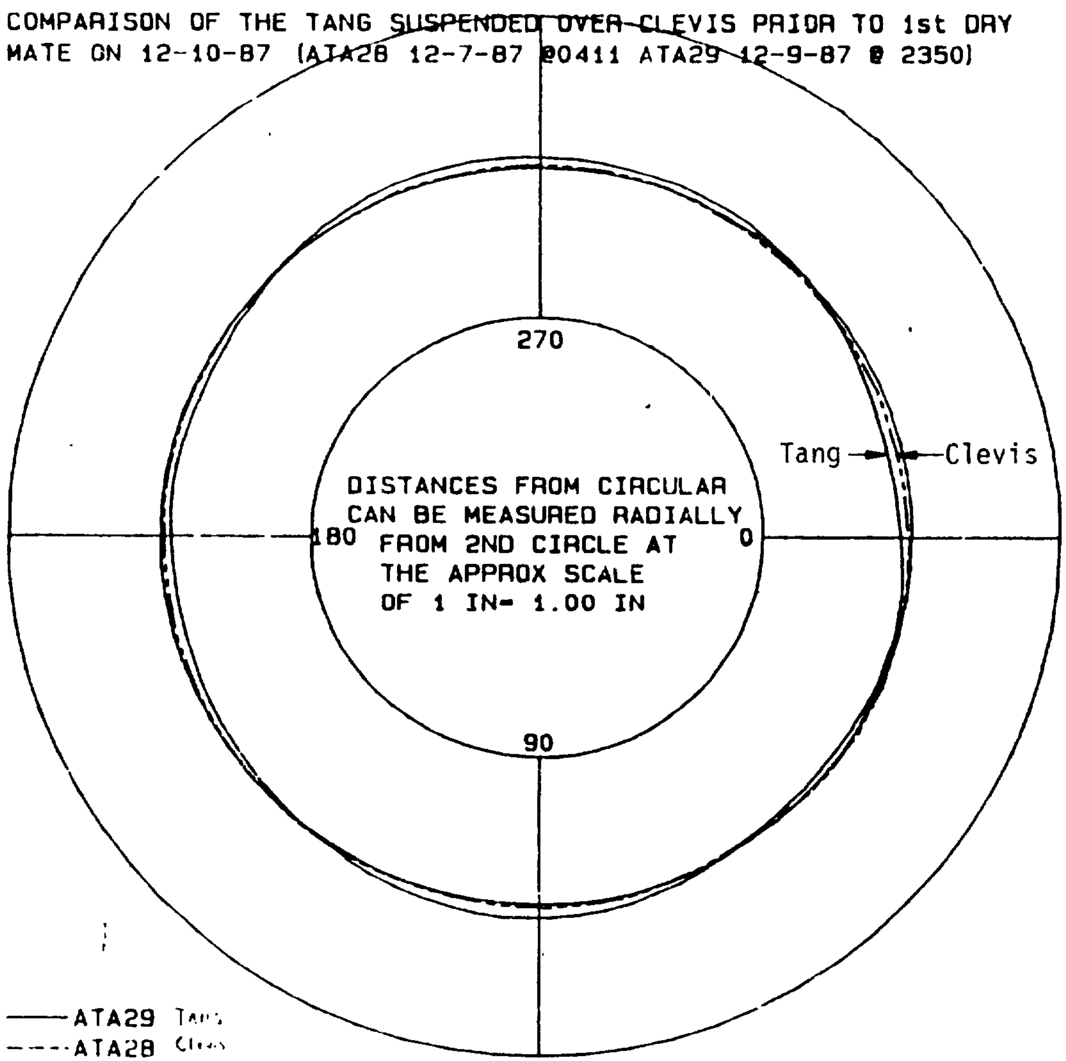

DIFF IN DELTAS FROM CIRC

ANGLE	DIFF	ANGLE	DIFF
0	-0.042	320	0.003
10	-0.020	330	-0.030
20	-0.025	340	-0.059
30	-0.046	350	-0.065
40	-0.052		
50	-0.026		
60	0.013		
70	0.042		
80	0.059		
90	0.076		
100	0.083		
110	0.060		
120	0.024		
130	-0.006		
140	-0.028		
150	-0.044		
160	-0.053		
170	-0.054		
180	-0.047		
190	-0.043		
200	-0.048		
210	-0.047		
220	-0.024		
230	0.013		
240	0.047		
250	0.063		
260	0.059		
270	0.047		
280	0.042		
290	0.048		
300	0.049		
310	0.033		

Figure 4-7. Tang and Clevis Shape Comaprison Prior to First Full (dry) Mate

4.4 FIRST FULL MATE (dry mate)

The dry mate began on 10 Dec 1987 about 0130 hr. Figures 4-8 and 4-9 show the out-of-parallelism and lowering rate for the dry mate insertion. As with the first partial mate, an approximate 0.2 in. out-of-parallelism was recorded during initial FJAF engagement, which is indicated by Point B in Figures 4-8 and 4-9. At Point C, insertion was stopped for approximately one hour for tang to O-ring land clearance measurements. Segment lowering between Points D and E was interrupted due to exceeding the out-of-parallel redline. It was initially 0.035 in., then changed to 0.060 inches. Each change required paper processing. At Point E lowering was stopped again. A PR disposition to proceed was required because the segment was cocked slightly. During this interval (E to F) the out-of-parallel redline was also increased to 0.075 inches. When segment lowering was reinitiated, the out-of-levelness on the 0- to 180-deg axis jumped to 0.087 in. for two data frames (2 sec) before returning to the initial value. This lurch can be seen as the spike at Point F in Figure 4-8. Insertion continued until Point G was reached, when the operation was again suspended.

An engineering meeting which included Morton Thiokol, SPC, and NASA (KSC and MSFC) personnel was held to reevaluate the redline out-of-levelness criteria, and to consider if the joint mating should proceed. It was agreed that an out-of-parallelism redline of 0.25 in. would be used for the remaining insertion. These agreements were made between Points G and H in Figures 4-8 and 4-9. The segment movement indicated on the charts between these points was due to segment settling. Insertion was restarted about 1000 hr and was completed within 20 min. The maximum out-of-parallelism during the final insertion (between Points H and I) was 0.175 in. on the 90- to 270-deg axis. At Point I, The hydraset load was increased 15,000 lb and the FJAF was detorqued. The final 0.25 in. was lowered by the hydraset, and the last pin installed at 2350 hr. Joint gap measurements were then taken, the pin clips installed, and the tang and clevis gap measurements were repeated. The lifting beam was disconnected from the aft center segment and moved back to the transfer aisle.

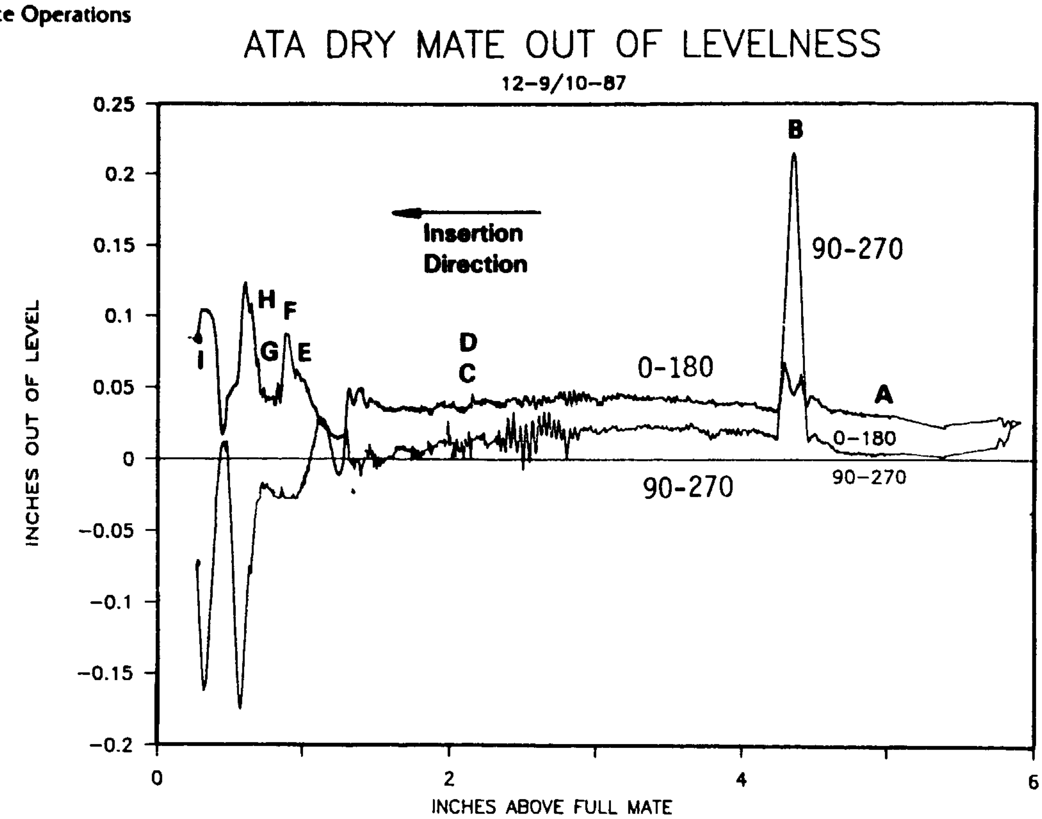

Figure 4-8. First Full (dry) Mate Out-of-Level Versus Vertical Position

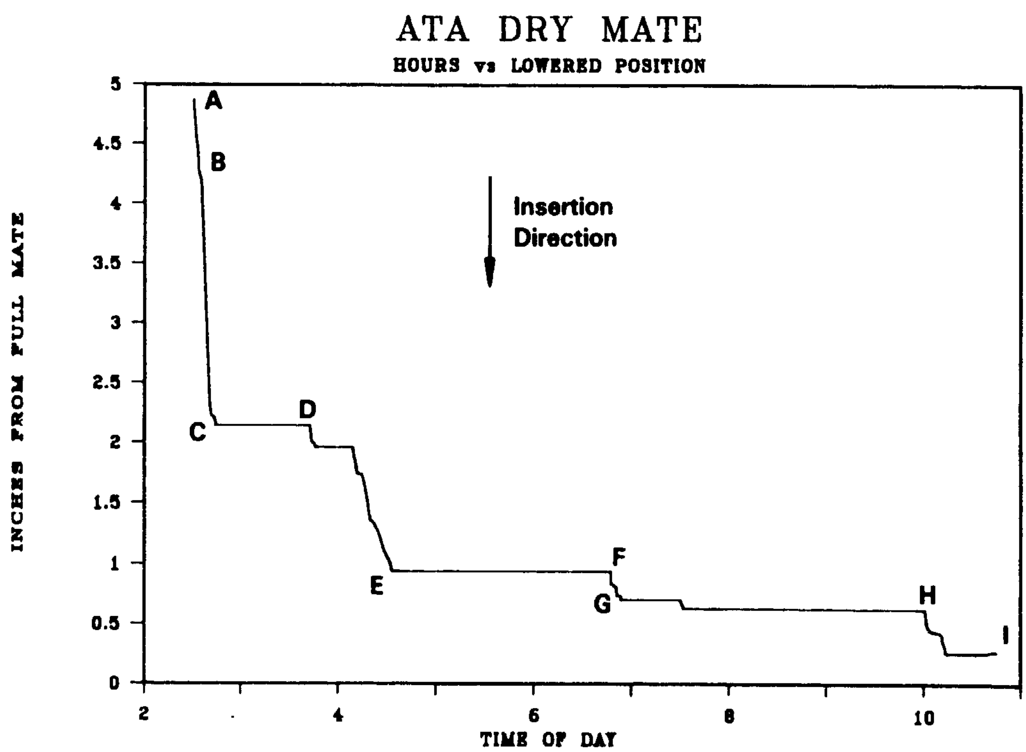

Figure 4-9. First Full (dry) Mate Vertical Position Versus Time

Numerous problems were encountered the next few days during the joint leak check procedure. These included both hardware and software discrepancies. Evaluation of the leak check equipment and process performance is contained in Section 7.1.3, as well as a discussion of the results. It is noted here the segment joint passed all leak criteria with ample margin.

Preparations were then made for segment separation. This included assembly of a work scaffold around the test article that allowed personnel access during the VSF assembly and operation. The scaffold assembly required extensive effort, and took about 16 hr to complete.

On 13 Dec 1987, the lower section of the VSF was installed on the aft segment. Upon tightening, some segment paint was gouged and a girth gage was destroyed due to some missing rubber on the VSF. The missing rubber was replaced, and the remaining parts of the VSF were installed. A complete evaluation of the VSF performance during the ATA test, including all recommendations for use on flight stacking, is contained in Section 7.1.3. The 4-point lifting beam was reattached to the upper segment, and the weight of the upper segment and beam was applied to the hydraset. Pin removal was then initiated.

All loose pins were then removed from the segment joint. When pin removal was complete within five pins of an alignment pin slot, reinsertion of the alignment pin was attempted. (The alignment pins had been removed after joint pin installation.) Alignment pin insertion was completed at the 118- and 240-deg location, but could not be done at 0-deg location after extensive effort. It was decided to demate with the two inserted alignment pins and omit the 0-deg location.

In addition, extreme difficulty was encountered attempting to remove the joint pin at the 164-deg location. In an attempt to unbind this pin, a separation load was applied to the hydraset. The 0-deg location rose approximately 0.375 inch. This action was in direct violation of the planning documents and could have resulted in critical damage to both tang and clevis. Fortunately, post-test inspection revealed no anomalies. Final pin extraction required the use of the hydraulic pin removal tool.

No similar process of trying to unbind a pin by segment movement should be ever at be attempted in the future.

4.5 DRY MATE SEPARATION

Joint separation was started on 15 Dec 1987 at about 2130 hr. Initial segment movement due to hydraset loading was upward at 90 deg and slightly downward at 270 deg (about 0.20 in.). Pressure in the VSF was increased to 500 psi, and movement was only seen at the 90-deg location. All VSF rams were then shutoff, except for the two near the 270-deg segment location (rams No. 7 and 8). A pressure of 850 psi was applied to those rams, and the 270-deg side was raised even with the 90-deg side. The 850 psi pressure was then applied to all VSF rams. Upward segment movement was faster than the hydraset could compensate for at this point, hence the VSF pressure was cutoff to allow the hydraset to catch up. The VSF pressure was then readjusted to 500 psi. When this pressure was again applied to all rams, segment elevation only occurred at 90 deg. The 270-deg location rams were again isolated from the others, and a 650 psi pressure was applied to relevel the segment. Then 500 psi pressure was again reapplied to all rams, and again, only the 90-deg side rose. Releveling was done by application of 550 psi to rams No. 7 and 8, as had been done before. This varying load application was repeated several more times, causing the segment to jockey back and forth during removal. Not only did just one side rise at a time, but while it was being raised the opposite side would settle or lower slightly. This erratic movement can be seen in Figure 4-10. Note that the curve loops, or doubles back along the X-axis at the points where the segment settled back down having once been raised. Also note all erratic movement occurred during the first 0.9 in. of demate. It is emphasized that lack of operator training, and not the tool design, was the primary cause of dissatisfactory tool operation. Once capture feature interference had been disengaged, segment separation was relatively smooth for the remaining demate.

Postmate joint inspections were then made. No damage to any parts were observed, and the J-joint insulation contact medium profile was very

MORTON THIOKOL, INC.
Space Operations

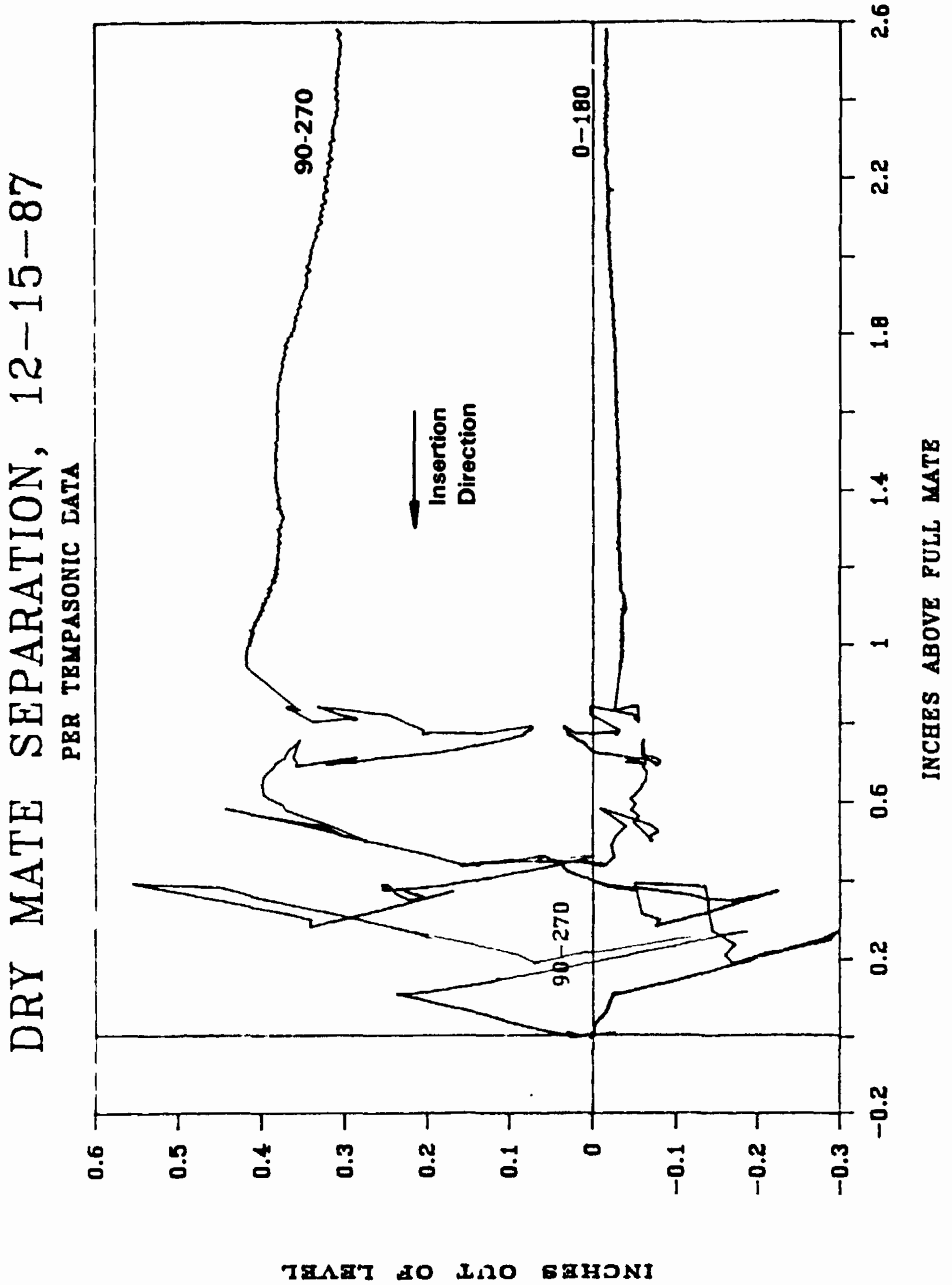

Figure 4-10. Dry Mate Separation Out-of-Level Versus Vertical Position

close to the predicted results. Detailed results of the metal parts and soft goods (O-rings, etc.) inspection are discussed in Section 7.2, while the transfer medium and insulation results are documented in Section 7.3.

After VSF removal from both segments, the aft center segment was lifted back to the transfer aisle. Joint preparation for adhesive application was then intiated. The insulation abrasion process on the aft center segment, which was a preparation step, was temporarily suspended due to suspected asbestos contamination. Environment tests however, verified no contamination was present.

4.6 SECOND FULL MATE

On 18 Dec 1987, joint preparations for the wet mate were completed. Some delays were encountered due to grease contamination in the adhesive. Minute bubbles in the applied adhesive also generated some concern, but were determined to be no constraint. The aft center segment was reshaped from a round to a more oval configuration to evaluate a worst case condition, as had been done on the second partial mate. An overlay of the premate tang/clevis shapes can be seen in Figure 4-11.

Segment mating was initiated 19 Dec 1987, about 0745 hr represented by Point A on Figures 4-12 and 4-13. During tang engagement with the FJAF guide blocks, the 0-deg location lagged the 180-deg location insertion by a maximum 0.22 in. (Point B). This value was consistent with past full and partial mates, and was expected. (Remember from Figure 4-11 the long axis was 0 to 180 deg). Tang insertion continued smoothly until Point C was reached, when mating was stopped for tang/clevis gap measurements. When reinsertion was begun, shown as Point D in Figures 4-14 and 4-15, the descent rate was held as constant as possible, and the out-of-parallelism values remained close to zero, as indicated between Points D and E.
At Point E tang insertion was inadvertently stopped. (It had been agreed that the descent rate would be slowed at that point, but rather than just slow down as was intended, the segment was stopped.) Upon tang insertion continuation, the out-of-parallelism values increased as was expected,

COMPARISON OF CLEVIS (12-17-87) TO TANG (12-19-87) PRIOR TO WET MATE.

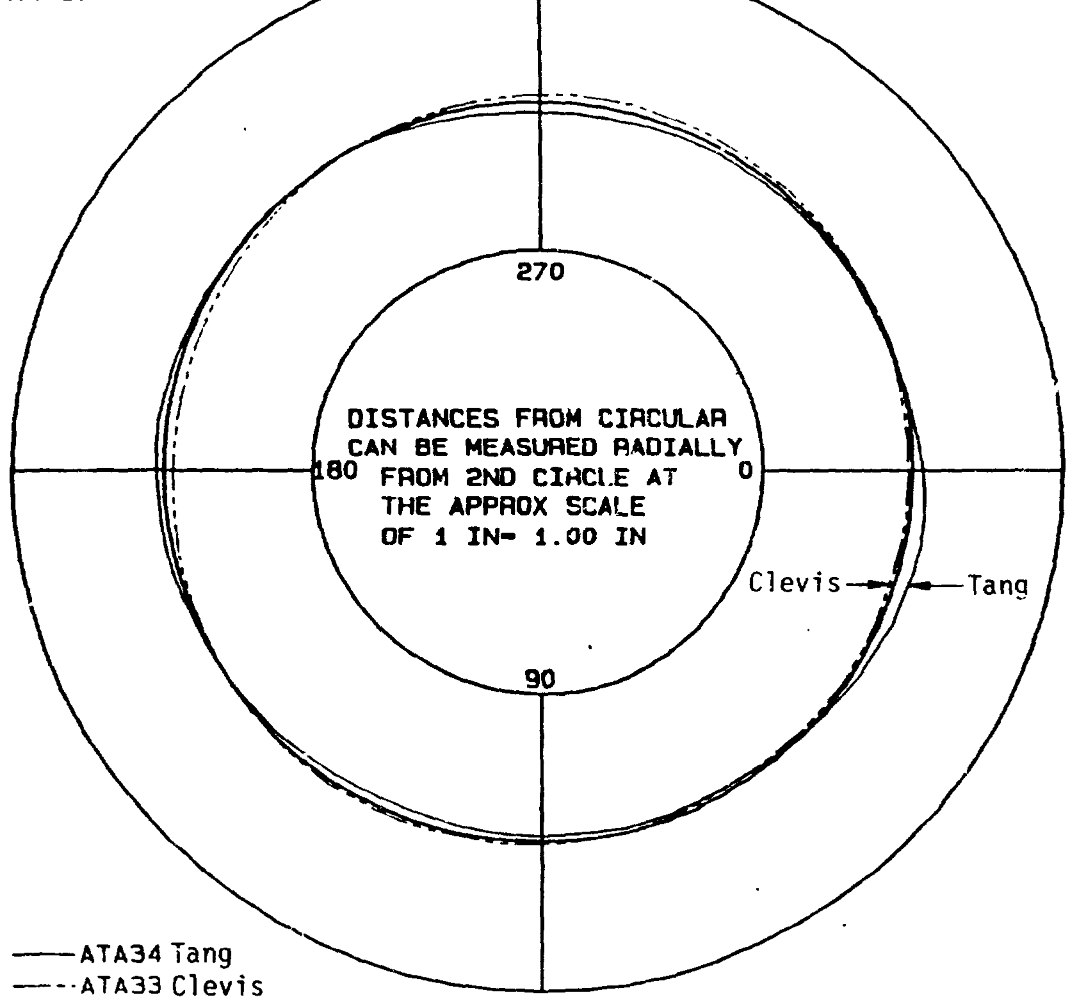

DIFF IN DELTAS FROM CIRC

ANGLE	DIFF	ANGLE	DIFF
0	0.101	320	-0.044
10	0.134	330	-0.028
20	0.119	340	-0.004
30	0.077	350	0.041
40	0.036		
50	0.015		
60	0.003		
70	-0.017		
80	-0.043		
90	-0.060		
100	-0.068		
110	-0.078		
120	-0.079		
130	-0.059		
140	-0.023		
150	0.014		
160	0.049		
170	0.084		
180	0.113		
190	0.119		
200	0.100		
210	0.074		
220	0.051		
230	0.028		
240	-0.007		
250	-0.050		
260	-0.094		
270	-0.124		
280	-0.128		
290	-0.108		
300	-0.083		
310	-0.062		

Figure 4-11. Tang and Clevis Shape Comparison Prior to Second Full (wet) Mate

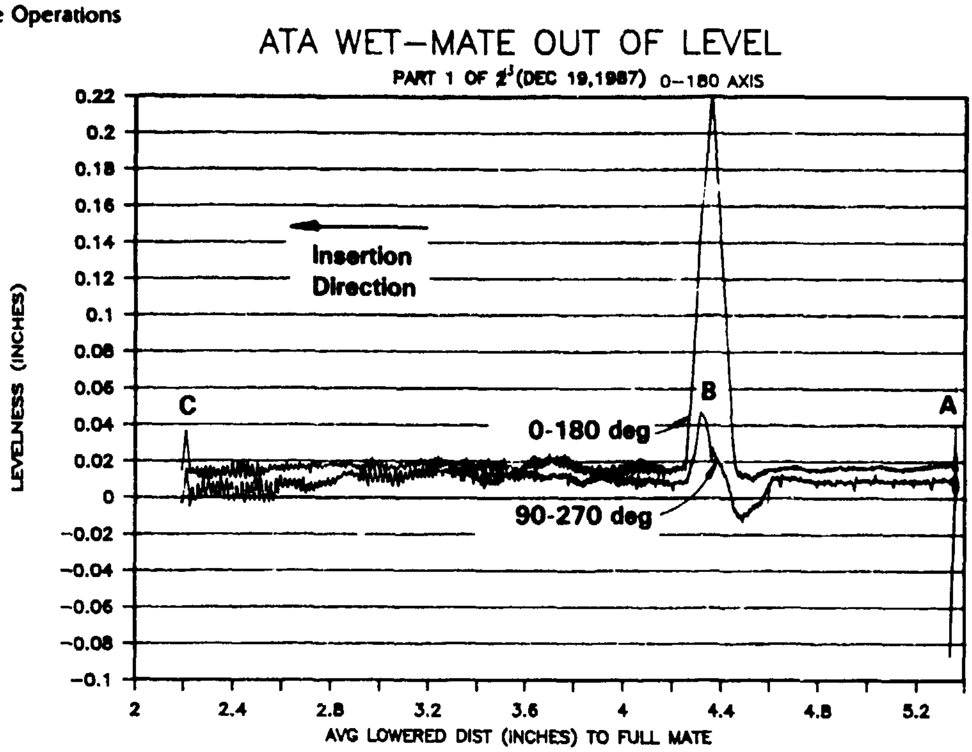

Figure 4-12. Second Full (wet) Mate Out-of-Level Versus Vertical Position

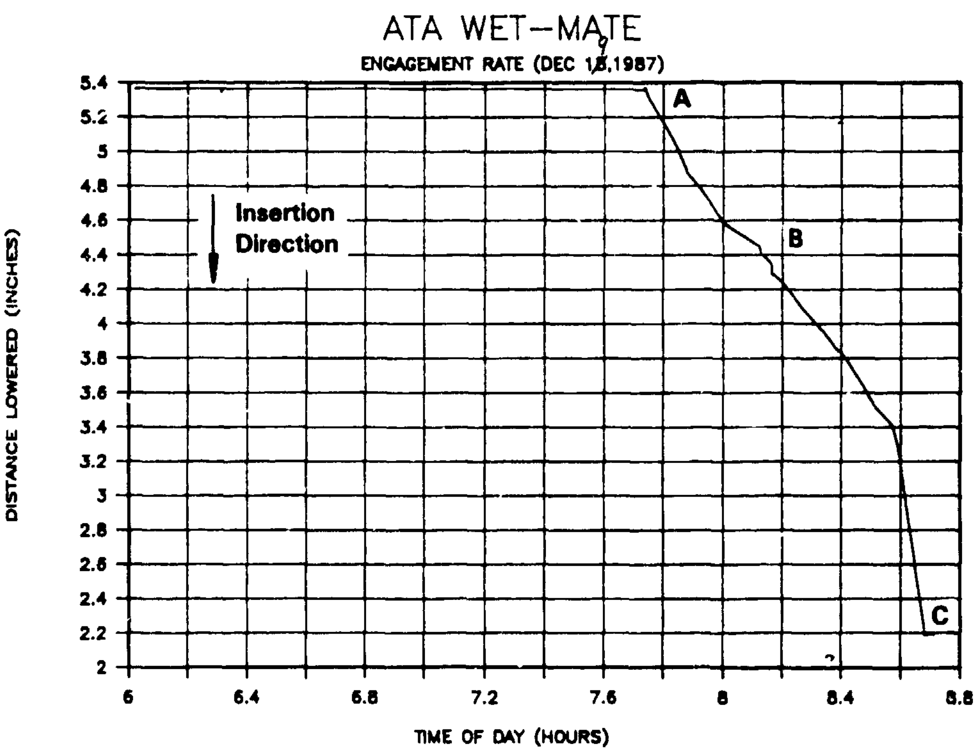

Figure 4-13. Second Full (wet) Mate Vertical Position Versus Time

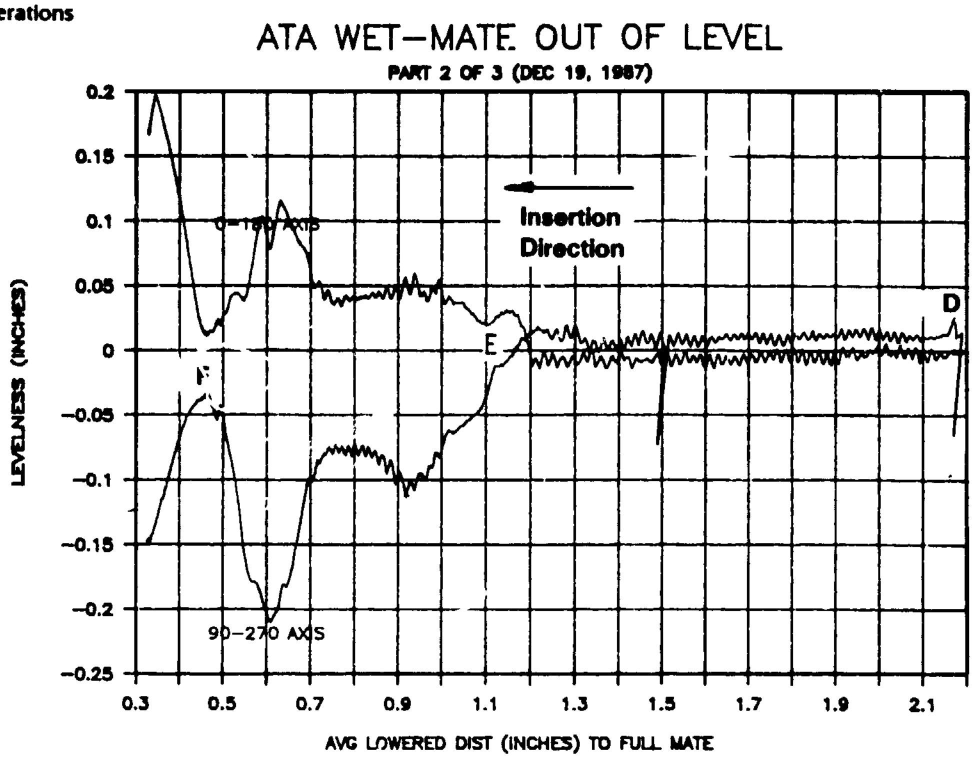

Figure 4-14. Second Full (Wet) Mate Out-of-Level Versus Vertical Position

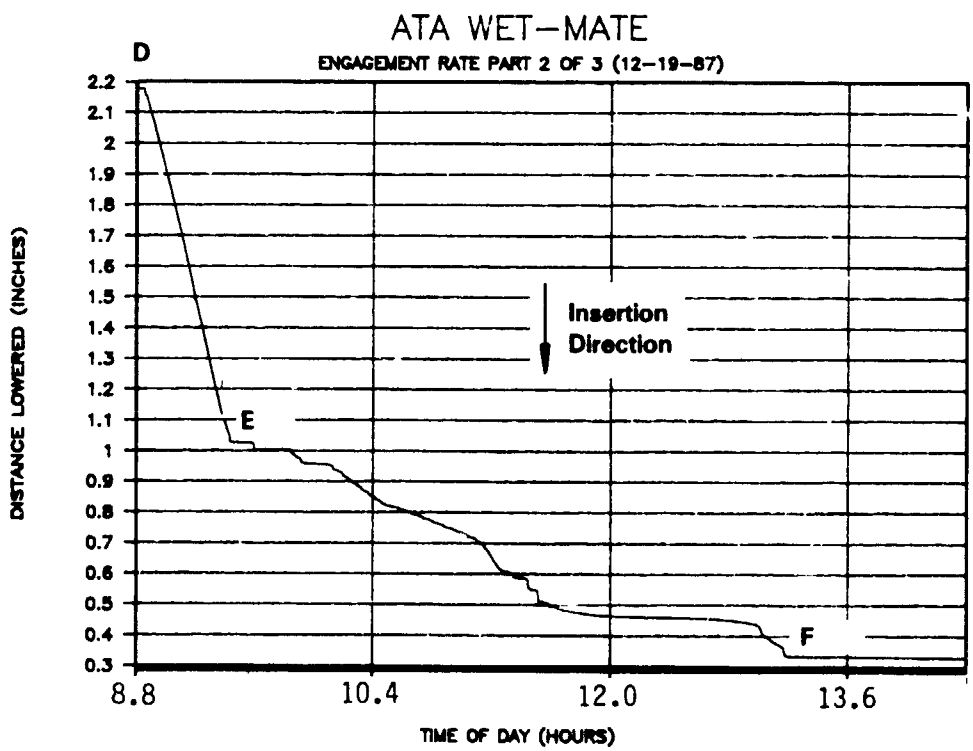

Figure 4-15. Second Full (wet) Mate Vertical Position Versus Time

due to the effects of static versus dynamic friction values, and engagement of the capture feature on the clevis. Insertion continued, and no stops were made until Point F was reached. At this time the FJAF was detorqued, the hydraset load increased, and the remaining 0.32 in. of insertion was done with the hydraset. Due to the alignment pin installation problems on the first full (dry) mate, is was decided to use the FJAF alignment pins during the wet mate. The FJAF remained on the joint after it was detorqued. Pin installation took approximately 45 min., and was completed about 1645 hr.

After removal of the 4-point lifting beam, a man was lowered down the motor bore to visually inspect the joint. The visual inspection results were very positive, as details are discussed in Section 7.3. The lifting beam was then reattached to the aft center segment, and the hydraset load was increased to match the segment weight to allow joint pin removal. Pin removal went smoothly, as no significant pin sticking was encountered.

Due to schedule constraints, some test plan requirements were deleted. This included the assembled joint measurements, leak check, and installation of the pin retaining band (also not possible because the FJAF was still in place).

4.7 WET MATE SEPARATION

Segment demate was initiated about 0600 hr, 21 Dec 1987. No VSF was used. There was concern that the segment might separate suddenly and bounce, damaging either or both segments. To reduce this possibility, the initial separation load was limited to the weight of the aft center segment and beam plus 15,000 lb. Segment out-of-parallelism plotted as a function of position can be seen in Figure 4-16. For the approximate 18 hr span between Points A and B, the segment moved very little. During this time, paper work was generated to enable redistribution of the load on the four beam points, to help the segment reshape and work it's way out. It was also decided that the total beam load could be increased 5,000 lb, allowing a calculated 20,000 lb separation load on the segment. (The entire segment and beam load had been estimated, so that load plus 20,000 lb

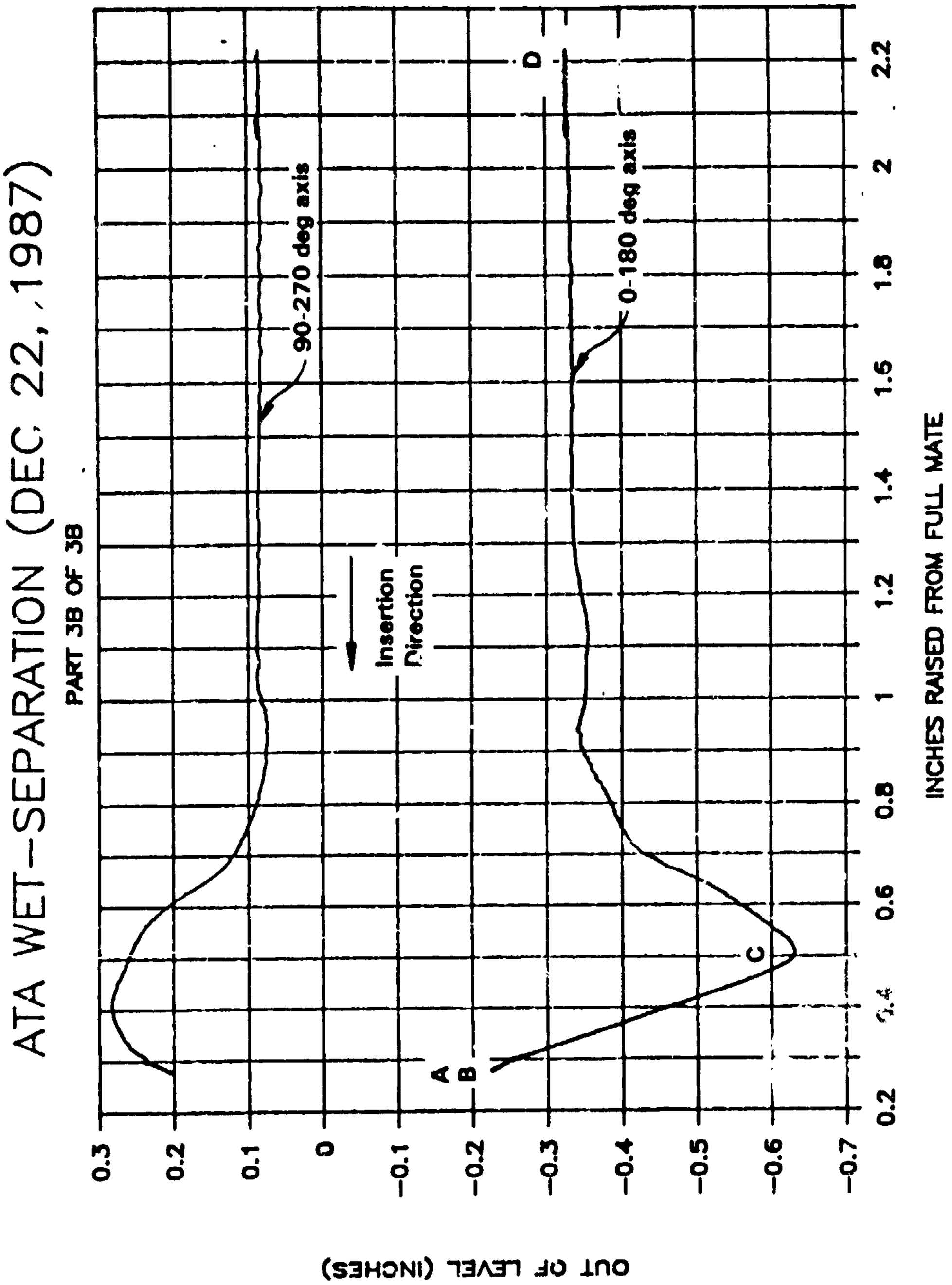

Figure 4-16. Wet Mate Separation Out-of-Levelness Versus Vertical Position

was allowable on the hydraset.) Significant segment separation finally started about 2330 hr, represented by Point B. At Point C the maximum out-of-parallel values during the separation were recorded. From Point C to Point D it can be seen the aft center segment returned to a more parallel position, and separation was smooth and continuous. No bounce effects were measured or noticed during joint separation.

After separation, post mate inspections were made of the joint. As with the first full (dry) mate, these results were very close to analysis predictions and are discussed in Sections 7.2 and 7.3.

The aft center segment was lifted to the transfer aisle, where is was readied for transfer to the RPSF. All further post-test inspections and profile measurements that were not deleted, are examined in their respective sections.

4.8 SUMMARY AND CONCLUSIONS

4.8.1 Segment Mate/Demate Operations

Prior to the first partial and first full mates the tang/clevis shapes (roundness) were relatively close (with a maximum variation of 0.055 in. radially). Prior to the second partial and second full mate, the tang/clevis shapes were relatively uneven (with a radial variation as much as 0.167 in.).

Segment separation of the first full mate was accomplished using the case VSF, while only the hydraset and 4-point lifting beam were used for the second full demate. Insufficient operator training using the VSF contributed to erractic joint separation while it was in use. Similar segment movement was seen, however, during the second full demate when only the 4-point lifting beam and hydraset were utilized. All contingency segment separations during flight stacking should use the case vertical separation fixture.

Evaluation of the insulation J-joint dry powder transfer medium was done following the first full demate. Adhesive performance evaluation was also done after the second full demate. Both inspections verified the insulation J-joint contact was as expected, with no damage to the insulation.

Post-separation inspection also confirmed no damage to the O-rings or soft goods occurred. The integrity of these seals was also confirmed by affirmative leak check results. Although some difficulty was encountered during various pin insertion and removal operations, no damage to the metal parts was observed.

The two partial mates, and two full-segment mates and demates adequately verified that assembly/disassembly of flight RSRM segments is possible in the vertical position, without damage to the insulation, metal parts, or seals.

4.8.2 Procedural Verification

Procedures for the RSRM segment handling and assembly/disassembly as specified in TWA-791 were validated during ATA. Both motor segments were received, processed, stacked, and demated using the existing facilities. In addition, the aft center segment was prepared for shipment and shipped again, while the aft segment was stored in the existing facilities.

Numerous deviations and problems were encountered with the operating tasks as specified in the OMI throughout the ATA test. These requirements were corrected, edited, or deleted. This procedural refining process was time consuming and often frustrating, yet was one of the overall key purposes of the ATA test. The specifics of these procedural changes are discussed in the applicable sections.

Evaluation of the segment operations during ATA resulted in the establishment of flight segment mating criteria. This consisted of:

a. Premate relative position (centering).
b. Premate segment relative concentricity (shape).
c. Insertion rate versus position.
d. Relative parallelism (levelness) versus position during joint mate.

The specifics of this criteria were discussed in Section 3.1.2.1.

It was also shown during ATA, the RSRM segment and joint design adequately considered operating, test, and maintenance personnel tasks. All three groups of personnel were able to perform their required operations (including complex and critical tasks) with adequate accessibility and safety. Crew training was provided. Areas where additional training is required were identified, and are also discussed in their applicable sections.

4.8.3 GSE Certification

The other key purpose of the ATA test was certification of the GSE to be used for flight segment inspection and stacking. Use of this GSE was mentioned briefly above, whereas detailed performance evaluation, and all recommended changes, are contained in Section 7.1.

5

INSTRUMENTATION

5.1 INTRODUCTION

A summary of the instrumentation initially installed on the ATA test article and the supporting GSE used during the test is listed below in Table 5-1. The instrumentation used to support ATA is documented in drawing number 7U75781, and the instrumentation listing from that drawing is included as Appendix 1, contained in Volume II of this report.

5.2 OBJECTIVES

The instrumentation used on the ATA test hardware and supporting GSE was used tc directly support the following test objectives from the D&V plan:

m. Gather actual data for analytical comparison.

k. Determine mate/demate loads on hardware and GSE (including bondline stress).

5.3 DISCUSSION

The majority of the instrumentation was installed on the ATA test segments 20-24 Nov 1987. As this test was performed at KSC, and involved numerous support organizations, instrumentation data was not reduced in one central location. Some data was reduced by Morton Thiokol personnel in the VAB, other was recorded on disk and taken to Hangar AF to be reduced and plotted, and still other was recorded by Grumman equipment, which required a significant time delay until final data reduction. There are still outstanding data plots at this writing. Extensive coordination with the interfacing was required on the gages, and some miscommunication did occur.

Table 5-1. ATA Instrumentation Summary

	FJAF (GSE)	Test Article	Total Gages
Temperature	3	3	6
Displacement	72	--	72
Strain	4	32	36
Stress	--	12	12
Total	79	47	126

Just prior to the first partial mate, it was found that the strain gages on the segment joint were ranged in the positive direction only (+2,000 min./in.), and would not correctly record both compressive and tensile loads. The signal conditioning units were reranged to ±1,000 min./in. to correct this problem, but as a result only incomplete gage performance was available during the partial mates.

Other difficulties were encountered with the instrumentation system during the ATA test. This included gage adhesive and label placement, coordination of paperwork, and gage cable installation. Solutions were found and all were adequately resolved.

A summary of all gages that failed to function properly, and the reason for the failures if known, is listed below in Table 5-2. A * symbol indicates these gages were approved and recognized by design and project engineering as pretest nonfunctional gages.

Table 5-2. Instrumentation Discrepancies

Gage Type/Measurement: Pressure Transducer/Bondline Stress

Inst No.	Discrepancy/Cause
S005-S0016* (12 gages)	*Gages migrated out of position during cure. All were removed due to shipping schedule impact.

Gage Type/Measurement: Thermocouple/Joint Temperature

Inst No.	Discrepancy/Cause
T001-T003* (3 gages)	*Gages were removed with bondline stress gages listed above.

Table 5-2. Instrumentation Discrepancies (Cont)

Gage Type/Measurement: Uniaxial Strain/Outer Clevis Leg Deflection

Inst No.	Discrepancy/Cause
S071-S074* (4 gages)	*Solder on tabs and gage coating interfered with FJAF. Trimming of tabs destroyed gages.

Gage Type/Measurement: Girth/Tang Radial Growth

Inst No.	Discrepancy/Cause
G009 (1 gage)	Broken by a mallet strike during installation of pin retainer clip at the 296-deg location.

Gage Type/Measurement: Girth/Clevis Radial Growth

Inst No.	Discrepancy/Cause
G003 (1 gage)	Metal/metal contact during VSF installation pinched gage at the 114-deg location.

Gage Type/Measurement: Biaxial Strain/Axial Tang

Inst No.	Discrepancy/Cause
S023 (1 gage)	Connection wire at 180-deg location broken by scraping type blow during VSF installation.

5.4 CONCLUSIONS

The instrumentation system used during the ATA test performed well, and adequately supported the gathering of data for analytical comparison. Mate/demate loads on the test hardware and GSE was determined, however, no bondline stress loads were measured due to gage removal prior to the test.

6

PHOTOGRAPHY

Still photographs were taken to document the various procedures and inspections throughout the ATA test. The complete collection of still photograph negatives are stored in Building M-9 at Morton Thiokol Space Operations. A photographic summary of the key events during the ATA test will be compiled from these negatives.

Video documentation of the ATA procedures was not allowed by Morton Thiokol personnel due to legal/contract issues. Those issues have been resolved, and Morton Thiokol personnel will be allowed video access for all future tests at Kennedy Space Center. Unfortunately, untrained personnel on the video equipment used during ATA resulted in out-of-focus and poorly lighted documentation.

Permanently mounted video cameras were also present to monitor the activities in the transfer aisle and high-bay level. These cameras were for general activity monitoring, and were not intended to be used for test process documentation and evaluation.

7
TEST RESULTS AND DISCUSSION

7.1 GSE CERTIFICATION/EVALUATION RESULTS

7.1.1 Introduction

The stacking of the RSRM segments on the MLP is one of the first steps in the building up of the entire space transportation system (STS) configuration. In order to ensure the segments can be mated without any damage to the hardware, seals, and insulation, additional GSE has been designed for use.

The GSE used during ATA can be separated into two general types: 1) use for segment inspection, and 2) use for segment assembly/disassembly. Prior to motor flight use, various inspections must be performed on the segment hardware and insulation to verify acceptance criteria. This includes determination of any case and insulation edge unbonds, and the J-joint insulation profile measurements. These inspections must be performed without disturbing or altering the insulation and propellant configuration, or NDE must be completed.

Before any of this GSE can be used to evaluate and/or aid in the stacking of actual flight segments, the equipment must be certified for use. Numerous GSE changes have been made as a consequence of the shuttle redesign, as well as an introduction of several new GSE articles. One of the primary purposes of the ATA test was to provide an opportunity for this GSE certification, as well as evaluate the equipment performance.

7.1.2 Objectives

The D&V Certification Plan Objectives, as they related to GSE certification during the ATA test, are listed below.

Certify use and operating procedures of the following GSE:

	Equipment	Model No.	Configuration
1.	Pin Retaining Wedge Kit	A77-0424	8U75930
2.	Alignment Pin Kit	H77-0438	8U52624
3.	Field Joint Assembly Fixture	H77-0442	7U75170
4.	Joint Measuring Fixture	A77-0448	8U75901
5.	Vertical Disassembly (separation) Fixture	H77-0451	7U52919
6.	Leak Check System	C77-0457	8U75902
7.	Auxiliary Shaping Tool	C77-0470	8U75900
8.	Mechanical Case-to-Insulation Bondline Inspection Kit	C77-0475	2U129799
9.	Comparator	A77-0477	8U75903
10.	Ultrasonic Case-to-Insulation Bondline Inspection Kit	C77-0479	2U129431
11.	Joint Insulation Profile Measuring Kit	C77-0481	2U129541
12.	J-seal Terminus Inspection System	C77-0485	2U129541
13.	J-seal Bondline Inspection Tool	C77-0484	8U76225
14.	Assembly Instrumentation		
	Temposonics	C77-0487	8U75919
	4-point Beam	H77-U0384	
15.	Slump Measuring Tool	C77-0488	8U75923

7.1.3 Results and Discussion

a. Pin Retaining Wedge Kit (A77-0424) Not Certified. Pins were inserted in the joints during both full mates of the ATA test. During the first full (dry) mate, pin retainers were also installed (pin retainers were not used during the second full mate due to the FJAF being left on the joint). Ease of pin retainer installation, however, eliminated the need for the use of the pin retainer wedge kit, hence no tool certification was done during ATA, and no evaluation of the kit is included in this report.

b. Alignment Pin Kit (H77-0438) Certified. The purpose of the 8U52624 pin alignment kit is to index and align field joint pinholes during mating, aiding pin installation. Three alignment pins are used, located at 0, 118, and 240 deg. During the first full mate separation, one alignment pin could not be reinserted in the pinhole at the 0-deg location. Measurements of the hole and pin revealed a maximum material condition, or the pin was at the large end of tolerance and the hole was at the small end. After evaluation, a .0005-in. reduction on the pin diameter was recommended. The applicable drawings are being updated to reflect this dimensional change. With the above mentioned change, the alignment pin kit is qualified for use on flight segments.

c. Field Joint Assembly Fixture (FJAF) (H77-0442) Certified. Extensive testing and evaluation of the 7U75170 FJAF was done during the ATA test. Detailed analysis evaluation of the FJAF is contained in TWR-18067, as only a generalized evaluation is given in this report. A schematic diagram of the FJAF GSE tool can be seen in Figure 7-1. The FJAF is a fixture designed to conform the tang and clevis to the same shape, minimizing possible damage to the O-rings during the mating operation. As can be seen in Figure 7-1, the FJAF is composed of four sections, each weighing about 85 lb. Handles are attached at each section end for operator maneuvering. After the four FJAF sections are placed on the outer clevis leg, bolts and pins are used to secure the pieces together. The final ID of the FJAF is smaller than the outer clevis leg OD, so the clevis leg is compressed during this operation. This circumferential squeezing, or bearhugging, compensates for the ratcheting, or yielding effects of the clevis that occur during the segment hydroproof cycles. Shims of a precalculated thickness are placed between each section joint prior to the torquing down of the assembly bolts, to obtain the correct final FJAF diameter and amount of bearhugging for each particular segment clevis.

The FJAF is designed not only to conform the clevis to the correct shape, but also the tang during segment mate. An illustration of the tang and clevis with the FJAF just prior to mating can be seen in Figure 7-2. As the tang is inserted inside the FJAF guide block bore,

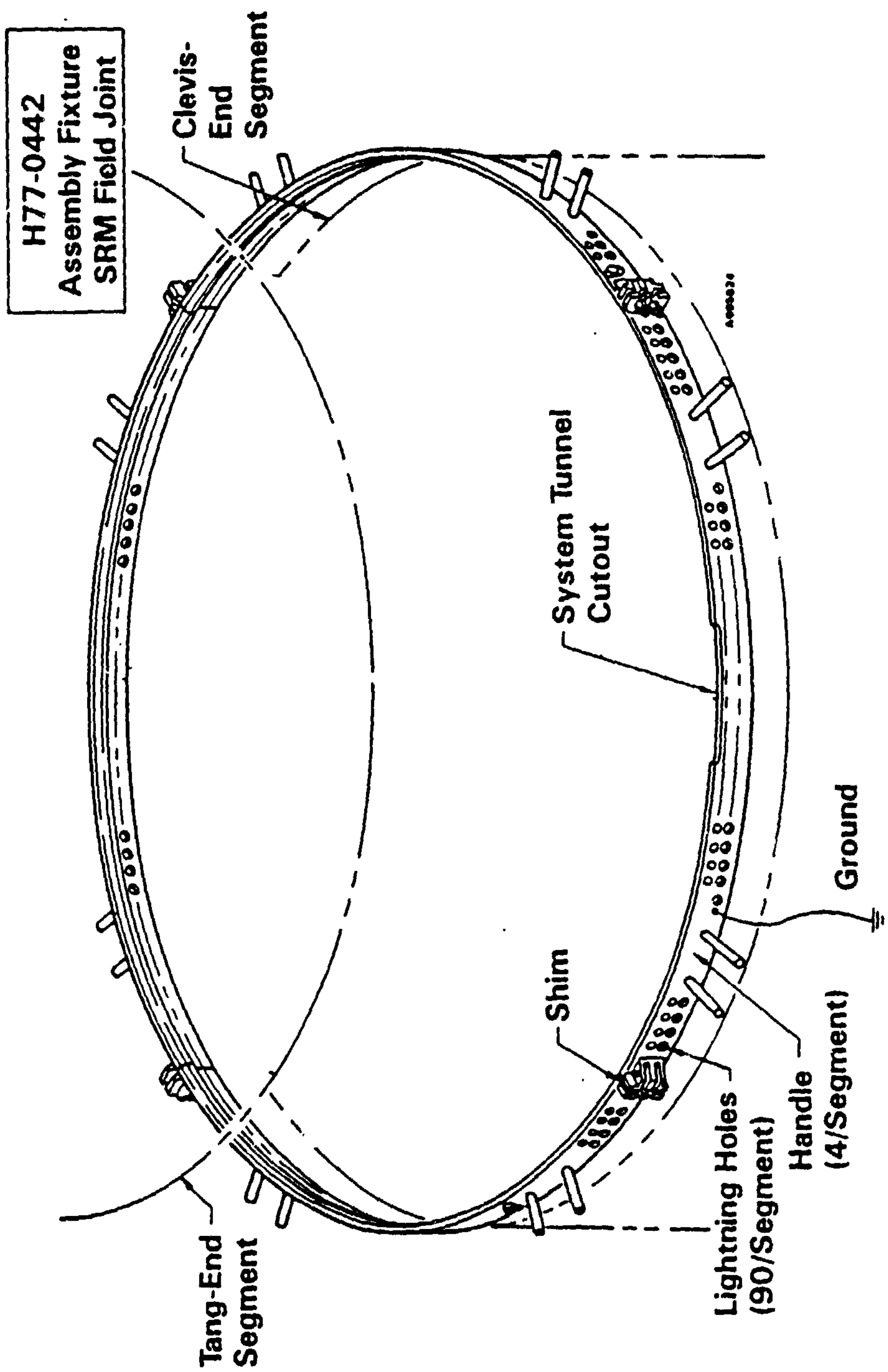

Figure 7-1. Field Joint Assembly Fixture (FJAF)

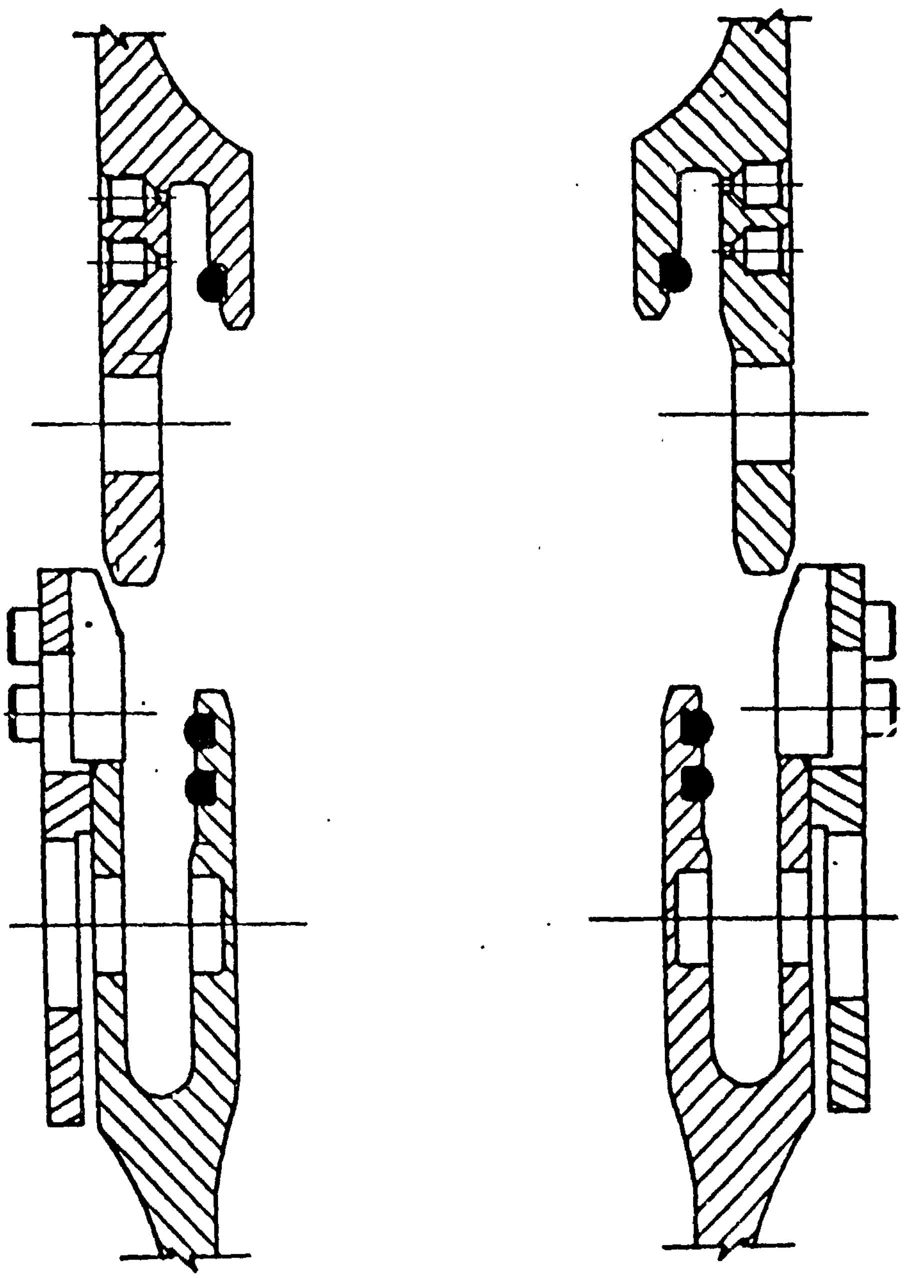

Figure 7-2. Tang Just Prior to FJAF Guide Block Engagement

the tang is circumferentially squeezed. This inward deflection not only compensates for the ratcheting effects on the tang (that occurred during hydroproof), but ensures proper tang and clevis positioning so as to avoid O-ring damage during mating. During segment mating, once the capture feature has engaged the inner clevis leg, the FJAF can be de-torqued and segment insertion can be completed.

As previously discussed in Section 4, the segment shapes were varied during the partial and full mates to fully evaluate the FJAF performance during worst-case, out-of-round conditions. During the second partial mate separation between the FJAF contact band and outer clevis leg was observed as well as separation between that tang and FJAF guide blocks. The degree location and separation amount is listed in Table 7-1. FJAF contact band separation was also noticed during the second full (wet) mate, and the measurements are contained in Table 7-2. Both mates were done when the tang and clevis shapes varied by more than 0.25 in. along the 0- to 180-deg axis, so the area of separation in both cases was in the area of maximum interference. After evaluation of the FJAF performance during the above mentioned mates, it was determined sufficient tang and clevis shaping will be done providing the FJAF/case separation gap is less than 0.005 inch. During flight stacking, if the FJAF contact band separates from the outer clevis leg by more than this amount, PR disposition will be required before the mating operation can be continued.

Table 7-1. Measured Gap Between the FJAF Segments

Location (deg)	Gap (in.)	Location (deg)	Gap (in.)
0	closed		0.013
2	0.008	254	0.015
4	0.013	263	0.015
6	0.015	267	0.015
8	0.015	271	0.015
10	0.014	215	0.015
12	0.014	279	0.015
14	0.012	283	0.015
16	0.008	283	0.015
18	0.006		
20	closed		

Table 7-2. Gap Between FJAF and Outer Clevis Leg During Second Full Mate

Location (deg)	Gap (in.)
2	closed
4	0.007
6	0.007
8	0.007
10	0.007
12	0.007
14	0.004
16	closed

An evaluation of the results showed the FJAF was extremely sensitive to any bolt torquing. Partial mate No. 1 showed an average diametrical squeeze of 0.033 in. after bearhugging, while partial mate No. 2 showed an average 0.037 in. of bearhugging squeeze for the same shim configuration. This difference was attributed to differences in the FJAF joint rattlespace during the two partial mates. During partial mate No. 1, there was an approximate 0.060-in. rattlespace, whereas on partial mate No. 2 a 0.068-in. rattlespace was left in the FJAF joints prior to bearhugging. It was determined a rattlespace of 0.070 ±0.005 in. should be in the four FJAF joint locations prior to the bearhugging sequence.

The ATA test did demonstrate the segment ratcheting effects were eliminated by the FJAF, and much information was gathered. The joint contact band shim packs were determined for the STS-26 flight stacking. It is recommended, however, that additional evaluation be done concerning the bearhugging and shim pack calculations. To achieve this, a premate bearhug evaluation will be performed on each joint during the STS-26 stacking. If it is found that initial shim calculations are in error, the shim thicknesses will be changed. Similar bearhugging measurements will also be done the first time the new 8U75686 FJAF is used for flight segment stacking (probably STS-27).

Also determined during ATA were the recommended changes to be made on the 8U75686 FJAF, which will replace the 7U75170 used during ATA.

These changes include:

1. The FJAF back thickness dimensions will be increased. The minimum dimension has been changed from 0.377 to 0.407 in., and the maximum has been changed from 0.440 to 0.460 inch.

2. The joint shim tolerance will be changed from ±0.010 to ±0.001 inch.

3. The pin clearance hole size will be changed from 1.50 to 1.25 inch.

4. The above changes will increase each FJAF section weight from about 86 lb. to approximately 100 lb. The current handle locations will be changed, and a third set of handles will be added to allow a third person help with the section handling.

During the ATA test, peeling of the FJAF Teflon® coating was a problem. This was due to overspraying or double coating of the Teflon® coating during application. Light sanding of the FJAF will eliminate this problem. In addition, the joint welds on each quarter section will be nondestructive tested, and the weld areas where the Teflon® has been stripped will be coated with rubberized paint for corrosion protection. (Removal of the rubberized paint will allow easy weld access for future nondestructive testing.) Particular attention will be paid to the inside face of the guide blocks and contact band. During nonuse, these areas will be covered with HD-2 grease to avoid corrosion.

During the ATA test, the 7U75170 FJAF was adequately certified for use on flight segment stacking. The 8U75686 tool will be certified by similarity prior to use on flight segments.

d. <u>Joint Measuring Fixture (sine bar) (A77-0448) Certified</u>. The purpose of the joint measuring fixture, or sine bar, is to obtain the shape of the clevis and tang. This allows the tang shaping to begin hours before the mate when the upper segment is suspended in the transfer aisle. A schematic diagram of the 8U75901 sine bar used on the ATA test, and the support equipment, can be seen in Figure 7-3. Note that in addition to

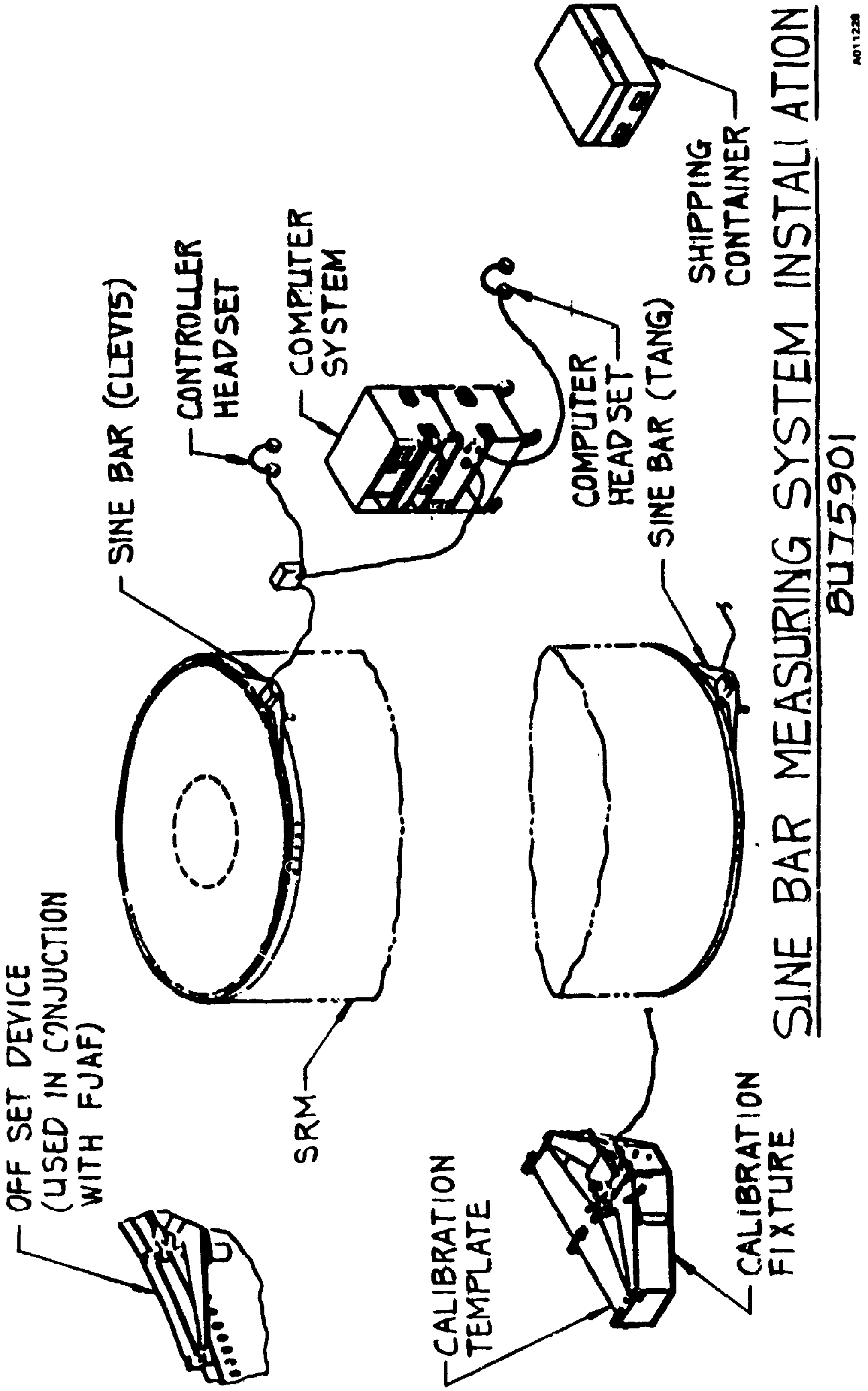

Figure 7-3. Joint Measuring Fixture (sine bar)

the actual fixture, the sine bar configuration includes a calibration template to verify the sine bar's LVDT sensor is functional, i.e., the electronic gain and physical offset of the transducer are correctly set prior to use. The tool's one LVDT measures the arc height of a 36-in. chord. Thirty-six of these readings (one every 10 deg) make up a set of data which can be used to determine the shape of the tang or clevis surface. Guide fingers on the fixture insure proper positioning is achieved during measurements. The LVDT data is acquired and processed by a portable computer system programmed specifically for sine bar use. After measurements are complete, an X-Y plotter can print out a plot comparing the tang or clevis shape to a perfect circle. This makes it easy to visualize the segment shape. The quantitative measurement values are also printed on the plot, making detailed shape or interference calculations possible. Tang and clevis measurements can also be printed on a single plot, making shape comparison very easy. (Comparisons of the tang and clevis shapes prior to mating were presented in Section 4.)

During the ATA test, 34 sine bar measurements were performed. These are in sequential order in Appendix 2, found in Volume II of this report. The equipment performed well for all mating and shaping analysis, and proved to be consistent with micrometer data. It should be noted that the sine bar does not determine absolute size, but rather relative shape. Absolute size and shape was determined on ATA segments by the use of pi tapes and the sine bar.

Although the sine bar performance during ATA was very good, various improvements have been recommended and are being made. One of the four guide fingers was modified to eliminate an interference problem with a connector. Computer software modifications are being made to include flags to alert the operator if an LVDT reading goes out of range. This audible alarm also includes a message on the screen which indicates possible solutions, which are:

1. First LVDT reading out-of-range, message indicates that rezeroing of the LVDT may be desirable.

2. Any out-of-range reading in the opposite direction (from the first reading) indicates that either this segment is greater than 9 in. out-of-round, or there is some anomaly in the sine bar system.

3. The second LVDT reading out of range in the same direction (plus or minus) as the first reading indicates that LVDT rezeroing is desirable.

4. The third out-of-round range reading in the same direction (of the previous two) indicates that LVDT rezeroing should be performed.

Because the equipment acquisition and processing of data is computer controlled, additional operator training along these lines was recommended and is being implemented. This includes general familiarity with personal computers, and specifics relating to the sine bar software. A menu-driven standard plot title format, which contains the important information necessary for future reference and data evaluation, is also being included in the software changes. A copy of all future plots and/or printouts made are to be included in the OMI during segment stacking.

Sine bar use during the ATA test adequately demonstrated the tool is qualified for use during flight segment stacking.

e. Vertical Disassembly Fixture (H77-0451) Certified. The 7U529 VSF was used to aid in segment separation during the first full (dry) . .e. Certification of this tool was required due to contingency separation during flight stacking. A schematic diagram of the tool can be seen in Figure 7-4. The tool consists of two bands that are made up and attached to each segment. Eight hydraulic rams and load spacers are connected between bands, as shown in the Figure 7-4. Hydraulic lines from the control unit provide pressurized fluid to actuate each ram. The control unit rests on a movable cart.

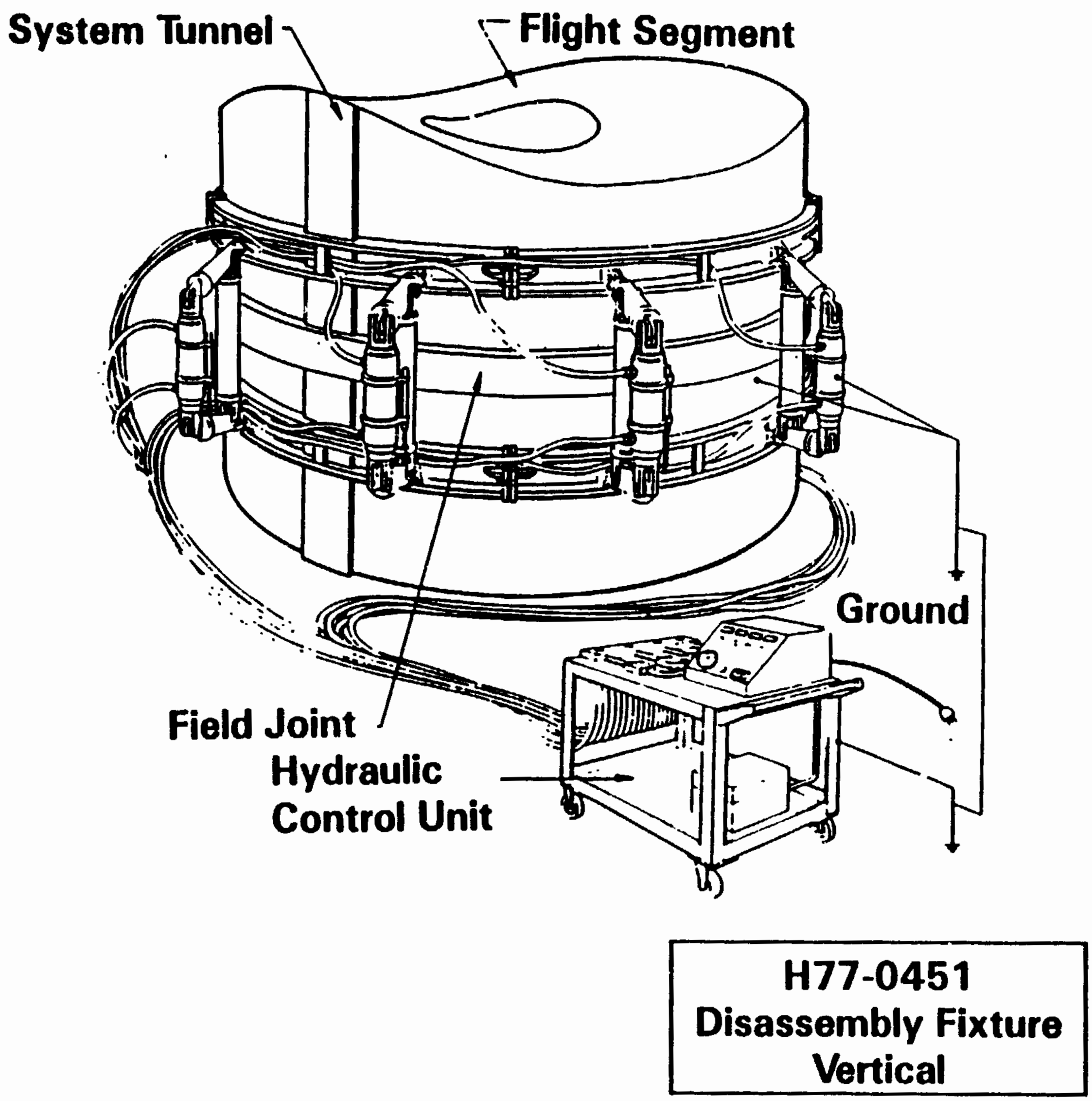

Figure 7-4. Vertical Separation Fixture (VSF)

As explained previously in Section 4, segment separation while using the VSF was erratic and uneven. One side of the segment would rise, and while the other side was being raised the first side would settle back down slightly. The VSF was not used for the second full (wet) mate separation, as the FJAF alignment pins were used. This required the FJAF to be left on the joint (although it was detorqued), which prevented VSF installation.

Some of the difficulties encountered during tool use were due to lack of operator familiarity with the equipment, however, recommended changes are being made to the 8U fixture prior to contingency use during flight stacking. This includes:

1. Reduction of the size of the hydraulic cart. The previous size made it very difficult to move the cart through the doorways and around the levels required.
2. Lengthening of the hydraulic hoses by three feet (at least). The hydraulic cart will be placed on the levels to determine the actual hose lengths required for use. This information will be used to update the appropriate drawings.
3. The sensitivity of the main control valve will be reduced. This will lower the chance of inadvertent operator error due to turning the valve too far.
4. The LVDTs will be eliminated that are currently on the cylinders. LVDT use was previously for segment movement monitoring, however, the temposonics gages are now used.
5. The directional adjustable control valves will be replaced with a fixed orifice.
6. Evaluation of the main pressure gage readout scale is being done. It is recommended that the gage be replaced with one that is scaled for easy readability in the sensitive operating range.

Addition of the above mentioned changes will qualify the tool for contingency demate during flight segment stacking.

f. Leak Test System (C77-0457) Certified. Leak checks are required on every field joint during SRB stacking. This process not only ensures the primary and secondary field joint seals are functional, but verifies the primary and secondary O-rings are seated in the proper position prior to ignition pressure application. During the ATA test, a leak check was performed on the test joint during the first full (dry) mate. A leak check on the second full mate, was deleted

The 8U75902 leak test system was used on ATA, and the same system is planned for use on the Qualification Motors (QMs) and flight stacking. An illustration of the leak check equipment and test joint schematic can be seen in Figure 7-5. The two principle components consist of: 1) the data acquisition panel, and 2) GN_2 leak check panel. A facility or K-bottle supply is used to provide the GN_2 for joint leak evaluation. The test joint and system components were connected with hard lines, or nonflexible tubing.

Due to this test (ATA) being the first use of the upgraded system (a prototype was used on the DM-8, DM-9, and JES-3B tests), some problems were naturally encountered with the hardware. The primary problem was valve sticking. The valves used on the equipment were custom made, and it was found that the operators would tighten them too much, causing the valve needle to bind. During the test, this was temporarily resolved by removing the handle and gently striking the valve with a soft hammer. This problem will be resolved by incorporation of a torque limiting ratchet type handle, that will free spin once the preset torque limit is reached. Also the surface finish of the port components were changed from 32 to 20, to reduce the possibility of sticking. Other improvements to the hardware under consideration include incorporation of convoluted flex lines to replace the currently used hard tubing (it was found common flex lines leak). Tests are currently being performed to ensure the convoluted flex line volumes do not change with pressurization, thus adversely effecting the leak rate calculations.

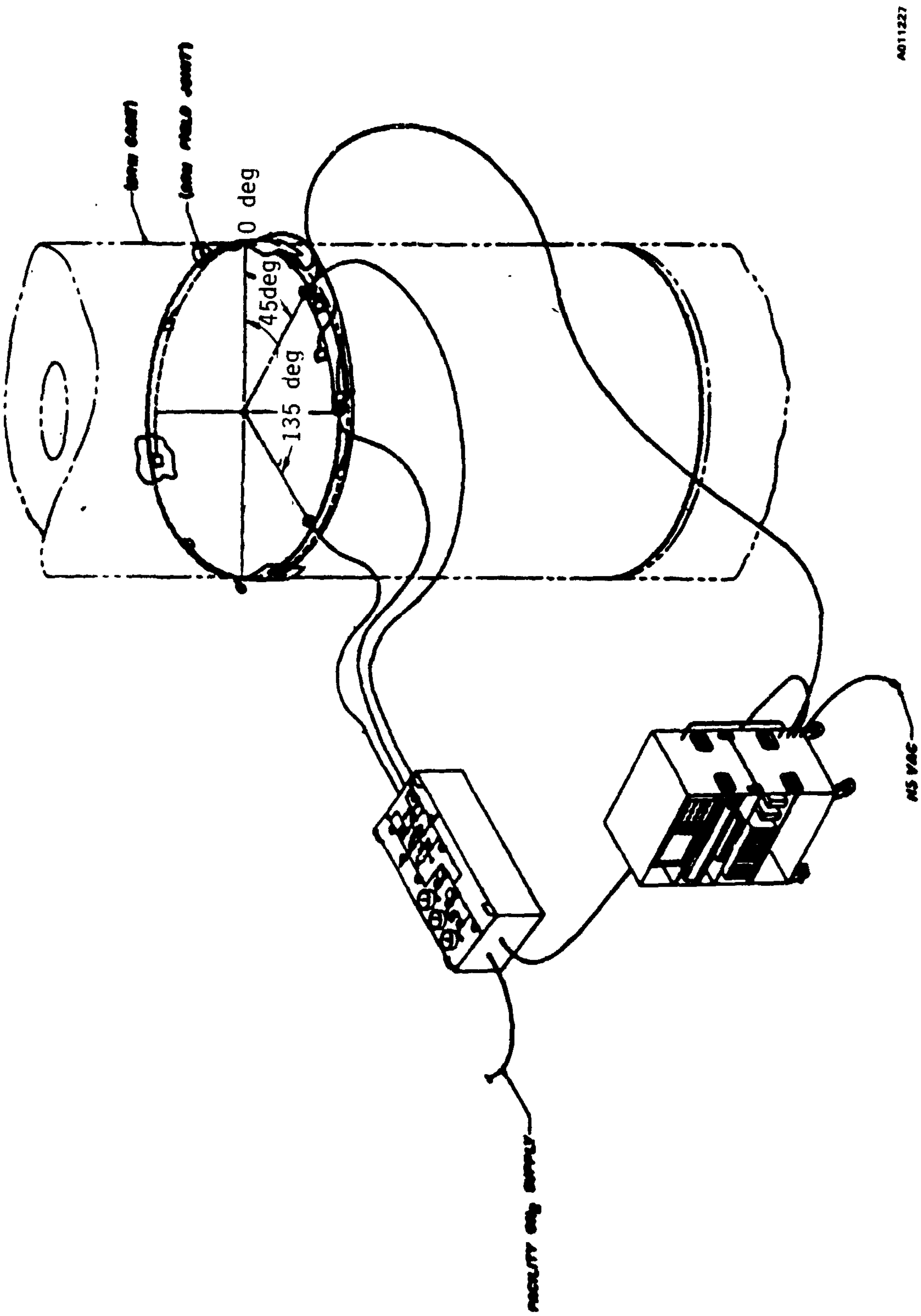

Figure 7-5. Joint Leak Check System

Some program software discrepancies were also determined. The software program contains over 8,800 lines of code, and no time had been available to completely debug the program prior to use up on the test level. There were no problems with data acquisition and recording (so no measurements repeats were necessary), but discrepancies were found in the data reduction. Some real number syntax errors were also found. These were subsequently corrected and the joint leak results were determined. Other software improvements being made deal with operator interaction. Before, sequence initiation and termination were driven by the computer clock. If the operators were not able to perform the right function in a specified time (such as opening or closing a valve), sequence continuation would still occur. Changes have been made so the operator starts and ends the various test sequences, allowing verification of proper equipment functionality prior to measurement. Updates are also being made to display measured values as they are acquired, allowing hand calculations during the procedure if desired. When the leak check process is complete, a final summary is printed for review.

The final leak check results from the ATA test are discussed in Section 7.2. Both high and low pressure tests were performed on the primary/secondary O-ring cavity and primary/capture feature O-ring cavity. All four leak rates passed the limit criteria by ample margin. A very slight negative leak rate was measured during the low pressure primary/secondary volume test. This negative value is consistent with other leak tests in the past, and is due to gas exudation from the O-rings. This test sequence occurs at 30 psi, and follows the 1,000 psi test. During the high pressure test, GN_2 is absorbed into the O-rings, and exudes when the pressure is reduced. In this case the gas release rate from the O-ring exceeded the cavity leak rate, hence the negative value. This undesirable condition has been investigated and eliminated with a change in the pressurization sequencing.

Recommended improvements to the leak check procedure include leak check solution application training. Upon joint disassembly, rust was found at the 45-deg leak check port. This was attributed to excess leak check solution being dribbled down the segment into the joint. No rust was found at the 135-deg point because (possibly) a rag was placed below the port (a rag can easily be placed below that port, whereas at the 45-deg location it cannot). Updates to the planning are being made to alleviate this problem in the future.

Use of the leak check equipment, and evaluation of the procedures certify the leak check equipment for use during flight motor segment stacking operations.

g. Auxiliary Shaping Tool (H77-0470) Not Certified. The auxiliary shaping tool is a contingency device to aid in segment mating. If satisfactory segment tang shaping cannot be obtained by manipulating the load between the two-beam axis, tool use is required. The tool was not used during the ATA test.

h. Mechanical Case-to-Insulation Bondline Inspection Kit (Air Load Test) (C77-0475) Certified.

1. Clevis Inspection. On 11 Dec 1987 the air load test was performed on the ATA aft center clevis. An evaluation of the unbond inspection results are discussed in Section 7.3, as this section deals primarily with the tool use. An illustration of the 2U129799 air load tool as used on the clevis can be seen in Figure 7.6. An 80 ±5 psi air source is used for the air jet supply, while the guide block ensures correct jet placement. The video probe (shown in the guide block) is connected by cable to the recording and monitoring equipment. The video and air filter systems were placed on the platform above the clevis (B level) during tool use. The air filtering and drying system was connected to the facility air on D roof. Prior to actual inspection, a mellon, (oil and particulate) sample of the air was taken in order to verify the hazard analysis requirement, (MSFC Proc. 404 Spec).

The actual inspection operation took under 5 hr. Due to procedural training and equipment familiarity that has since occurred, future inspection timeline estimates are 3 to 4 hr per joint.

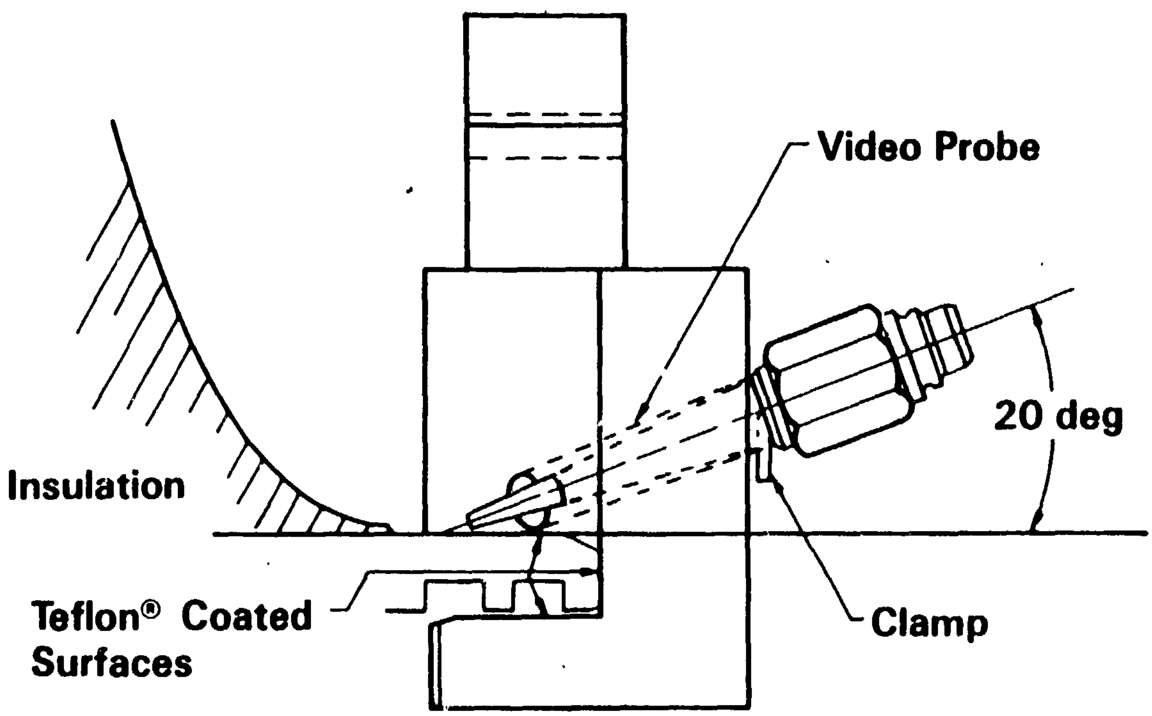

Figure 7-6. Mechanical Case-to-Insulation Bondline Inspection (air load on clevis end)

The operation procedure was altered slightly from that as originally intended. Instead of pushing the tool for a clockwise inspection, the tool operated more smoothly by pulling (counter clockwise). The speed of inspection varied from 100 sec/10 deg to 60 sec/10 deg. The video field of view was 0.718 inches. Unbonds were plainly detectable and visible. Inspection results indicate the air jet does not enlarge unbonds. If the air does cause a previously undetected unbond to open up, it is felt that good case bond was not present initially.

One difficulty encountered during tool use was communication problems between the tool and key board operators, due to excessive air flow noise. This problem could be eliminated through a headset intercom system between the tool an keyboard operators. Also, the weight of the video and air lines caused a torquing of the plastic air probe, making precise placement difficult. Support added to these lines would eliminate this problem. Grease left on the inner clevis leg was blown into the unbond, which creates significant grease removal and unbond repair problems. It is recommended that all inner insulation surfaces be thoroughly cleaned of all grease prior to tool use.

2. Tang Inspection. The air load bondline inspection tool was not used to inspect any segment capture feature (tang) during the ATA test. The planned procedure for capture feature bondline inspection specifies the tool speed will be no greater than 5 sec/deg, and the tool operator will call out a signal every 2 deg. This will then be annotated on both the video screen and data sheet. Unbond measurements, if any, will then be taken and recorded on the data sheet.

Air load test equipment use during the ATA test sufficiently demonstrated tool performance for use on flight segments. Even though no inspections were performed on the tang during ATA, equipment use on other segments (DM-9) qualify the tool for use on flight segments.

i. Comparator (A77-0477) Not Certified. The comparator was not used during the ATA test, thus, an evaluation of the tool operation is not included in this report.

j. Ultrasonic Case-to-Insulation Bondline Inspection Kit (C77-0479) Certified. Ultrasonic inspections are for detection of unbonds between the case and insulation in the critical segment joint area. During ATA, ultrasonic tests were conducted on the aft center segment tang and the aft segment clevis joint areas. An illustration of the 2U129431 inspection probe as used on the tang capture feature inner wall is in Figure 7-7.

1. Tang Inspection. The inspection of the aft center segment tang was conducted on 18-19 Nov 1987. Duration of the test was approximately 9 hr. This inspection was performed without the advantage of a calibration standard; an actual piece of a segment with a known good bond and a known bad bond was used to adjust the inspection system. A calibration standard will be used on all future inspections, but at the time of the ATA test none were available. The test revealed consistent ultrasonic response throughout the circumference of the segment, indicating a good bond in the entire tested area (assuming the tool was correctly calibrated).

2. Clevis Inspection. Inspection of the aft segment clevis was conducted on 20-21 Nov 1987 and lasted approximately 20 hr. Figure 7-8 illustrates how the probe is placed during use. A calibration standard was available and used for this test. Once again the test revealed a consistent ultrasonic response, indicating no unbonds in this area. Local pinhole scan results also indicated no debonds.

Prior to use on flight segments, the plastic spring covers will be replaced. The 20[illegible] and pinhole scanners will be tethered to protect them from being dropped. Use of a smaller transducer on the capture feature will also be introduced.

For future tests it is recommended a second magnetic track be procured. This will reduce test time by allowing the scanner to

MORTON THIOKOL, INC.
Space Operations

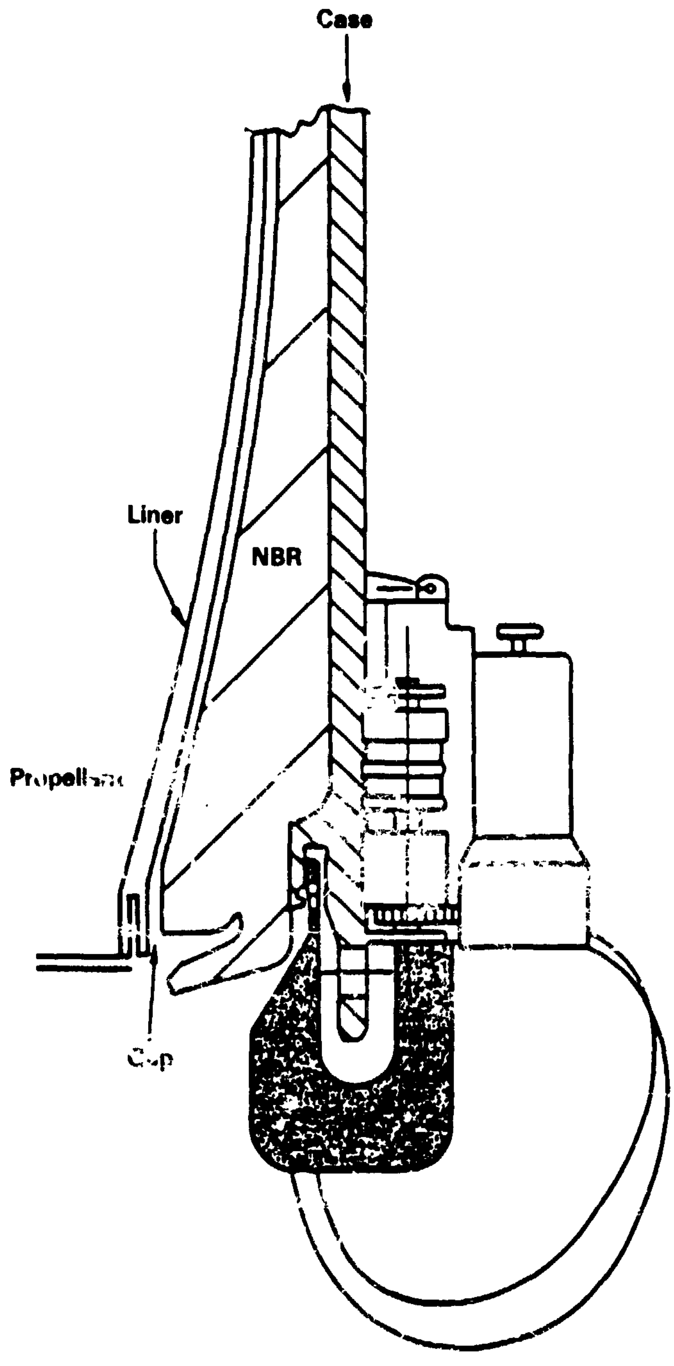

Figure 7-7. Ultrasonic Inspection--Inner Wall of Capture Feature

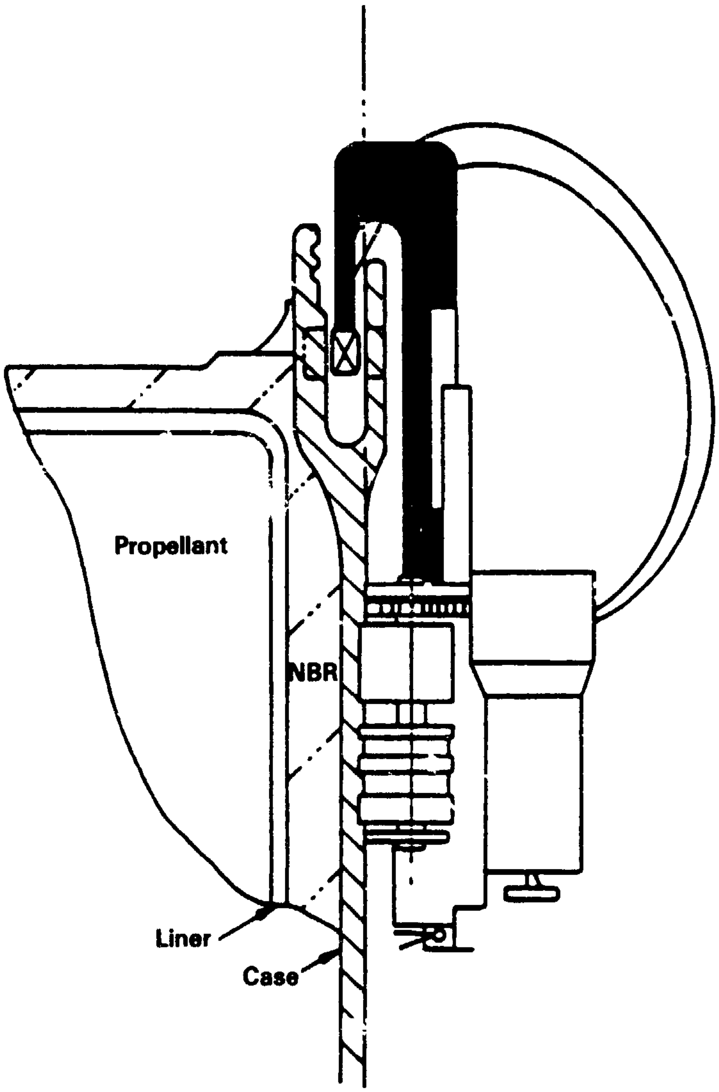

Figure 7-8. Ultrasonic Inspection--Inner Clevis Wall

88086-15C

roll from one test track to the next. During the ATA test, only one track was available, which required removal of the scanner from the track, track repositioning, and reinstallation of the scanner. The test system is delicate and should not be moved more than absolutely necessary. It is recommended a permanent location be selected where the equipment can be kept, and then be moved only when necessary.

Tang and clevis inspections performed during ATA (and DM-9) satisfactory qualify the tool for use on flight stacking.

k. Joint Insulation Profile Measuring Kit (J-seal Profile) (C77-0481) Certified. J-seal profile measurements are made on both the joint tang and clevis to determine the interference profile prior to joint mate. The measurement results are discussed in Section 7.3, as only the tool use is discussed here.

A schematic diagram of the 2U129541 profile inspection tool as used on the clevis can be seen in Figure 7-9. The clevis profile measurement took over 17 hr with the use of two tools (180 pinhole locations). After equipment familiarization and operator training, the expected inspection time is 8 min per/pinhole, or 12 hr with two tools. The current tool design is simple, but tool use could be made easier and quicker with the advent of a second depth micrometer.

The clevis measurements are easily taken (working over the segment), whereas tang measurements require working under the segment. The tool as set used on the tang is illustrated in Figure 7-10. The operators are required to always be looking up, and continually have a hand on the depth rod so as to not to let it fall to the ground. The tang measurements took more than 19 hr with the use of two tools (180 pinhole locations). Clevis and tang measurement times could possibly be decreased by using a third tool, but then equipment and personnel interference may occur, as well as a problem with the number of persons available or qualified to operate the tools.

Future design changes and improvements include another profile tool designed to attach to each end of the propellant slump tool. This new

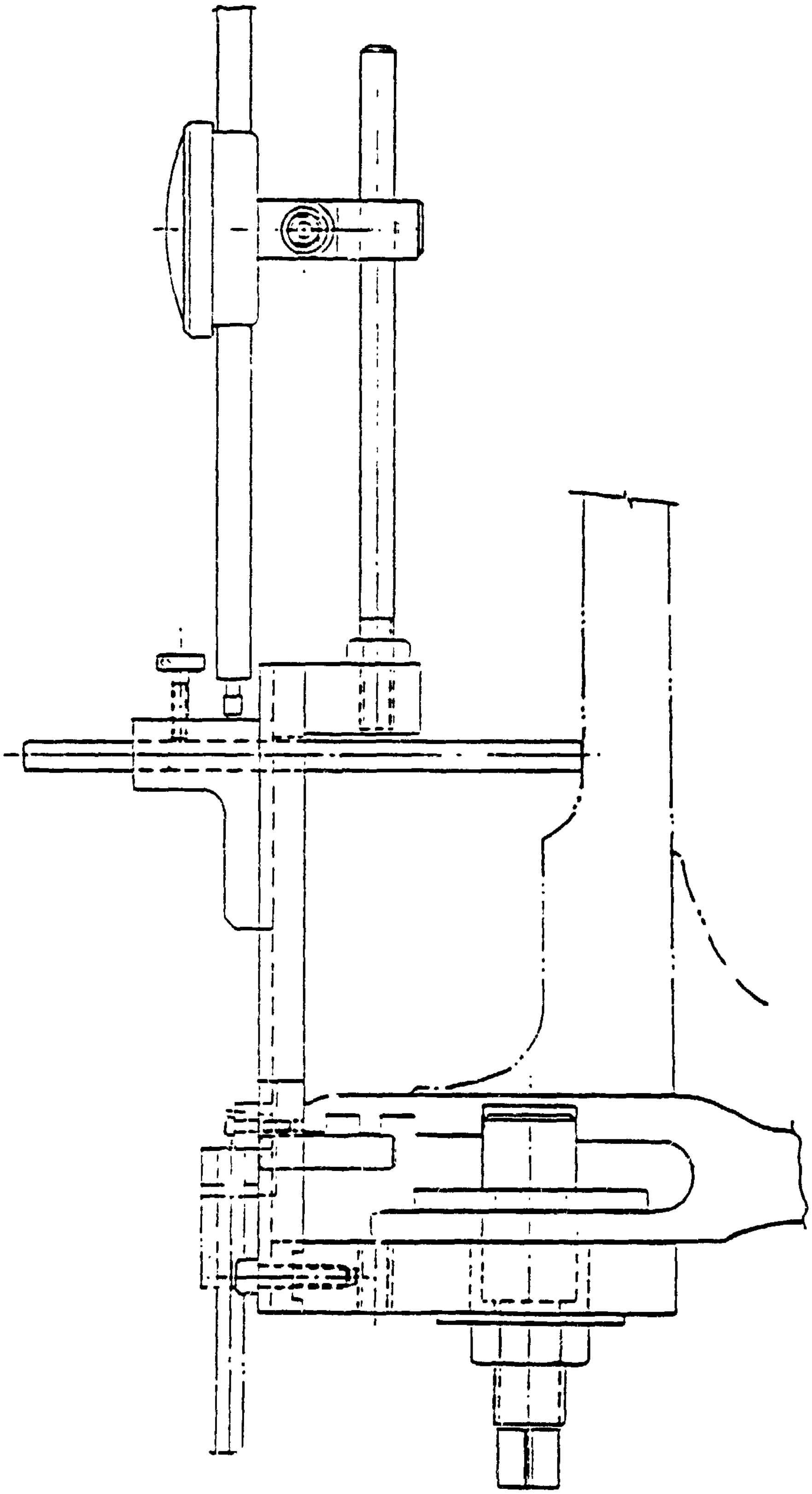

Figure 7-9. Manual J-seal Profile Inspection (clevis end)

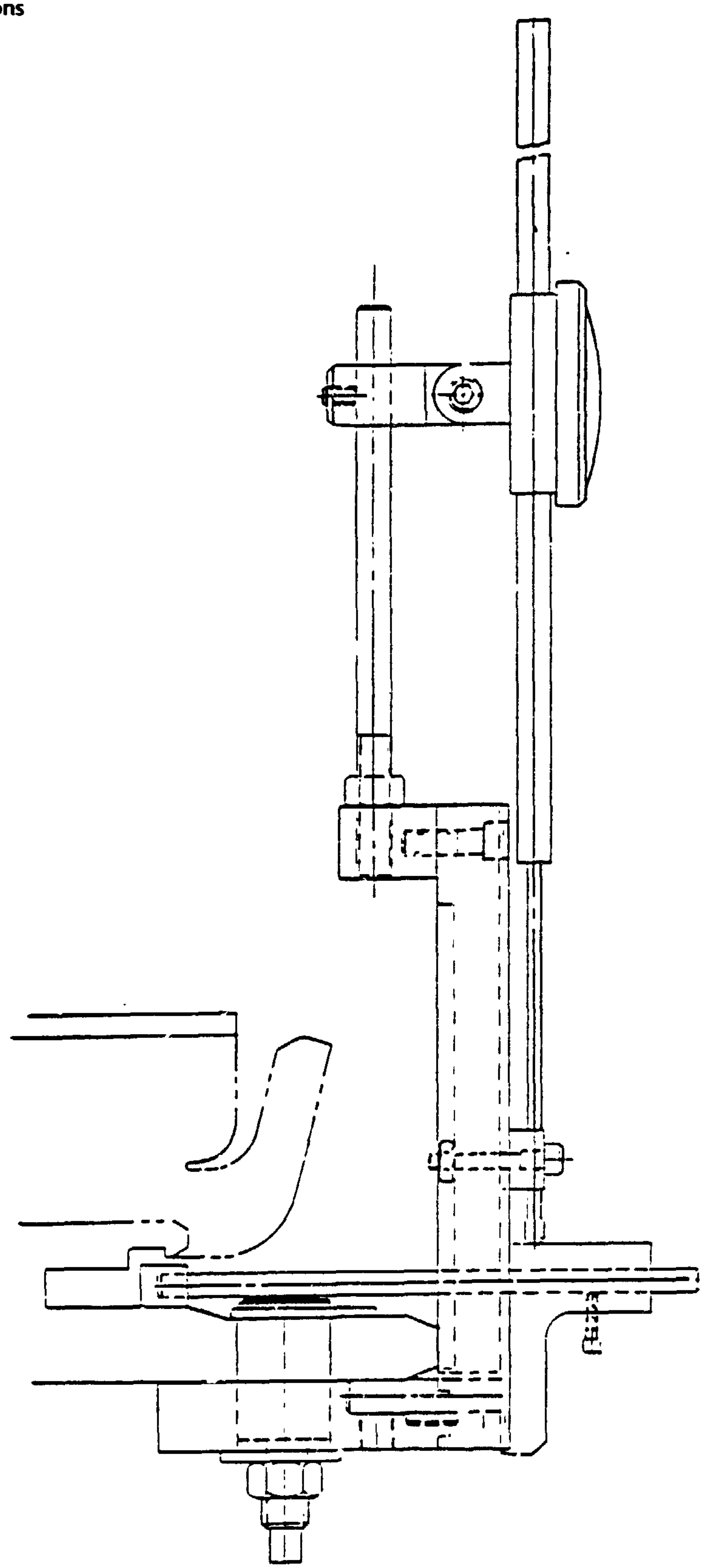

Figure 7-10. Manual J-seal Profile Inspection (tang end)

tool design uses glass scales and LVDTs to take the same measurements as the original profile tool. A critical design review (CDR) presentation and hazards analysis will be performed prior to qualification test use. Long range planning is also in effect for an auto-laser profile tool.

Although both tang and clevis measurements were very time consuming and design improvements are being implemented, the tool is currently qualified for use on flight segments. As significant changes are made, certification will be made either by separate tests or tool similarity.

1. <u>J-seal Terminus Inspection System (Fiber Optics) (C77-0485) Certified</u>. The purpose of this inspection is to reveal any cracks, cuts or tears present in the J-seal terminus region. An illustration of the 2U129578 wand placement during inspection is in Figure 7-11. Terminus inspection is performed with the fiber optic probe inserted into the region by means of probe head. The fiber optic image is then carried to the camera and recorded on videotape, while being displayed simultaneously on a monitor. Slight downward pressure is then applied to the probe, causing the J-seal terminus to open. This expansion causes existing defects to become more obvious to the observer.

Tang inspection was done while the aft center segment was hanging in the transfer aisle. Locations every 10 deg were recorded on videotape for future reference. About 11 hr were required. After additional operator training, examination time can probably be significantly reduced to about 3 hr.

A relatively large amount of dirt and/or dust was found in the terminus area. No abnormalities other than the above mentioned dirt and dust were found in the J-seal terminus area around the entire circumference. One suspect area was noted at approximately 57 deg, but was later determined to be some type of debris, either dirt or dust. Debris was also found to be concentrated around the rubber mold flashing approximately every 15 deg. This was to be expected and was not a cause for concern. No transportation or handling defects were found in the J-seal terminus area prior to joint mating.

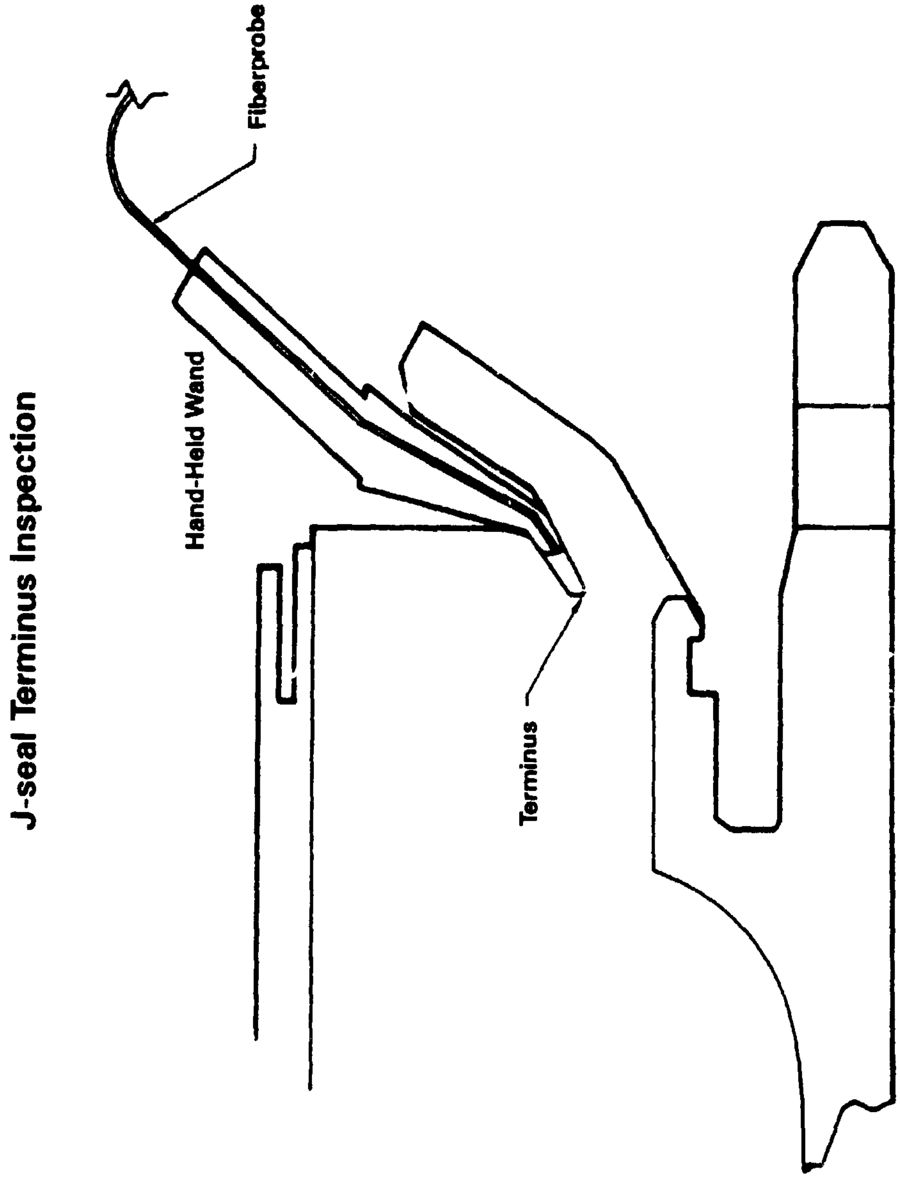

Figure 7-11. J-seal Terminus Inspection

A recommended improvement to this GSE equipment is a reduction of the current wand width. This would allow easier lateral movement within the J-seal, avoiding the need to remove the wand and reinsert it at the new measurement position. The fiber optic cable connection to the camera needs to be dead ended to prevent rotation, otherwise determining crack orientation is not possible. It is also recommended that offline computer enhancement and characterization be done to further evaluate future inspection results. If this cannot be done, a leader should be produced on the inspection tape to explain the images.

Although areas of tool improvement were identified, tool use was qualified for flight segments during the ATA test.

m. J-seal Bondline Inspection Tool (C77-0486) Not Certified. The J-seal bondline inspection tool is used to evaluate the joint insulation contact during segment mate. The use of this tool was deleted from the ATA test. Inste a J-seal bondline inspection was performed by a man entering the b re by Boson's chair and inspecting the area visually without any magnification or fiber optics.

n. Assembly Instrumentation (C77-0487) Certified. A schematic diagram of the ssembly instrumentation used during ATA is shown in Figure 7-12. The principle components shown are the hydraset, the 4-point lifting beam (which is also used to shape the suspended segment), and the four temposonic height gages, each located 90 deg apart on the segment. The various electronic support equipment is also shown.

1. Hydraset. Directly underneath the crane block and above the lifting beam is the hydraset, which is a hydraulic device that allows extremely sensitive vertical movement control in either the up or down direction. Segment movement from the transfer aisle to a small distance (2 to 3 in.) above the lower SRB stack is accomplished by the crane, as is also the segment centering, or relative axis position alignment. Critical vertical movement during mate and demate operations is controlled by the hydraset, enabling the required sensitivity to meet the lowering and separation rates.

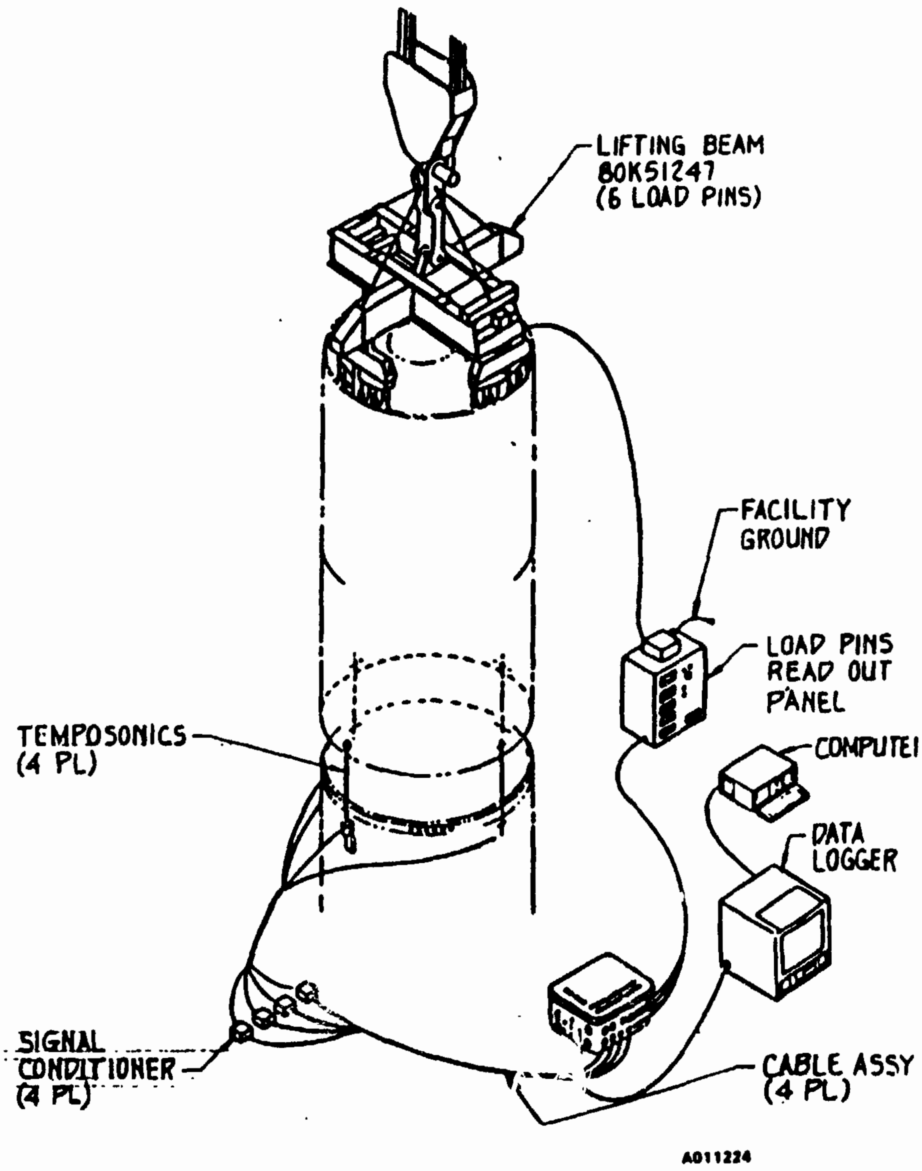

Figure 7-12. Assembly Instrumentation

Although this criteria was met during the ATA test, it is felt that additional operator training should be done to ensure all future stacking operation rates are met. It was also found that segment movement lags the indicated hydraset load slightly. Operator awareness of this fact is important during critical operations in order to avoid over correcting the hydraset for segment movement.

During the ATA test, hydraset control and monitoring was done at a different station from where the beam loads were displayed and the temposonic data were output. Operator communication was ensured with the use of headphones and an intercom system. Incorporating the hydraset readings into the temposonic data acquisition system would not only provide a central readout point during mate and de-mate operations, but aid in data analysis as well. The feasibility of this is currently being investigated.

2. <u>4-Point Lifting Beam (H77-V0384)</u>. The 4-point lifting beam has the capability to vary the weight between a complete 2-point suspension on one axis to a complete 2-point lift on the opposite axis, and any 4-point lift combination in between. Sixteen segment suspension pins are used at each location, making a total of 64 pins used to support the segment weight. Each beam drop contains a load pin, used to determine the load at that location. The load pin display panel shows the load on each of the four beam load pins, the combined load for each beam axis, and the total beam load. As with the hydraset readout, this display panel was independent of the other assembly instrumentation. Load pin data is presented and discussed in Section 7.2. It was recommended and is being implemented that the beam load readings be incorporated into the temposonic data acquisition system. It was also found that the load pin readings were often discrepant, and would vary from hydraset readings by as much as 10,000 lb. The reasons for this and any recommended solutions are currently being investigated.

Premate segment parallelism, or the parallel variation between the bottom of the tang and top of the clevis prior to mating, was easily achieved during the ATA test with the use of the lifting beam. The beam contains two pneumatic actuators oriented 90 deg to one another which are capable of tilting the segment and beam with a force of 10,000 lb each. The loads from the load pins in each actuator are also displayed on the beam load readout panel. These actuators worked well, but it is recommended that a scale be attached to each so the physical extension or retraction can be known.

a) Segment Shaping. Segment shaping capability during the ATA test was adequately demonstrated, but insufficient data were gathered to generate a reliable model. Extensive shaping tests, as defined in the test plan, were not performed due to schedule constraints. A simplified presentation of data gathered can be seen in Figure 7-13. Those data are loads from the 384 beam and sine bar deviations from circular.

The solid square at Point 1 indicates while the 0- to 180-deg axis had a load of about 155 kips, there was a positive 0.29 in. deviation from circular along that same axis. The hollow square at Point 1 indicates while an approximate 155-kip load was on the 90- to 270-deg axis (or when the segment was in an even 4-point lift), there was a negative 0.27 in. deviation from circular along that axis. In other words, the segment was oval in an equal 4-point suspension lift. This ovality was also seen in the old type hardware to approximately the same valve. The boxes, labeled 2, show how the axis lengths changed with beam load variation. The weight was increased to 230 kips on the 90- to 270-axis (hollow square), and decreased to 70 kips on the 0- to 180-deg axis (solid square). Both axis lengths shifted approximately 0.1 in. towards the zero position. The significant points of this plot are Points 3 and 4. They show that the axis lengths were closest to each other (or the segment was most round) when most of the segment weight was on the 90- to 270-deg

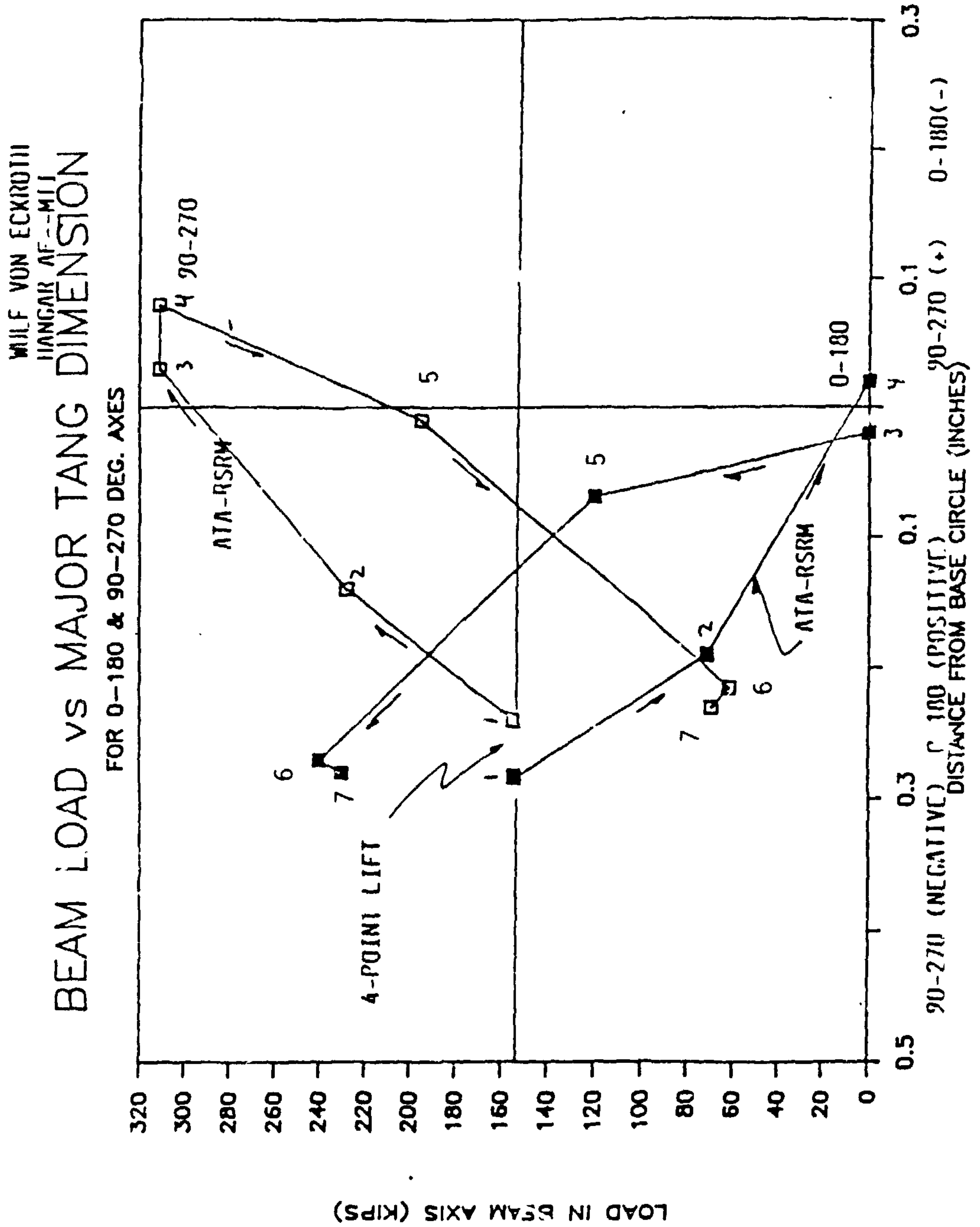

Figure 7-13. Aft Center Segment Shaping During the ATA Test

axis. The shift between Points 3 and 4 represents the segment continuing to shape while in that same load suspension. Due to the segment size, shape, and propellant modulus characteristics, there is a significant time delay between application of the beam loads and final segment shape response. It is for this reason that segment shaping tests require so much time, and they were severely impacted by schedule constraints. Points 5, 6, and 7 indicate the remaining segment response and hysteresis effects (path up is different from path down) of continued beam load variations.

The important points learned from the segment shaping performed during ATA are: 1) in a 4-point lift the segment was not round, 2) hysteresis effects can be seen from the segment shaping, and 3) more energy is concentrated along a segment axis in a 2-point lift than a 4-point lift. (Shape changes with respect to time are greater in a 2-point lift than a 4-point lift).

In conclusion, insufficient shaping data were acquired during the ATA test. It is recommended more segment shaping data be analyzed during flight stacking, to enlarge the data base and refine the segment shaping model.

3. Temposonics (C77-0487). The temposonic gages are used for all mating and demating operations to monitor the segment vertical position. Four modified 8U75919 gages were placed at the 2-, 92-, 182-, and 272-deg locations during the ATA test. Not only can each location's vertical position be determined, but segment out-of-parallelism can readily be monitored by taking the difference between the two opposite points on each axis. Numerous figures of temposonic data were presented and discussed in Section 4. The temposonic data are acquired and reduced by a personal computer, where it is displayed real time on the screen and recorded on a hard disk. This real-time display proved extremely useful during mating and demating procedures. After a file has been generated, the data are dumped onto a floppy disk where they are taken to another computer for plot generation and tabular listings.

As mentioned above, the hydraset and beam load readings are displayed elsewhere, so operator coordination during critical sequences is achieved through the use of headsets and an intercom system. The beam loads are being incorporated into the temposonic data display and acquisition system, and the feasibility of including the hydraset readings is currently under study.

Throughout the ATA test, the assembly instrumentation used indicates it is certified for use on segment stacking for flight motors.

o. Slump Measuring Tool (C77-0488) Certified. The 8U75923 slump gage was used during the ATA test to measure propellant/insulation surface axial dimensions. Measurements were performed on the aft segment clevis end and both ends of the aft center segment. A schematic diagram of the tool can be seen in Figure 7-14. It can been seen the gage uses (LVDTs) to measure 14 locations along the segment diameter. Data are routed through the various support electronic equipment, and are recorded by the data logger.

The slump tool setup procedures as initially outlined in the OMI were refined during the ATA test. Once the tool was setup and calibrated, however, all measurements were made quickly and easily (in about 15 min). The initial tool setup and calibration took over 5 hr, however, with the increased operator tool familiarity it now takes about 2 hr. During initial operation some minor problems were encountered and quickly resolved. In one instance, an inboard LVDT plunger missed the propellant surface and extended into the bore. This occurred at one location and was due to the oval segment shape.

A recommendation currently being worked for improved future slump tool use is incorporation of the computer data system in place of the data logger. A lighter but stiffer beam would also increase performance, as the current beam weighs about 150 lb. All data printouts in the future will also be included immediately in the OMI, rather than just recorded as was done in the past.

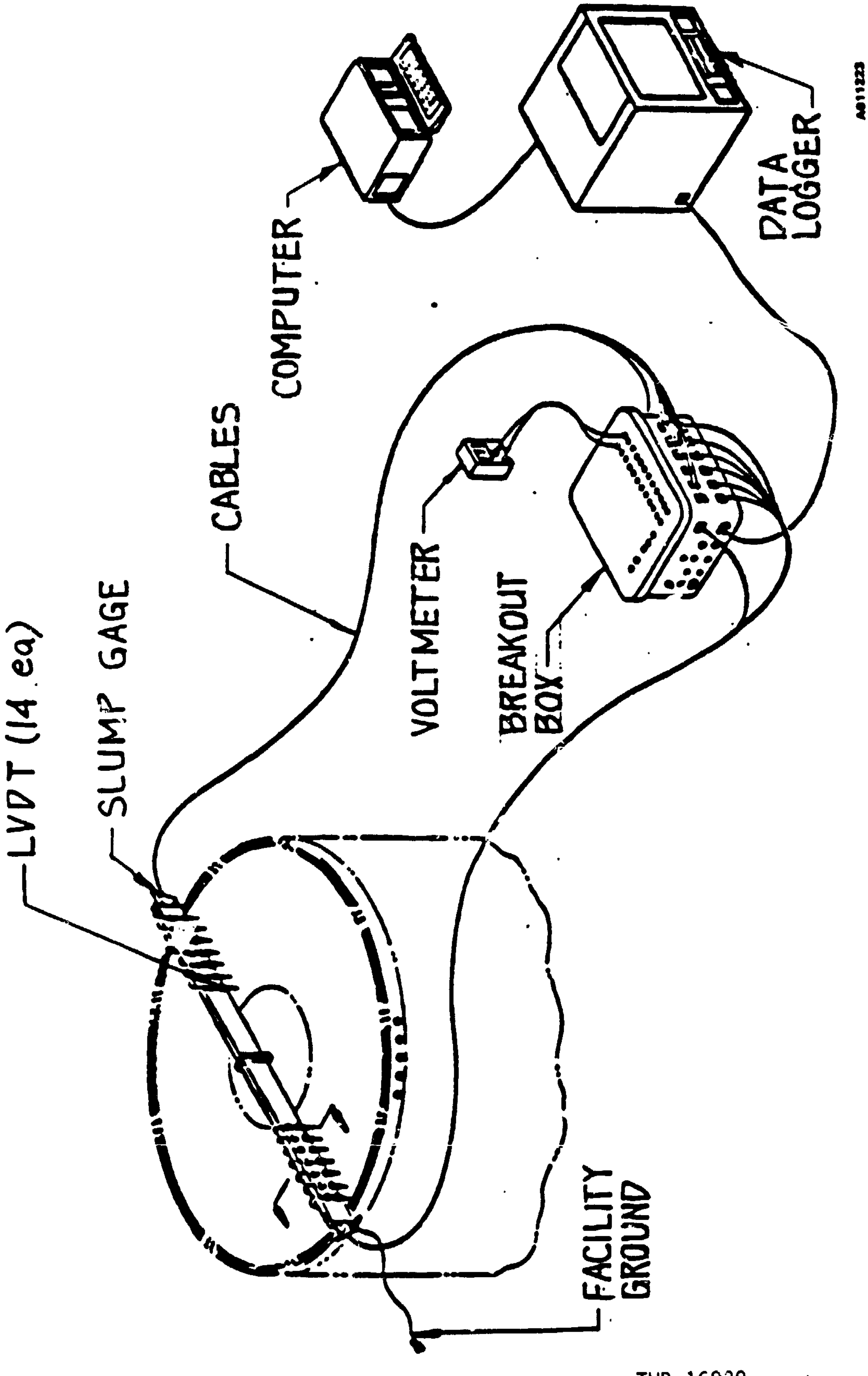

Figure 7-14. Propellant Slump Measuring Tool

Compared to the previous mechanical slump tool performance, the resulting reduction in data collection time is significant. Improved accuracy is also achieved with new slump gage use. In conclusion, the slump measuring tool is qualified for further use.

7.2 STRUCTURAL APPLICATIONS

7.2.1 Introduction

This section discusses the structural applications areas of interest of the ATA test. Of primary interest were the metal parts, soft goods (O-rings, V-2 filler), and leak check. Evaluation of the metal parts includes grease application prior to segment mating, hardware strains and stresses induced during FJAF torquing and mating, and postmate inspections for marring, scratching, or damage. Soft goods evaluation concerns the greasing, compression, and inspection of the soft parts for damage both prior and after mate. The leak check equipment was discussed in Section 7.1.3, as only an evaluation of the results is presented here.

7.2.2 Objectives

The structural applications certification objective covered by the ATA testing is:

> Certify that the leak test method is compatible with the field joint insulation to verify joint seals.

Developmental structural test objectives that were met are:

a. Determine mate/demate loads on hardware.
b. Evaluate baseline joint configuration fit during and after mate.
c. Gather actual data for analytical comparison.
d. Validate procedures for RSRM assembly/disassembly and handling.
e. Evaluate condition of hardware and components from post-test measurements, inspections, and data.

Also of interest was the evaluation of the following GSE.

a. Field Joint Assembly Fixture (FJAF)
b. Leak Test System
c. Vertical Separation Fixture (VSF)

7.2.3 Results and Discussion

The main document used to stack/destack the ATA test article is KSC document OMI B5145. The OMI document has Operational Maintenance Requirements Support Document (OMRSD) requirements in it that are critical to the stacking integrity. Morton Thiokol supplies document TWA-791 which is Morton Thiokol input for the OMI.

The majority of test procedures that were of interest to structural applications are contained in Drawing 7U75782. This drawing specifies the components to be used in the mating of the aft skirt joint (aft skirt/aft segment), and components used for mating the ATA field joint (aft segment/aft center segment). It also specifies grease application, and installation of the O-rings, V-2 filler, joint pins, and pin retainer clips. The leak check of the RSRM field joint cavities after assembly is also called out.

7.2.3.1 Grease Application. A new grease application procedure (STW7-2999) was introduced and incorporated on the ATA test components. This procedure, which has been used on DM-8 and DM-9 in a preliminary stage, utilizes the same grease as the SRM design but employs a lighter application on the sealing surface areas. Past data indicate excessive grease can directly effect the leak check criteria. Accordingly, an application procedure was written to be leak check compatible, as well as be corrosion preventive. This grease specification has been reviewed and is currently being updated to correct any errors and resolve the review item discrepancies (RIDSs). The procedure also provides installation instructions for the O-rings and V-2 filler, and lists the installation tools required for this procedure.

The bare metal surfaces were cleaned before the application of the Conoco HD-2 (STW5-2942) grease was performed. After the grease was applied the Viton® V-2 filler (STW3-3353) was installed in the root of the capture feature, then the O-rings (7U75204) were installed prior to the first full mate. (Clevis primary/secondary and tang capture feature).

The O-rings used on ATA were 7U configuration. The manufacturing specifications of 7U O-rings are different from those of 1U flight configuration O-rings but were determined adequate for assembly tests.

Disassembly inspection of the dry mate showed no major problems with the soft goods (O-rings and V-2 filler) or joint metal regions. Grease on the metal surfaces was nominal, while the O-rings were slightly over-greased. The Viton® V-2 filler was still properly seated with no evidence of overfill or damage.

The grease application for the second full assembly on bare metal and O-ring surfaces was completed per STW7-2999. The O-rings had a wet look but were not heavily coated with grease. After the grease was applied and the O-ring were installed, the insulation adhesive (STW5-3479) was applied to the J-joint area.

Postmate inspection revealed the cleanliness of this mate was not as good as the dry mate because the transfer medium powder used to check out the J-joint during the first full mate was not completely cleaned off of the clevis surface. The powder was found all over the wet mate sealing surfaces. It was attached to the grease all over the joint area. The contamination could not be determined to be a problem, as the leak check was deleted from the wet mate.

7.2.3.2 Mate/Demate Loads. Load monitoring devices consisted of a 250-ton hydraset in the lifting arrangement (between the crane and the 4-point lifting beam) and load pins installed in the lifting arrangement to mate the clevis end of the aft center segment with the lifting beam. Comparison of these loads can be found in Tables 7-3 and 7-4.

Assembly Loads. The measurements of the mating forces were widely varied. Hydraset data (see Table 7-3) indicates an assembly force of 9,000 lb for the dry mate, while load cell measured values were 35,000 lb. The highest assembly load was seen on the second mate (wet mate) which indicated an assembly load of some 56,000 lb.

Disassembly Loads

The first full mate disassembly load of the ATA segments (calculated from the VSF hydraulic pressure) was no greater than 42,000 lb, which is also explained on Table 7-3. The actual separation load was probably less,

Table 7-3. Dry Mate Load Summary

Hydraset			OMI Sequence
Before Mate = 326,700 lb			(10-102)
After Mate = 317,700 lb			(10-136)

Hydraset assembly load calculation--before mate load minus after mate load equals assembly load

326,700 lb - 317,700 lb = 9,000 lb

Load Pins			
Before Mate			(10-102)
	0	= -1,400 lb	
	90	= 162,100 lb	
	180	= 2,100 lb	
	270	= 148,100 lb	
	0-180	= 700 lb	
	90-270	= 310,200 lb	
After Mate			(10-145)
	0	= -1,500 lb	
	90	= 145,350 lb	
	180	= 0 lb	
	270	= 277,500 lb	
	0-180	= -1,500 lb	
	90-270	= 277,500 lb	

Load cell assembly load calculation equals - Before mate totals of 0-180 and 90-270 minus after mate totals of 0-180 and 90-270.

310,900 lb - 276,000 = 34,900 lb

Separation Tool

Maximum system pressure achieved on separation tool = 850 psig square Area of piston (in inches) plus mechanical advantage of system

Assuming eight cylinders are being used = 49.02 in.^{2}

805 lb/in.^{2} gage x 49.02 in.^{2} = 41,667 lb

Disassembly force from separation tool = 42,000 lb

Table 7-4. Wet Mate Load Summary

Hydraset — OMI Sequence (11-113)

Before Mate = 326,900 lb
After Mate = lb

Hydraset assembly load calculation--before mate load minus after mate load equals assembly load

lb - lb = lb

Load Pins — (11-113)

Before Mate

0	=	86,900 lb
90	=	69,600 lb
180	=	87,700 lb
270	=	58,300 lb
0-180	=	174,600 lb
90-270	=	127,900 lb

After Mate

0	=	lb
90	=	lb
180	=	lb
270	=	lb
0-180	=	lb
90-270	=	lb

Load pin assembly load calculation equals--before mate totals of 0-180 and 90-270 minus after mate totals of 0-180 and 90-270.

302,500 lb - 246,300* lb = 56,200 lb

Separation Tool--Not used

*Monitoring of assembly loads from load pins from D. Cummings notebook.

as extreme rapid upward segment movement was seen when this load was applied. During the wet mate disassembly, the highest demate load was estimated to be 20,000 lb. This load was deduced by estimating the weight of the upper segment and lifting beam, and then adding 20,000 lb. This total sum load was then applied to the hydraset.

7.2.3.3 <u>Leak Check Results</u>. A field joint leak test was performed on the ATA in the VAB. This leak test represented the first full scale test for the upgraded SU75902 GSE leak test panel. The leak test employs the method of pressure decay to calculate leak rates. The leak test equipment is used to pressurize and isolate the test joint. Test equipment provides real-time monitoring of pressure and temperature during the isolation period. Changes in pressure and temperature are then used to calculate the joint leak rate.

The leak check procedure (STW7-3447) was used for the first time on full-scale flight hardware stacked in the vertical positions. This procedure proved technically sophisticated and very sensitive and quite prone to problems of software support calculations. ATA was finally determined to have passed the leak check criteria of STW7-3447 after two days of debugging the system. The procedures and equipment still need refinement to make it adaptable to the common worker and environment it needs to operate in at KSC. The leak test results are presented in Table 7-5. Test results show all joints to have acceptable leak rates.

7.2.3.4 <u>Metal Parts Inspection</u>. For the dry mate disassembly, the 7U52919 VSF was used. The crane lifting arrangement was connected and the weight of the aft center segment and dead weight of upper tension band was pumped up on the hydraset. All loose pins were then removed until removal came within five pins of an alignment hole, then the alignment pins were inserted. This worked at 118 and 240 deg but not at the 0-deg location. It was decided to go ahead and demate using the two alignment pins (118 and 240) instead of all three.

Also during the dry mate disassembly one single pin would not come out at the 164-deg location. The segment was moved at the 0-deg location 0.375 in. out-of-level to try and free the pin. It was finally removed by

Table 7-5. Leak Test Results

Joint	Cavity	Test Pressure (psig)	Maximum Allowable (sccs)	Measured Leak Rate (sccs)
	P-S	1,000	0.32	0.0066
	(P-C)	Ambient	-0.32	-0.0001
	P-S	30	0.0082	-0.0003
ATA	(P-C)	Ambient	-0.0082	0.0000
Field	P-C	100	0.051	0.0039
	(P-S)	Ambient	-0.051	-0.0003
Joint	P-C	30	0.0082	0.0005
	(P-S)	Ambient	-0.0082	-0.0001

sccs = Standard Cubic Centimeters Per Second
P-S = Primary--Secondary Cavity
P-C = Primary--Capture Feature Cavity

releveling the segment and using the hydraulic pin removal tool. This action was in direct violation of the planning documents, and could have resulted in critical damage to both tang and clevis. Post test inspections revealed no anomalies. No similar process (of trying to unbind a pin by segment movement) should ever be attempted in the future.

Further disassembly inspections after the dry mate found raised metal at 0 deg on the clevis outer leg hole and on the tang alignment slot. This was a result of the above mentioned difficulty encountered while trying to reinsert the alignment pins. Slight burnish marks were also found on the inner clevis inside diameter due to interference fit with the tang capture feature. Similar marks were also observed on the tang outside diameter due to the interference of the tang segment and FJAF guide blocks.

7.2.3.5 <u>Nozzle Plate Static Analysis</u>. Structures Design Research Corporation, Inc. (SDRC) conducted a static analysis (Project No. 40680-24) to provide information about the effects of replacing an actual nozzle assembly on the ATA with a 0.75 in. thick cover plate over a nozzle fixed housing. It was desirable that the ATA structure with a fixed housing and cover plate exhibit similar stiffness characteristics as the actual nozzle configuration.

To determine the joint ovality, two finite element models were assembled to represent the two configurations. These global static models predicted three-dimensional deformations due to gravity. The finite element models used for the study include the ETA segment with the new 360-deg ring, the aft segments with three sets of stiffeners, the aft dome, an actual nozzle or fixed housing and cover plate, the aft skirt and the MLP pad holddown post stiffness.

ATA sine bar measurements of the fixed housing with cover plate configuration show good correlation with analyses of the actual nozzle configuration. The 0- to 180-deg axis sine bar measurements from ATA showed -0.042 in. ovality, the analyses indicated this same value. The sine bar 90- to 270-deg axis measurements were -0.046 in. while analyses showed -0.038 inch.

The results of the study indicate that the nozzle cover was an acceptable replacement for the nozzles on the ATA aft segment.

7.2.3.6 Strain and Deflection Measurements. Developmental strain gages (biaxial and girth) provided microstrain data monitoring of the hardware during the bearhugging of the FJAF to the outer clevis leg (Figure 7-15) and when mating the tang with the clevis (Figure 7-16).

Girth gages were placed on the outer clevis leg 3.48 in. from the leg tip (on the flat machined surface), and 5.25 in. from the clevis end (in the transition region where the machined surface of the clevis bends into the membrane area of the cylinder).

During the torquing of the FJAF, these gages measured an average of -60 μin./in. and -28 μin./in. microstrain respectively. This microstrain can be converted to deflection when multiplied by the cylinder diameter at the gage location. Calculations indicate that the outer clevis diameter at the gage locations compressed or straightened 0.009 and 0.004 in. respectively.

Biaxial gages were also placed under the FJAF on the outer clevis leg 1 in. from the end. The average hoop microstrain reading was as expected and shows that the outer clevis leg was circumferentially squeezed inward as much as 0.030 in. during the FJAF torquing prior to mating. The biaxial gages also showed uniform microstrain distribution around the segment at the 0-, 90-, 180-, and 270-deg locations. Girth gages on the aft center segment tang indicated the tang was compressed inward 0.002 in. during the mating processes. See Tables 7-6 and 7-7 for a complete list of all strains from testing.

Strain gauge monitoring of the hardware show no indication of material concerns from the bearhugging of the FJAF on the outer clevis, or during assembly/disassembly of the tang segment with the clevis segment. Highest microstrain readings were approximately 200 μin./in. which is well below any critical areas of the cylinder D6AC steel material.

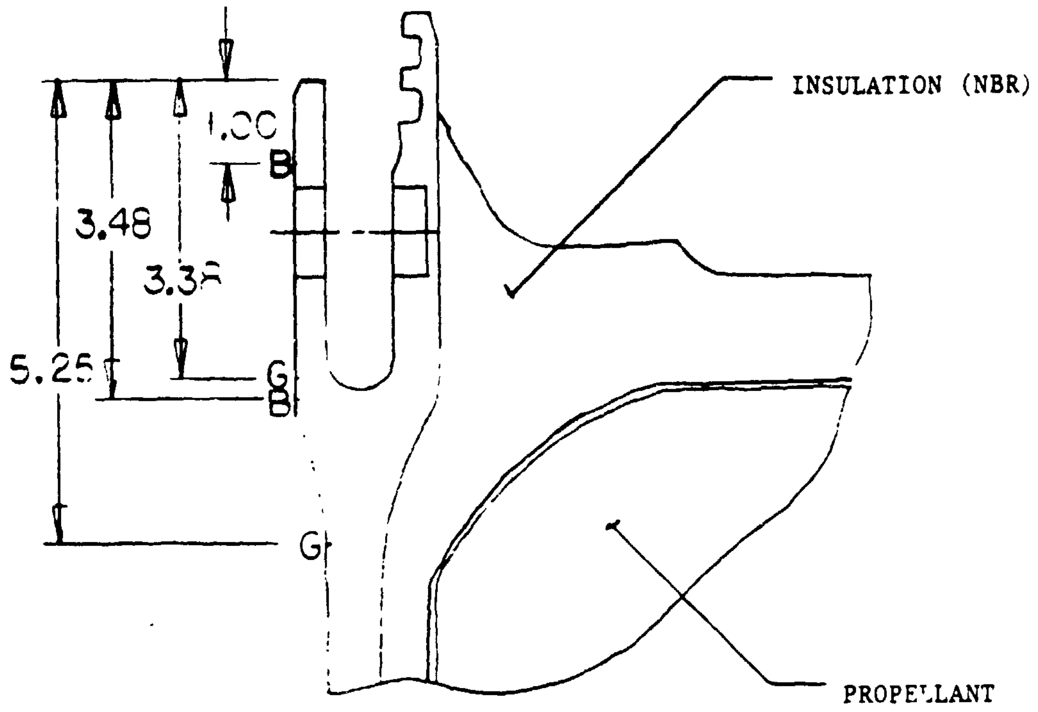

B = BIAXIAL STRAIN GAUGE

G = GIRTH GAUGE

Figure 7-15. Clevis Segment Instrumentation

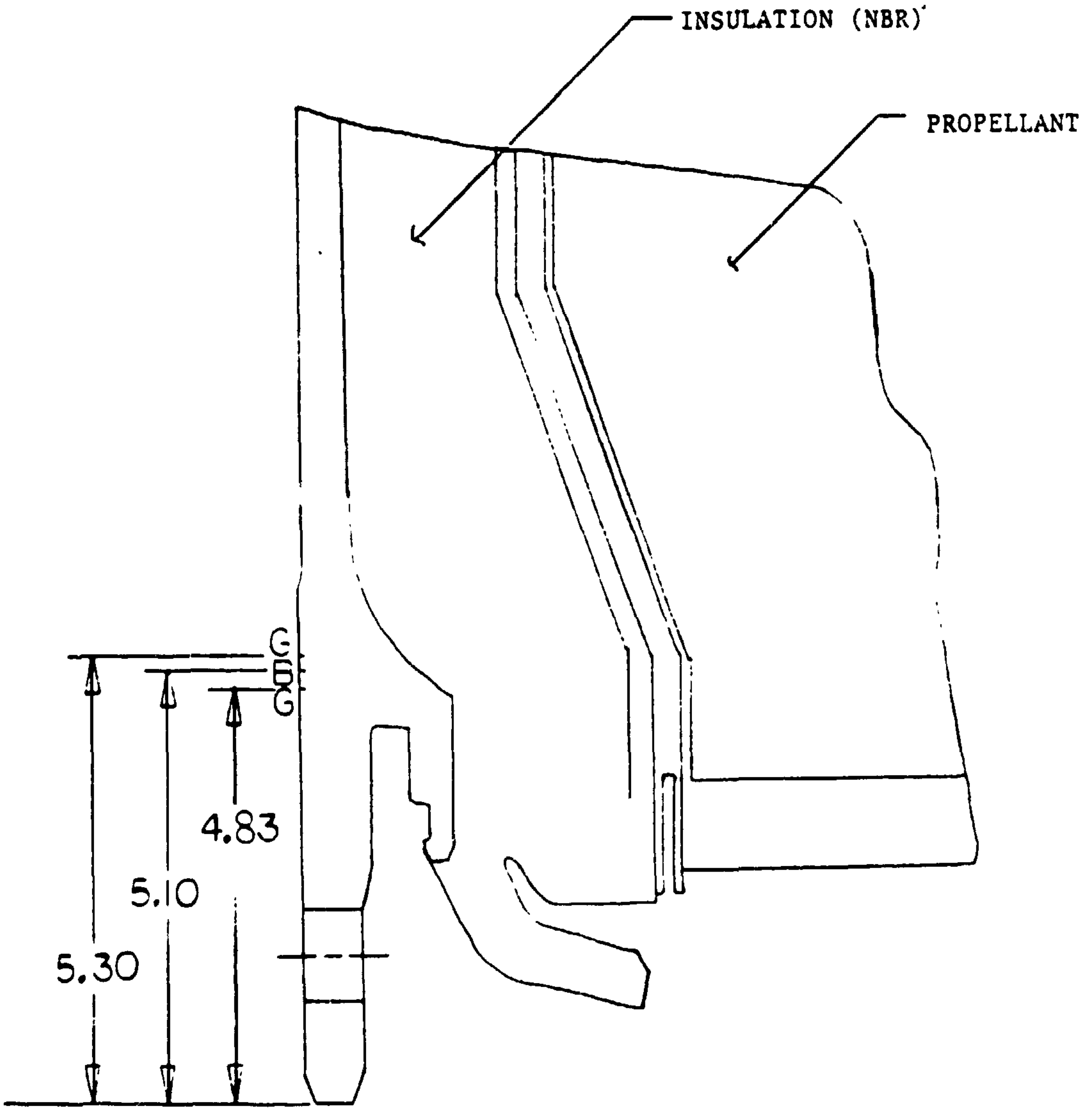

B = BIAXIAL STRAIN GAUGE

G = GIRTH GAUGE

TANG SEGMENT INSTRUMENTATION

Figure 7-16. Tang Segment Instrumentation

Table 7-6. Dry Mate Strains Results

Gage No. Clevis	Gage No. Tang	Description	Change in Microstrain From Zero
S039		Clevis axial microstrain monitoring from bearhugging clevis with FJAF	+190
S041			+236
S043			+202
S045			+206
		Average =	+209
S040		Clevis hoop microstrain monitoring from bearhugging clevis with FJAF	-50
S042			-52
S044			-50
S046			-48
		Average =	-50
S047		Clevis axial microstrain monitoring from bearhugging clevis with FJAF	--
S049			+26
S051			+26
S053			+24
		Average =	+25
S048		Clevis hoop microstrain monitoring from bearhugging clevis with FJAF	--
S050			-220
S052			-202
S054			-190
		Average =	-204
			Deflection (in.)
G003		Clevis girth gage monitoring of diametrical deflection from torque of FJAF	-0.004
G004			-0.009
			Change in Microstrain From Zero
	S019	Tang axial microstrain monitoring from initial tang/FJAF engagement	-16
	S021		-32
	S023		--
	S025		-26
		Average =	-25
	S020	Tang hoop microstrain monitoring from initial tang/FJAF engagement	-124
	S022		-102

Table 7-6. Dry Mate Strains Results (Cont)

Gage No. Clevis	Gage No. Tang	Description	Change in Microstrain From Zero
	S024		-90
	S026		-46
		Average =	-91
			Deflection Microstrain in (in.)
	G008	Tang girth gage monitoring of diametrical initial tang/FJAF engagement	-0.006
	G009		-0.006
			Change in Microstrain from zero
S039		Clevis axial microstrain monitoring from initial tang/FJAF engagement	-2
S041			+18
S043			-52
S045			4
		Average =	-8
S040		Clevis hoop microstrain monitoring from initial tang/FJAF engagement	+80
S042			+70
S044			+62
S046			+28
		Average =	+60
S047		Clevis axial microstrain monitoring from initial tang/FJAF engagement	-2
S049			-12
S051			-16
S053			-8
		Average =	-10
S048		Clevis hoop microstrain monitoring from initial tang/FJAF engagement	+90
S050			+154
S052			+118
S054			+100
		Average =	+116
G003		Clevis girth gage monitoring of diametrical initial tang/FJAF engagement	+0.002
G004			+0.006

Table 7-6. Dry Mate Strains Results (Cont)

Gage No. Clevis	Gage No. Tang	Description	Change in Microstrain From Zero
	S019	Tang axial mircrostrain monitoring from final assembly	-38
	S021		-8
	S023		-22
	S025		-24
		Average =	-23
	S020	Tang hoop microstrain monitoring from final assembly	-98
	S022		-70
	S024		-58
	S026		-28
		Average =	-64
			Deflection in (in.)
	G008	Tang girth gage monitoring of diametrical final assembly	-0.003
	G009		-0.003
			Change in Microstrain from Zero
S039		Clevis axial mircrostrain monitoring from final assembly	-194
S041			-218
S043			-204
S045			-186
		Average =	-201
S040		Clevis hoop microstrain monitoring from final assembly	+124
S042			+44
S044			+106
S046			+68
		Average =	+86
S047		Clevis axial microstrain monitoring from final assembly	-56
S049			-22
S051			-32
S053			-28
		Average =	-35
S048		Clevis hoop microstrain monitoring from final assembly	+390
S050			+228

Table 7-6. Dry Mate Strains Results (Cont)

Clevis	Tang	Description	Deflection (in.)
S052			+308
S054			+238
			Average = +291
G003		Clevis girth gage monitoring of	+0.006
G004		diametrical final assembly	+0.014
			Change in Microstrain From Zero
	S019	Tang axial microstrain monitoring	-20
	S021	from disassembly	-26
	S023		--
	S025		-34
			Average = -27
	S020	Tang hoop microstrain monitoring	+82
	S022	from disassembly	+42
	S024		+88
	S026		+28
			Average = +60
	G008	Tang girth gage monitoring of dia-	+0.005
	G009	metrical deflection from disassembly	--
			Change in Microstrain From Zero
S039		Clevis axial microstrain monitoring	+92
S041		from disassembly	+64
S043			+176
S045			+154
			Average = +122
S040		Clevis hoop microstrain monitoring	-96
S042		from disassembly	0
S044			-122
S046			-48
			Average = -67
S047		Clevis axial microstrain monitoring	+51
S049		from disassembly	-2

Table 7-6. Dry Mate Strains Results (Cont)

Gage No. Clevis	Tang	Description	Deflection (in.)
S051			+8
S053			-22
			Average = +20
S048		Clevis hoop microstrain monitoring	-276
S050		from disassembly	-14
S052			-248
S054			-160
			Average = -175

Gage No. Clevis	Tang	Description	Deflection (in.)
	G003	Clevis girth gage monitoring of dia-	---
	G004	metrical deflection from disassembly	-0.007

Table 7-7. Wet Mate Strains Results

Gage No. Clevis	Gage No. Tang	Description	Change in Microstrain From Zero
S039		Clevis axial microstrain monitoring from bearhugging clevis with FJAF	+194
S041			+208
S043			+182
S045			+200
		Average =	+196
S040		Clevis hoop microstrain monitoring from bearhugging clevis with FJAF	-46
S042			-46
S044			-42
S046			-46
		Average =	-45
S047		Clevis axial microstrain monitoring from bearhugging clevis with FJAF	--
S049			+18
S051			+18
S053			+20
		Average =	+19
S048		Clevis hoop microstrain monitoring from bearhugging clevis with FJAF	--
S050			-190
S052			-166
S054			-176
		Average =	-177
			Deflection (in.)
G003		Clevis girth gage monitoring of diametrical deflection from torque of FJAF	---
G004			-0.004
			Change in Microstrain From Zero
	S019	Tang axial microstrain monitoring from final assembly	+6
	S021		-18
	S023		--
	S025		-14
		Average =	-9
	S020	Tang hoop microstrain monitoring from final assembly	-122
	S022		-6

Table 7-7. Wet Mate Strains Results (Cont)

Gage No. Clevis	Gage No. Tang	Description	Deflection (in.)
	S02?		-70
	S02?		--
		Average =	-66
	G008	Tang girth gage monitoring of	-0.003
	G009	diametrical from final assembly	--
			Change in Microstrain From Zero
S039		Clevis axial micr train monitoring	-98
S041		from final assembly	-196
S043			-94
S045			-202
		Average =	-148
S040		Clevis hoop microstrain monitoring	+32
S042		from disassembly	+26
S044			+24
S046			+30
		Average =	+28
S047		Clevis axial microstrain monitoring	-50
S049		from final assembly	-14
S051			-8
S053			-18
		Average =	-23
S048		Clevis hoop microstrain monitoring	+214
S050		from final assembly	+120
S052			+80
S054			+130
		Average =	+136
			Deflection (in.)
G003		Clevis girth gage monitoring of di-	--
G004		ametrical deflection from final assembly	+0.005

Table 7-7. Wet Mate Strains Results (Cont)

Gage No. Clevis	Gage No. Tang	Description	Change in Microstrain From Zero
S019		Tang axial mic: ıstrain monitoring	
S021		from disassembly	
	S023		
	S025		
		Average =	
	S020	Tang hoop microstrain monitoring	
	S022	from disassembly	
	S024		
	S026		
		Average =	
			Deflection (in.)
	G008	Tang girth gage monitoring of dia-	0.002
	G009	metrical deflection from disassembly	---
			Change in Microstrain From Zero
S039		Clevis axial microstrain monitoring	-152
S041		from disassembly	-10
S043			-24
S045			10
		Average =	-44
S040		Clevis hoop microstrain monitoring	12
S042		from disassembly	14
S044			10
S046			44
		Average =	20
S047		Clevis axial microstrain monitoring	--
S049		from disassembly	4
S051			0
S053			0
		Average =	1
S048		Clevis hoop microstrain monitoring	12
S050		from disassembly	28
S052			20
S054			82
		Average =	36

Table 7-7. Wet Mate Strains Results (Cont)

Gage No. Clevis	Gage No. Tang	Description	Deflection (in.)
	G003	Clevis girth gage monitoring of dia-	---
	G004	metrical deflection from disassembly	0.001

Measurements were taken of the outer clevis leg to tang while the crane was supporting the weight of the aft center segment. The average calculated gap from measurements was 0.033 inch. This same gap was taken when the crane was disconnected and was found to be 0.009 in. larger. Pi tape diameter comparisons of the clevis, next to the chamfer area, support these findings. The assembled pi tape dimension was 146.945 in. and the pi tape dimension prior to mate was 146.933 in. a diameter difference of 0.012 inch. Dividing this by two converts the diameter reading to a comparable radial dimension of the assembled gap measurement to 0.006 inch. This shows that the clevis outer diameter changes when the weight is transferred from the crane and is supported at the field joint. Pi tape procedure DI-1005 was followed for all pi tape measurements. Table 7-8 shows these values.

Assembled joint pinhole measurements were also performed to verify uniformity of the assembled clevis/tang gap. (The locations of these measurements are in Figure 7-17) The outer pin hole gap averaged 0.023 inch. The minimum gap was 0.030 in., located from 120 to 150 deg. The maximum gap of 0.035 in. was at the 330-deg locations. Inner pin hole gap measurements revealed an average 0.108 in. gap, with a minimum of 0.103 in. at the 0- through 30-deg locations, and a maximum 0.114 in. gap at 180 deg. These measurements are also listed in Table 7-8.

Measurements through the leak check ports were made for information only. The 135-deg port measurement revealed that the assembled clevis opening was 0.844 in., as compared to an average 0.839 in. unassembled opening, which is a difference of 0.005 in. This also compares to the gap/pi tape measurements mentioned above. The gap between the tang inside diameter and the inner clevis diameter, forward of the primary O-ring, was calculated to be 0.016 in., which was verified to be within design tolerances. Tables 7-8 and 7-9 presents these measurements and calculations.

The 45-deg port measurements show that the clevis gap opening when assembled was 0.830 in. which is less than the unassembled gap opening and that there is no clearance between the tang ID and the inner clevis diameter.

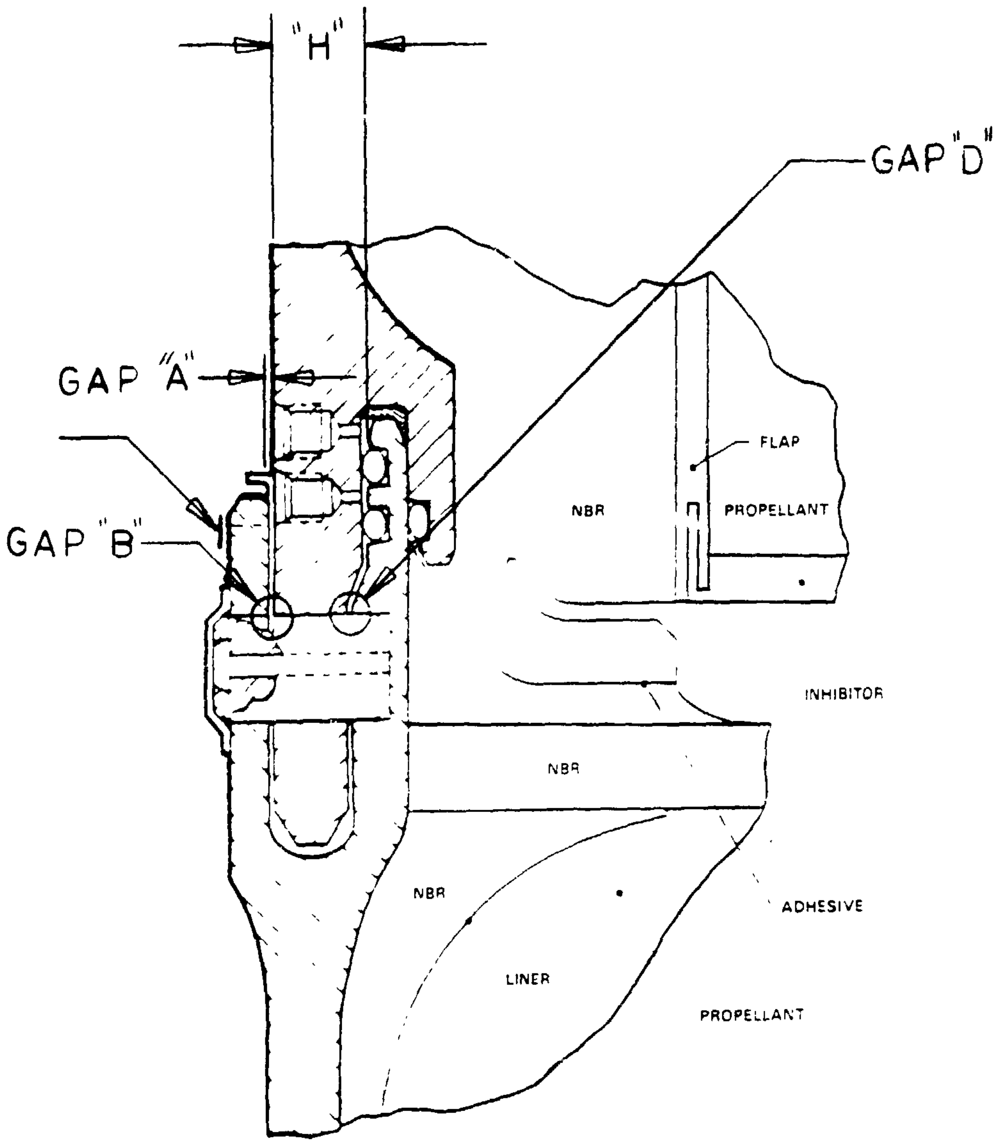

Figure 7-17. Assembled Joint Measurement Locations

Table 7-8. Assembled Joint Measurements

Clevis/Tang

Deg	Gap "A" Weight Not Supported by Crane	Gap "A" Weight Supported by Crane	Outer Pinhole Gap	Outer Pinhole Gap
0	0.040	0.033	0.033	0.103
30	0.044	0.041	0.032	0.103
60	0.044	0.038	0.031	0.104
90	0.043	0.035	0.031	0.104
120	0.042	0.038	0.030	0.110
150	0.042	0.038	0.030	0.112
180	0.041	0.033	0.031	0.114
210	0.042	0.036	0.034	0.111
240	0.042	0.034	0.033	0.110
270	0.042	0.036	0.031	0.107
300	0.042	0.031	0.034	0.108
330	0.042	0.035	0.035	0.108
Average	0.042	0.033	0.032	0.0108

Assembled pi tape of clevis 0.025 in. from chamfer

146.945 in.	Assembled field joint clevis measurement at KSC
-146.933 in.	Unassembled field joint clevis measurement at Morton Thiokol H-7
0.012 in.	Difference from unassembled to assembled diamters

Clevis Gap Opening Measured Through Leak Check Ports

135 deg

0.802 in.	From tang to inner clevis
+0.042 in.	Outer tang/clevis Gap "A" at 135 deg
0.844 in.	Clevis gap opening when assembled
0.802 in.	From tang to inner clevis
-0.786 in.	Tang thickness at 135 deg
0.016 in.	From tang inside diameter to inner clevis

45 deg

1.169 in.	From outer clevis to inner clevis
-0.339 in.	Outer clevis thickness at 45 deg
0.830 in.	Clevis gap opening when assembled

Table 7-8. Assembled Joint Measurements (Cont)

1.169 in.	From outer clevis to inner clevis
-0.044 in.	Outer tang/clevis Gap "A" at 45 deg
1.125 in.	
-0.339 in.	Outer clevis thickness at 45 deg
0.786 in.	
-0.786 in.	Thickness of tang at 45 deg
0.000 in.	From tang inside diamter to inner clevis

Table 7-9. Measurement Comparison Kennedy Space Center/H-7

Thickness Measurements

At 2.75/3.36 in. from end

Tang

Deg	H-7	KSC	Delta
0	0.786	0.780	0.006
30	0.786	0.783	0.003
60	0.786	0.781	0.005
90	0.787	0.783	0.004
120	0.786	0.781	0.005
150	0.786	0.783	0.003
180	0.785	0.782	0.003
210	0.785	0.780	0.005
240	0.784	0.781	0.003
270	0.785	0.782	0.003
300	0.785	0.782	0.003
330	0.785	0.781	0.004
Average	0.786	0.782	0.004

Outer Clevis Thickness

Clevis

Deg	H-7
0	0.339
30	0.339
60	0.339
90	0.339
120	0.339
150	0.339
180	0.338
210	0.338
240	0.339
270	0.338
300	0.339
330	0.339
Average	0.339

Table 7-9. Measurement Comparison Kennedy Space Center/H-7 (Cont)

Gap Openings

Clevis

Clevis Maximum Gap Opening

Deg	H-7	KSC	Delta	KSC After Testing
0	0.840	0.843	+0.003	0.839
30	0.839	0.835	+0.004	0.839
60	0.844	0.851	+0.007	0.845
90	0.838	0.837	+0.001	0.841
120	0.838	0.837	-0.001	0.838
150	0.840	0.837	-0.003	0.842
180	0.839	0.837	-0.002	0.842
210	0.840	0.836	-0.004	0.839
240	0.840	0.839	-0.001	0.840
270	0.838	0.836	-0.002	0.839
300	0.839	0.837	-0.002	0.841
330	0.839	0.837	-0.002	0.838
Average		0.840	0.839	0.840

Capture Feature Gap Opening

Tang

Deg	H-7	KSC	Delta
0	0.428	0.428	0.000
30	0.428	0.425	-0.003
60	0.428	0.430	+0.002
90	0.429	0.428	-0.001
120	0.429	0.428	-0.001
150	0.429	0.428	-0.001
180	0.429	0.428	-0.001
210	0.428	0.431	+0.003
240	0.428	0.430	+0.002
270	0.428	0.428	0.000
300	0.428	0.429	+0.001
330	0.428	0.429	+0.001
Average	0.428	0.429	0.001

Table 7-9. Measurement Comparison Kennedy Space Center/H-7 (Cont)

Pi tapes

Tang

	H-7	KSC	Delta	KSC After Testing
2.75 in. From End (No. 2)	146.198			
0.25 in. From Chamfer (No. 3)	146.210	146.203	0.007	

Clevis

	H-7	KSC	Delta	KSC After Testing
Inner Diameter (No. 4)	144.585	144.580	0.005	144.579
Outer Diameter 2.60 in. From End (No. 5)	146.922	146.932	0.010	
Outer Diameter 0.25 in. From End (No. 6)	146.933	146.926		146.925

Measurement comparisons between Morton Thiokol/H-7 refurbishment facility at Utah and KSC showed variations of 0.003 to 0.006 in. on tang thickness dimensions. KSC measurements before and after testing showed good correlations, however. (See Table 7-9 pi tapes). Clevis gap opening dimensions performed at KSC showed a 0.001 to 0.007 in. variance to those of Morton Thiokol/H-7 while the same measurements taken after test completion showed only a 0.000 to 0.003 in. maximum variance on the capture feature gap opening which is quite believable.

Pi tape data shows the worst comparison of KSC to H-7 measurements ranging from 5 to 10 mil less than those performed at H-7 Clearfield, Utah (see Table 7-2). KSC measurements before and after testing showed good repeatability.

7.2.4 Recommendations

a. Load monitoring needs to be better employed to understand what is happening during assembly/disassembly. A good correlation between hydraset, load pins and the mating/demating process needs to be established. The critical areas of the mating/demating processes need to have loads recorded to baseline the processes for evaluation of future assembly/disassemblies.

b. O-rings should be received, inspected and packaged at Morton Thiokol, Space Operations. The O-rings should be properly identified, greased, double bagged, and hard box packaged, shipped to KSC and opened at installation time. No further inspection should be needed except for shipping damage.

c. Hardware configuration during the assembly process is critical to the integrity of the joint. Better measurements techniques need to be developed to understand the correct interference fit. Reference memo L224:FY88:535.

d. Design engineering needs to review the KSC OMI document for stacking of the segments to maximize the integrity of this operation. This will improve O-ring grease application, joint assembly and disassembly (if required) load data gathering.

e. The leak check solution should be changed or improved to one that does not cause rust on the bare metal parts.

f. The paint to bare metal region on the tang segments at the field joints needs to be feathered out so that there is a smooth transition for the FJAF guide blocks. Grease should be applied over the paint 2 to 3 in. above the bare metal to paint region. This will improve the mating process.

g. Inspection of the clevis pinhole at 164 deg on the center segment and the matching location pinhole on the tang of the aft segment needs to be performed because of the cocking of the tang during the first disassembly.

h. The separation tool should be used on all field joint demates to insure that segments are not damaged.

i. The strain gages placed on the center segment tang surface are in line with the guide blocks of the FJAF. If the FJAF is not detorqued after the capture feature is engaged with the inner clevis the gages will come into contact with the guide blocks. Gage placement should be changed so that they are between the guide blocks of the FJAF and that any part of their placement is at least 5.1 in. from the end of the tang.

7.3 INSULATION DESIGN

7.3.1 Introduction

The ATA test was designed to demonstrate the vertical assembly of the new capture feature SRM hardware and redesigned J-joint insulation during a full mate, both as a dry fit using transfer medium and a full final mate using joint adhesive. The sequence of the process steps were also to be evaluated and then evaluated again in relation to process flow following the completion of each major task.

7.3.2 Objectives

Objectives of the ATA test, as they related to the field joint insulation, are listed as categorized below:

7.3.2.1 Qualification Objectives.

a. Certify assembly and disassembly of RSRM segments is possible in the vertical position in accordance with Assembly/Disassembly of Segments in accordance with Para 3.2.5.1 and 3.2.1.3.f of CPW1-3600A.

d. Certify that the design has considered tasks to be accomplished by operating, test, and maintenance personnel including considerations for safety, accessibility, critical tasks, complexity, and necessity for training.

g. Certify that the field joint insulation configuration will ensure that system performance and structural integrity is maintained during the assembly process.

h. Certify that the field joint insulation does not shed fibrous or particulate matter during assembly which could prevent sealing.

i. Certify that the field joint insulation will permit preflight demating. This shall not preclude insulation damage.

7.3.2.2 Development Objectives.

k. Determine mate/demate loads on hardware and GSE (including bondline stress).

l. Evaluate baseline joint configuration fit during and after mate.

n. Provide for crew training.

p. Validate procedures for RSRM assembly/disassembly and handling.

7.3.3 Results and Discussion

ATA testing in the VAB at KSC was supported by Insulation Design from 4-22 Dec 1987. Support activities included OMI review and making appropriate deviation changes, test activity inspection and reporting, and crew training and familiarization with redesigned joint procedures. Results of the reviews, inspections, test data, and the assembly process as they are applicable to the insulation assembly are described below.

7.3.3.1 Insulation Configuration. The ATA test field joint configuration was manufactured to the baseline field joint configuration which will be used for flight motors using mold tooling and processes common to the flight motors. The test field joint was the DM-9 configuration J-joint shown in Figure 1-2.

7.3.3.2 Joint Profile Inspection. ATA joint inspection was first made following insulation cure prior to propellant loading. Engineering analysis and experience has shown that loads created by slump change the joint configuration. Little change is seen in the tang joint profile because the propellant relief flap disengages the joint from the propellant shrinkage loads. However, the insulation configuration at the clevis changes significantly because of propellant slump except at the forward section Figure 7.18 which is a thin insulation section bonded to the steel case. The insulated level assembled joint analysis is given in Table 7-10. The gap at Point F is believed to be accurate even for the loaded motor segments. The other point gaps are presented for information to show the change in the analysis results caused by propellant slump as compared to the loaded segment joint analysis.

Engineering design shows the gap at Point F, near the capture feature, as 0.030 to 0.050 inch. ATA insulated level joint analysis shows all data for Point F with design limits except for a maximum value which is only 0.003 in. larger than the maximum design analysis gap of 0.050 inch.

The ATA test plan, CTP-0008, requests field joint profile measurements to be taken prior to the first full mate (dry fit), prior to the second full mate (wet fit), and again following final disassembly. Data from the first inspection was reduced by Morton Thiokol/KSC and showed the J-joint would contact the full radial length of the joint bonding surface (Figures 7-19 and 7-20) from the ID tip of the joint outboard to the radius except that contact would not be made at the radius from 96 to 102 deg. Reduced data at Morton Thiokol, using the same data, was in agreement. Inspection points were made at three locations, Points B, C, and D, along the J-joint bonding surface each 2 deg. Raw data noted an approximate 0.1 in. deflection at all

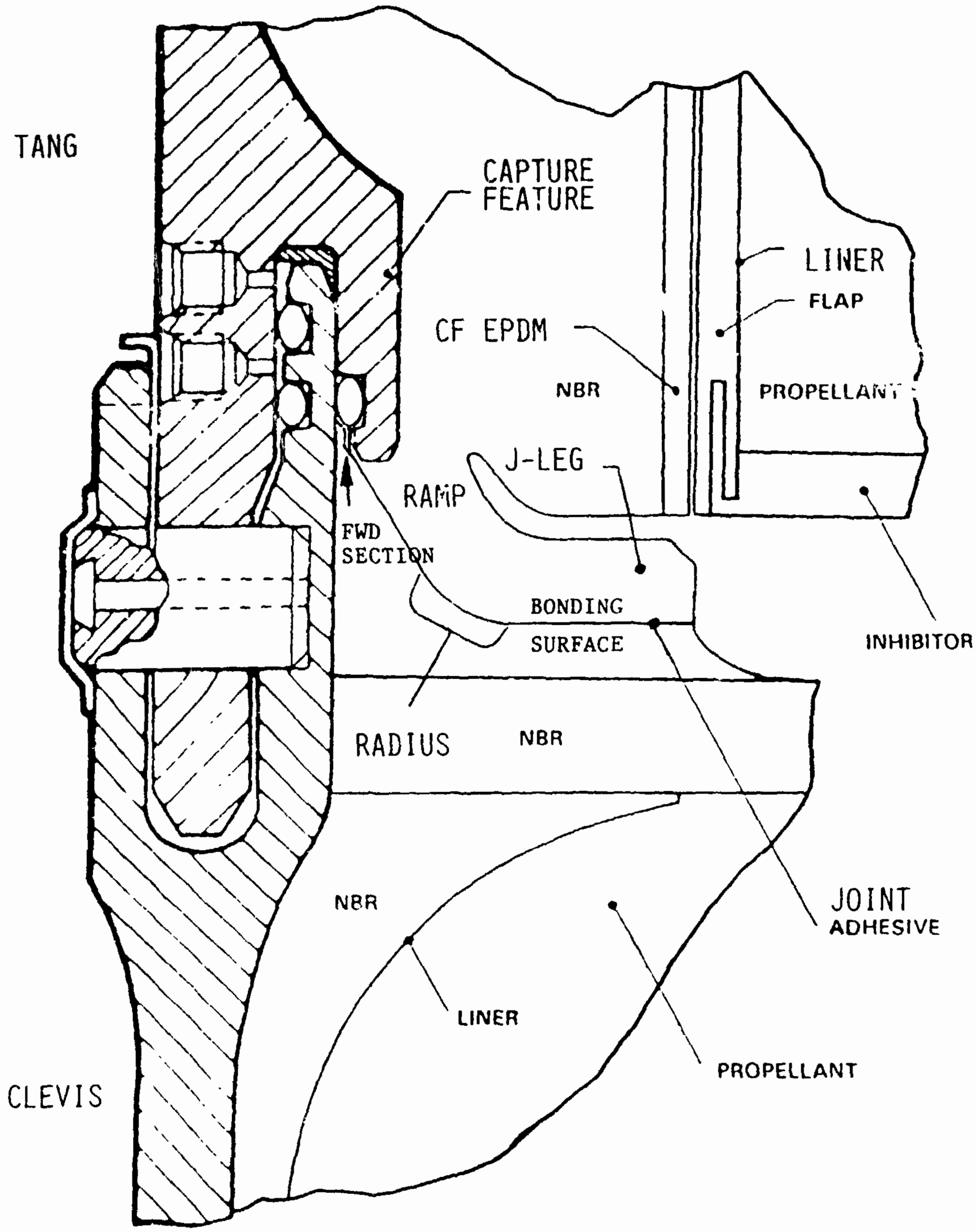

Figure 7-18. Assembled Field Joint Analysis Locations

Table 7-10. ATA Test Joint Gap Analysis

Location	A	B	C	D	E	F*
Engineering Design						
Minimum	0.000	0.000	0.000	-0.100	0.100	0.030
Nominal (75°F)	0.000	0.000	0.000	-0.299#	0.000	0.000
Maximum	0.000	0.000	0.000	0.000	0.220	0.050
ATA Pretest (insulated)						
Miniumu	-0.077	-0.203	-0.378	-0.576	-0.020	0.038
Maximum	-0.056	-0.177	-0.347	-0.536	-0.036	0.053
Average	-0.068	-0.193	-0.367	-0.557	0.006	0.046
ATA Pretest (loaded)						
Minimum	-0.074	-0.074	-0.296	-0.416	0.090	0.**
Maximum	0.030	0.070	-0.112	-0.269	0.310	0.**
Average	-0.031	-0.040	-0.220	-0.374	0.178	0.**
ATA Post-Test (loaded)						
Minimum	-0.026	-0.014	-0.154	-0.291	0.182	0.**
Maximum	0.011	0.024	-0.111	-0.242	0.223	0.**
Average	-0.005	0.010	-0.130	-0.262	-0.197	0.**

*The gap at "F" is not expected to change because of propellant slump in a loaded motor
**Dat was requested in the test plan but was not taken for the clevis joint
#Analysis at 75°F, vertical assembly

NOTE: " - " indicates interference

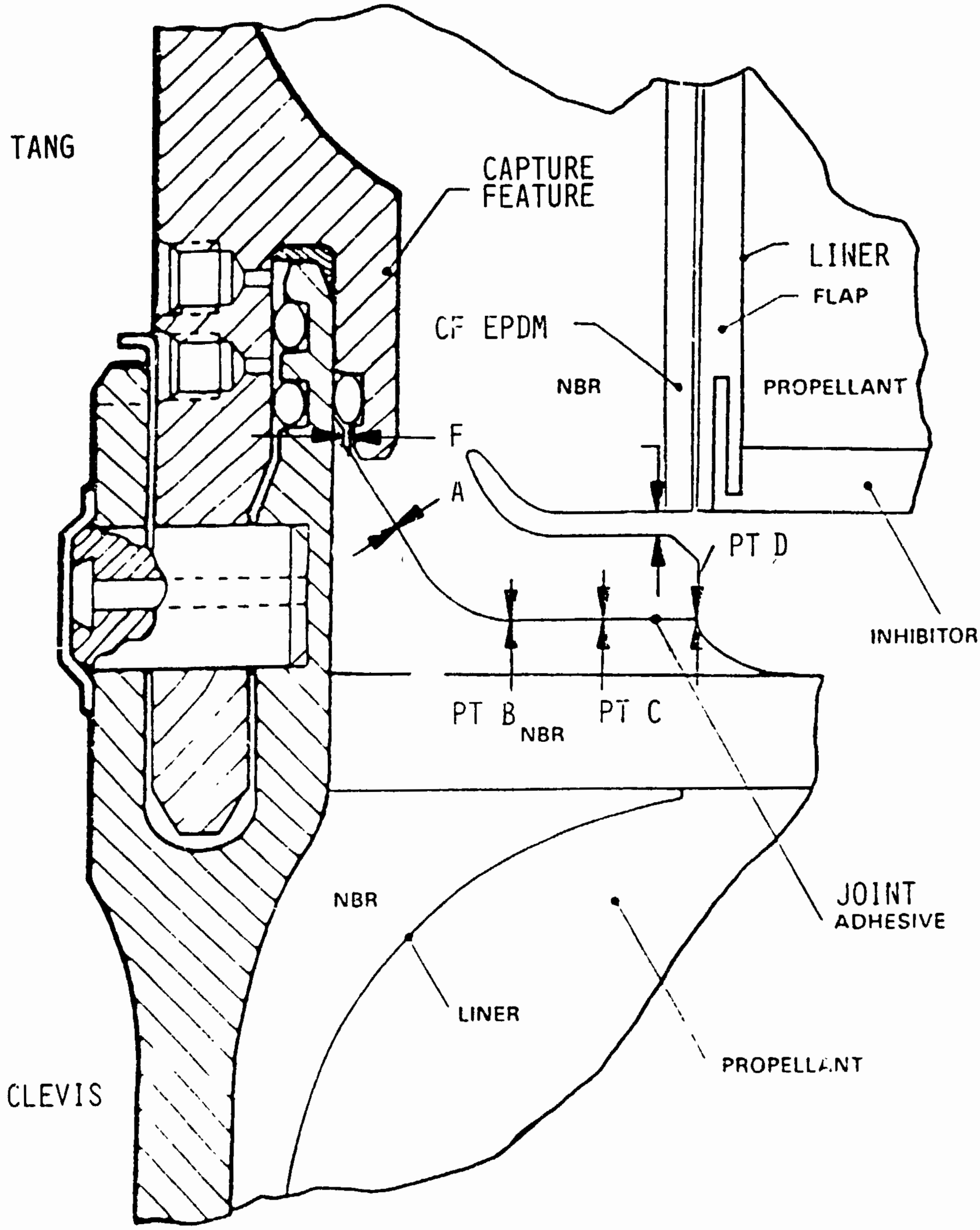

Figure 7-19. Assembled Field Joint Analysis Locations (Cont)

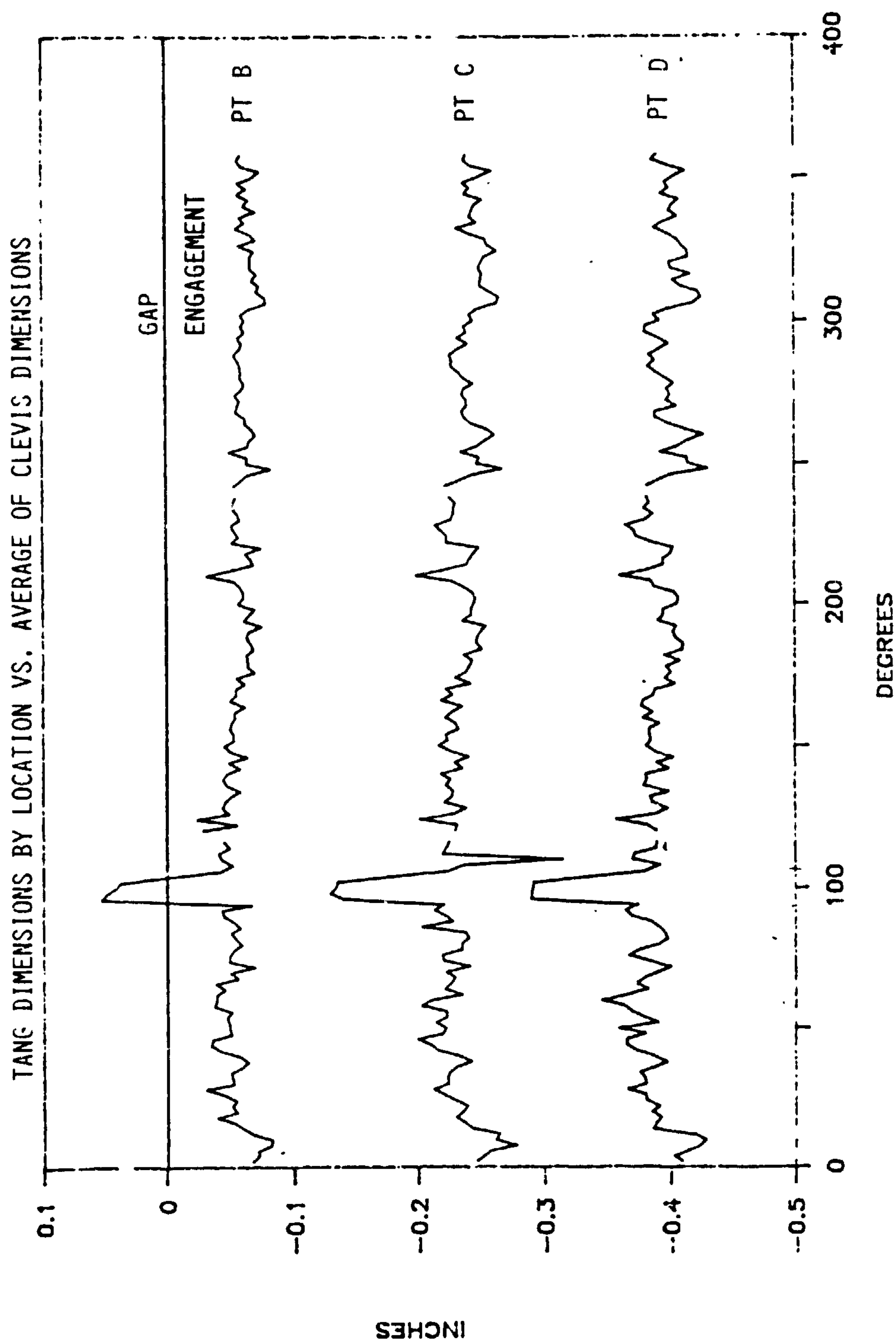

Figure 7-20. Flap-to-Flap Interference

three points. The joint insulation was deflected forward. Measurement data is dated 23-24 Nov 1987 and occurred in the RPSF building. One individual inspected the joint visually the dry inspection was made and noted the deflection. No one else reported any visible detection of the condition.

Inspections were made by insulation design on 5 Dec 1987 and did not note the deflected condition. A long (approximately 30 in.) straight edge was placed against the surface at the tip and again a little outboard of the tip and noted no deflection. Rough measurements were made with a straight edge and a 6-in. scale each 2 deg from 90 to 110 deg and at 60, 80, 120, and 140 deg. Not more than 0.030 in. variance was noted from minimum to maximum dimensions. The dry fit, performed later, did not indicate that the condition was present at that time.

Pretest loaded segment gap analysis shows a range of data having a maximum gap of 0.030 in. to an interference of 0.074 in. at Point A in the ramp. The engineering designed gap near this region (outboard of the capture feature ID tangent area shows a data range from 0.070 in. gap to 0.074 in. interference. At Point C, midway between the ID point of the radius and the ID tip of the J-joint, an interference range of 0.112 to 0.296 in. is shown and at the ID tip of the joint an interference range of 0.296 to 0.416 in. is shown. Minimum design interference at the joint engagement by profile analysis was met. The gap at Point E, the pressurization gap, had minimum and maximum conditions of gap opening which exceeded the design criteria, but the average gap dimension was near nominal design.

In comparison of the joint profile analysis with the dry fit and wet fit inspection results, defined in the following sections, the joint shows a configuration change at assembly. The joint profile analysis connotes continuous contact from the joint ID outboard to the radius, but the dry fit and wet fit inspections showed contact at the ID tip and through the radius only. No contact was indicated by these inspections at Points A or C. As the joint ID tip contacts at assembly, the tang insulation bends and rotates into the assembled condition. This action apparently changes the tang joint contour and eliminates the interference shown by the joint profile analysis at the ramp and between the radius and the joint ID (Points A and C).

The actual radial engagement of the joint was reduced at assembly by tang joint insulation rotation as explained above. This was apparent by joint inspection following both the dry mate and the wet mate.

Joint profile measurements requested per CTP-0008 prior to the final assembly were not taken due to schedule constraints. Profile measurements taken following the disassembly of the segments after the wet fit were taken and reduced to indicate a change in joint contour caused by slump and elapsed time and by material set caused by the assembled joint condition. The joint was demated 22 Dec 1987. Tang profile data was taken 22 Dec 1987 but clevis profile measurements were not taken until 6 Jan 1988. Most of the effects of material set are in the tang joint insulation, so effects of material set from this assembly should be noted by the data. Over a longer period of time the insulation material is expected to relax near to its original configuration. Prior to this inspection, the joint had been mated twice, and was in a mated condition for approximately 140 hr during the dry fit and 69 hr during the wet fit. Approximately 75 hr passed between disassembly at the dry fit and assembly at the wet mate.

Joint gap analysis following final demate showed that interference had decreased at all points along the joint mating surfaces. The average interference at Point A, in the ramp, was reduced by 0.026 in., and the 0.040-in. average interference at Joint B, the ID radius tangent, was reduced to 0.010 in. gap. The average interference at Point C, midway between Point B and the joint ID tip, decreased 0.090 in., and at Point D, the joint ID tip, 0.112 inch. Additional slump effects, caused by the increased time in a vertical position, could have resulted in small effects to the joint gap analysis as shown by the 0.019-in. increase at Point E, the slot gap. However, an undetermined amount of this possible variation may be attributed to inspection method accuracy.

7.3.3.3 Dry Fit--First Full Mate. Design engineering inspection found evidence of flashing in numerous places on the tang J-leg ID tip from the mold tooling sprue holes which was not removed at Morton Thiokol. Tape residue contamination was noted on tang/clevis joint surfaces. The joint was taped for masking at a previous procedure at Morton Thiokol. It is recommended that tape not be applied to the critical joint bonding surfaces for any procedures but that it be limited in application to the joint surfaces noted in TWA-1177 for joint masking. It is also recommended that joint surfaces be inspected for tape adhesive and other such residues and that they be solvent cleaned prior to joint abrasion processes.

A guard was fabricated from a thin sheet of Kevlar® (approximately 15 in. high by 30 in. wide by 0.0625 in. thick) to aid in the spray application. A phenolic block was attached 1.15 in. from the bottom of the Kevlar® sheet on each end to index the guard on the clevis end of the joint. This positioned the guard to cover the steel sealing surface on the ID of the clevis leg so that transfer medium application would be restricted to the NBR joint areas. A handle was also provided to hold the guard.

The guard was positioned and the application of the transfer medium was begun. Application of the dry fit transfer medium, Tinactin foot spray powder, was made on the clevis joint surfaces following grease application to the bare metal components. No abrasion was performed on the NBR joint surfaces at KSC prior to application of the spray. The powder spray was intended to be applied in a thin, full cover coat. It was soon noted that the application was not as uniform as most previous applications. As the spray hit the joint surface, it would jet up behind the guard and ball up. It would then either be blown over the tip of the clevis ID leg and drop into the clevis joint opening, contaminating the grease application, or it would roll down onto the NBR joint surfaces creating thick and nonuniform spray application. The use of the guard also created an effect like a blast shield which deflected the spray during application and adversely affected the application. The guard was removed after spraying approximately a 45-deg section of the joint and application results improved immediately. A fine overspray covered the inhibitor surface entirely and obviously got into the clevis joint as well. Joint leak check was a success, indicating that the overspray did not affect the O-ring sealing capability. The overall transfer medium application was not as good as most previous applications to test motors but was acceptable. Post-test inspection did not indicate that any of the application adversely affected the transfer for the test.

Several cans of the transfer medium were available during the application process and were rotated frequently. Application was made by Morton Thiokol engineers who developed and used the process at the Space Operations. The KSC technicians did not apply the material and only a few observed any of the application process. Probably only one shift of operators saw the finished application prior to joint mate. Additional training, specifically of the operators who did not observe the transfer medium application, would be warranted if dry fit testing of joints will continue for RSRM flight segment joints.

The O-rings were all installed just prior to joint assembly. The primary and secondary O-rings were installed with minimal effects but caused concern to insulation design that the O-rings might touch the sprayed joint surfaces and contaminate both the O-rings and the joint surfaces. The tang capture feature O-ring was raised into position and contacted the joint NBR at the radius full circumference. The O-ring was then pushed up the ramp area of the joint (outboard of the radius) and into the O-ring groove, leaving a grease film along the entire ramp. Following this finding, insulation design requested that all future final assemblies have the joint adhesive applied last, after the joint surfaces are inspected and determined to be clean. This would help ensure that during final assemblies, using joint adhesive, the bonding surfaces and adhesive would not be contaminated with grease. The recommended order of the assembly steps are detailed in a later section.

Following installation of the joint O-rings, a final joint inspection was made prior to joint assembly. It was noted that the FJAF tool had been coated with a Teflon® spray and that it was flaking off. Air ducts were blowing conditioned air into the enclosure and they were aimed at the segment. The air flow was picking up the Teflon® flakes and blowing them into the greased area of the joint and would also have blow them into the joint adhesive had this been a final joint assembly. Most of the contamination was painstakingly removed by hand prior to joint assembly. A recommendation was made that the tool be thoroughly cleaned prior to its next use and that future assembly instructions add an inspection step to catch similar contamination. The tool was cleaned and no such problem was encountered during the wet mate assembly.

The dry fit inspection of ATA, using transfer medium, showed contact full circumference at the J-seal ID tip (0.40 to 0.45 in. radial engagement typical) and at the joint radius (0.8 to 0.9 in. surface length around the radius) as shown in Figure 7-21. Radial contact was shown for short arc lengths from 0.35 in. minimum to 0.65 in. maximum. No contact was noted between the engagement at the ID tip and the engagement at the radius or between the engagement at the radius and the NBR/case interface. At assembly, the tang J-seal tip engaged and scraped 0.25 to 0.28 in. of powder off the clevis surface. Engagement stopped with the tang tip 0.08 to 0.09 in. outboard of the clevis seal surface ID. A portion of the engagement face of the tang J-seal was masked out by the powder being scraped off at engagement but did not significantly affect the demate inspection. Joint contact in the radius did not affect contact at the joint ID tip. Engineering design nominal radial contact at the tip is 0.201 in. with the segment vertical and the propellant mean bulk temperature (PMBT) at 75°F. Joint contact at the tip exceeded the design nominal despite the contact in the joint radius. Table 7-11 shows the deg locations and the radial contact distance at the ID tip of the J-joint tang leg as measured with a 6-in. scale.

Definition of joint contact using indications of transfer powder was somewhat subjective. Transfer varies from almost no transfer to heavy transfer and is affected somewhat by the local thickness of application, the J-joint assembled load, possibly by how level the segments are at assembly and disassembly, and possibly by environmental effects on the transfer medium. The degree of transfer noted during the dry fit inspection is summarized in Table 7-12.

Engineering design analysis, documented in TWR-16188 presents engagement lengths (radial surface contact) for four regions along the

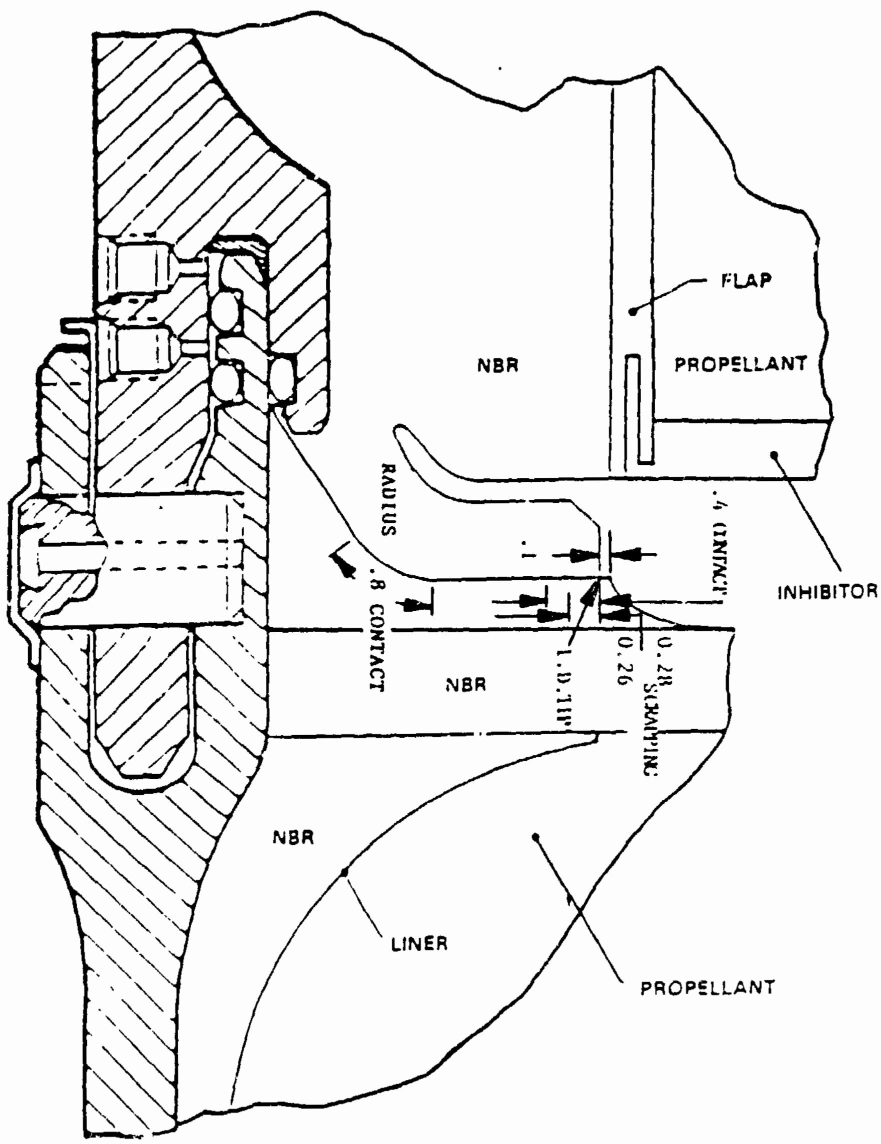

Figure 7-21. Dry Fit Inspection Summary

Table 7-11. Transfer Medium Inspection J-leg Tip Contact

Location (deg)	Radial Xfer (in.)	Location (deg)	Radial Xfer (in.)
2	0.35	134-148	0.42
4-6	0.40	150-158	0.45
8	0.45	160	0.40
10	0.50	162	0.45
12-16	0.40	163	0.55
18-20	0.50	164-168	0.45
22-38	0.40	170-172	0.55
40-54	0.38	174	0.34
56	0.40	176	0.32
58-70	0.50	178	0.45
72	0.45	180	0.50
76-78	0.43	182-188	0.65
80-82	0.45	190	0.55
84-88	0.38	192-206	0.45
90	0.34	208-264	0.40
92-94	0.38	266-270	0.50
96	0.40	272	0.54
98	0.50	274	0.56
100-106	0.45	276	0.58
108	0.30	278	0.55
109	0.15*	280-296	0.45
110	0.32	298-320	0.40
112-122	0.45	322-360	0.40
124-132	0.37		

*Local occurrence only--more indicative of transfer medium variance and not joint contact

Table 7-12. Dry Fit Inspection Summary

Location (deg)	Transfer	Location (deg)	Transfer
0 to 12	Medium	148 to 171	Medium to Heavy
12 to 16	Light	171 to 173	Heavy
16 to 32	Light to Medium	173 to 178	Light to Medium
32 to 46	Light	178 to 192	Medium to Heavy
46 to 58	Medium	192 to 238	Medium
58 to 72	Heavy	238 to 246	Light to Medium
72 to 84	Medium	246 to 254	Medium
84 to 94	Very Light to Light	254 to 264	Very Light to Light
94 to 104	Medium to Heavy	264 to 282	Medium
104 to 112	Light	282 to 300	Light to Medium
112 to 122	Medium	300 to 320	Nothing* to Light
122 to 132	Light	320 to 346	Very Light to Medium
132 to 142	Medium	346 to 360	Medium
142 to 148	Medium		

Where:
Light = Slight trace of powder transfer
Medium = Positive indication of powder transfer
Heavy = Continuous or caked indication of powder transfer
Nothing = Speckled transfer but no continuous band of transfer

insulation joint mating surface and are presented in the Table 7-13 for segments assembled in a vertical position.

The typical surface engagements distance of 0.40 to 0.45 in. and even the minimum distance of 0.35 in. and maximum distance of 0.065 in. are well within the defined engineering analysis results. The engagement distance of 0.8 to 0.9 in. through the radius exceeded the design analysis but does not seem to affect the ID tip engagement. No contact was noted on the ramp unless it was near the radius OD and that was not individually distinguished during the dry fit inspection. No contact was noted in the forward section either.

Three areas (0, 120, 240 deg) on the clevis joint had been repaired (very well) from a previous instrumentation assembly but the areas were still easily noted in the transfer medium during inspection.

The repair area at 0 deg showed a burp track through the transfer powder along the side of the repair at 359 deg. The transfer was reduced to approximately 0.25 in. in the radius at the local area. Transfer at the J-leg ID tip was not affected, nor was the burp track evident at the ID tip. The design of the J-joint allows air to be exhausted from the joint as pressure builds during assembly as well as achieving a joint contact at motor ignition. The burp track in the transfer medium indicated a path of concentrated air exhaust from the joint during the dry fit assembly and did not indicate a defective condition of the joint. The radius portion of the joint, where the burp track was noted, is not in the critical bondline of the joint nor will instrumentation and channel repairs be a part of flight motor field joints.

The slight protrusions remaining on the tang ID tip surfaces, from the mold tooling sprue holes, also showed up very well in the clevis surface inspection as heavy contact and scrape marks. Joint contact was noted adjacent to each protrusion, but at a lesser degree. Powder was also noted on the tang J-seal between the radius and the steel interface but appeared to have only settled in this area after being stirred up by exhausting air at joint assembly. The powder was not transferred by contact. No effects were noted which were attributed to the joint leak test.

Table 7-13. Joint Engagement Ranges

		40°F (in.)	75°F (in.)	90°F (in.)
Region 1 (ID tip)	Minimum	0.1348	0.1348	0.6739
	Maximum	0.2692	0.2692	0.7969
Region 2 (radius)	Minimum	N/A	Point	0.2500
	Maximum	N/A	0.0184	0.1783
Region 3 (ramp)	Minimum	0.1246	0.1246	0.2071
	Maximum	0.2071	0.2071	0.1246
Region 4 (forward section)	Minimum	Point	Point	Point
	Maximum	0.0530	0.0530	0.0530

A comparison of the dry fit results to the joint profile measurements does not show very good compatibility. The profile measurement analysis only defines probable engagement at specific inspection points while the dry fit with transfer medium shows positive contact anywhere in the joint. Even considering the large difference in the type of inspection results, no contact was noted along the bonding surface of the J-joint between the ID contact point and the beginning of the radius by the dry fit, whereas the joint profile analysis showed contact in this area full circumference.

Both inspection methods did indicate contact at the inside diameter of the J-joint, which is the most critical area, and at the radius.

7.3.3.4 Wet Fit--Second Full Mate With Joint Adhesive. Tang and clevis joint surfaces were wet abraded using abrasive paper and trichloroethane. The figure describing joint insulation abrasion, from TWA-1177, was added to the OMI by a deviation. Insulation design engineering aided with the abrasion and approved the final result prior to joint assembly. An engineer also donned a respirator, face shield, coveralls, and gloves and abraded approximately three-fourths of the tang joint surfaces while a hose from an atmosphere testing device was attached to him for asbestos sampling. The sample was taken continuously in excess of 10 min and sampled all particles, not just asbestos. The safety person operating the test equipment indicated he had registered 0.01 parts per cm^3 and was well below the allowable limits. The test apparatus did not discern if the sample contained asbestos or other airborne particles. Abrasion of the tang was accomplished using 180- and 220-grit abrasives.

The coarser abrasive did a better job in less time. The protuberances at the tang J-leg ID were removed and the J-joint surfaces were inspected and approved by insulation design. The protuberances should have been removed at Morton Thiokol prior to shipping. Criteria states that the protuberances shall be no more than 0.01 in. high. Quality has no way of measuring the height of the protuberances accurately in a timely manner. It is recommended that the inspection criteria be changed to indicate that protuberances be abraded until they cannot be felt by touch and that an inspection standard be provided if necessary.

A complete abrasion of the clevis joint surface was accomplished the first time using 600-grit abrasive paper and barely dulled the sheen on only a portion of the joint. The OMI called for 180 or finer grit abrasive to be used and 600-grit abrasive was available on the platform when the work began. The surfaces were abraded again using 180-grit abrasive paper. A request was made that the flight OMIs be changed to specifically request 180- to 220-grit abrasive to reduce the process time and ensure adequate abrasion of the joint surfaces. It is also recommended that a caution be added to the OMI that the ID corners of the tang J-leg and the clevis bonding surface not be rounded during the abrasion process. Rounding of the corners would cause a slight opening at the joint ID contact point.

Prior to abrading the joint surfaces, grease had been removed from the joint surfaces. The steel and NBR joint surfaces had been cleaned with trichloroethane. Following the abrasion process, the joint surfaces were again cleaned and the NBR portions of the joint were masked using Velostat® (black anti-static plastic sheeting) and aluminum conductive tape. The joint was masked as described in TWA-1177 and shown in Figure 7-22. TWA-1177 calls out the use of yellow vinyl tape and Kraft paper but the use of both materials was disapproved. Vinyl tape caused too much static charge when being removed from the tape roll and probably would have at removal from the masked surfaces also. The Kraft paper is flammable and was not allowed for use. The actual figures from TWA-1177 were added to the OMI by deviation with the above noted material changes included. It is recommended that TWA-1177 be changed to reflect the use of Velostat® and aluminum tape.

Transfer medium from the previous test had been removed from the joint surfaces and residues were cleaned out of the steel joint areas. However, the spray powder overspray was noted to extend to the bore of the segment but it was only cleaned from the joint inboard to an arms length. Morton Thiokol engineers requested that the overspray be entirely removed but were told that KSC operations did not allow anyone above or on the inhibitor surface to do such a cleaning operation. The ducted air blowing toward the segment stirred up the powder constantly, transferred it into the joint grease, and created quite a contamination problem. A recommendation was

NOTE:

1) ABRADE BETWEEN POINTS B AND C NOT TO EXCEED POINT D

2) APPLY VELOSTAT TO COVER POINTS B AND C. SECURE VELOSTAT WITH ALUMINUM CONDUCTINE TAPE OVER-LAPPING EACH END UP TO POINTS A AND D.

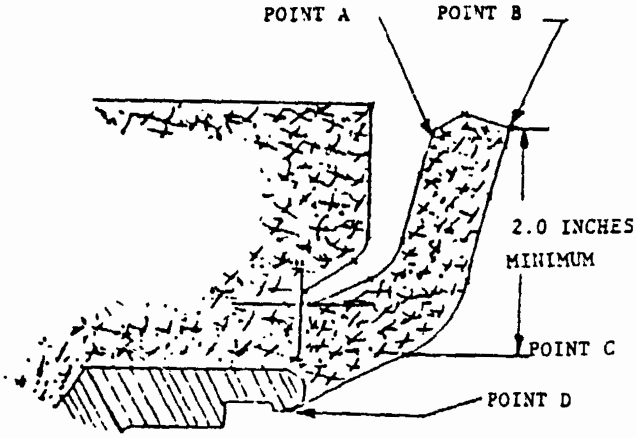

NOTE:

1) ABRADE BETWEEN POINTS B AND C. NOT TO EXCEED POINT D.

2) APPLY VELOSTAT TO COVER POINTS B AND C. SECURE VELOSTAT WITH ALUMINUM CONDUCTIVE TAPE OVER-LAPPING EACH END UP TO POINTS A AND D.

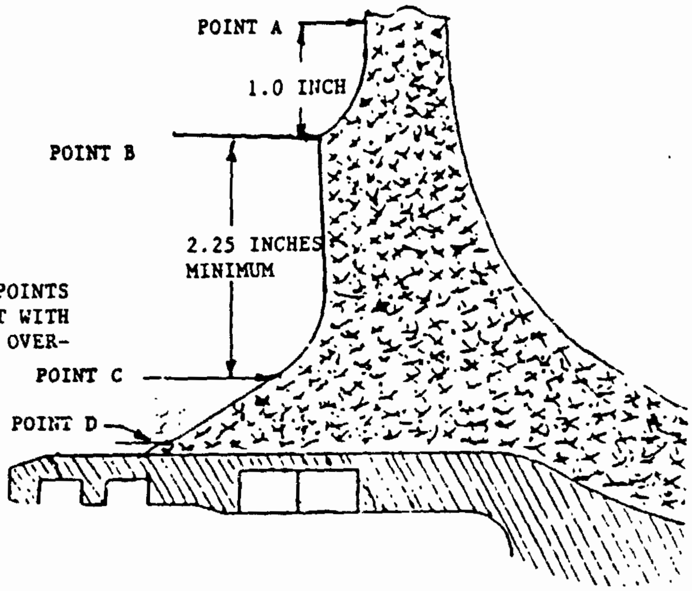

Figure 7-22. J-seal and Insulation Adhesive Surface Preparation

made that all transfer powder be cleaned off of segment surfaces in the future before proceeding with other tests.

Just prior to applying the adhesive, after removal of the masking, the joint surfaces were inspected by insulation design engineers for defects and contamination. Tiny rolls of insulation were noted which had balled up during the abrasion process and had not been removed by the solvent wipe. This condition would probably not affect the function or integrity of the joint except if the residue were excessive enough to act like a dust contaminant to the joint adhesive. It is recommended that a good joint inspection be accomplished prior to applying the adhesive to detect abrasion residues. It is also recommended that a ultraviolet light (blacklight) inspection be accomplished on the tang and clevis J-joint surfaces prior to adhesive application. Any indications of grease should be removed.

The solvent dispersed joint adhesive (STW5-3479) was applied using 2-in. wide foam brushes as described in TWR-1177 and shown in Figure 7-23. Insulation design engineers began the application to the tang joint surface to show the operators the method of application. The forward end of the aft segment was completely covered by Velostat® at this time to prevent adhesive from dropping and contaminating the clevis joint surfaces or the greased clevis surfaces. KSC operators then began the application of the adhesive from the starting point and progressed in both directions around the joint to completion. After removing the Velostat® from the aft segment, the clevis joint surfaces were also prepared with joint adhesive by KSC technicians using the same methods. Adhesive was applied to the joint surfaces as shown in Figure 7-23 and typically extended from the joint ID to halfway around the radius. It required less than 20 min and less than 1 qt of adhesive to prepare each joint, however, if a problem were to be encountered, the adhesive would most probably exceed its pot life prior to completing application and an additional kit would be needed. Small discrepancies were noted in the application where the adhesive was applied up into the radius area, out of the tolerance zone. This condition would

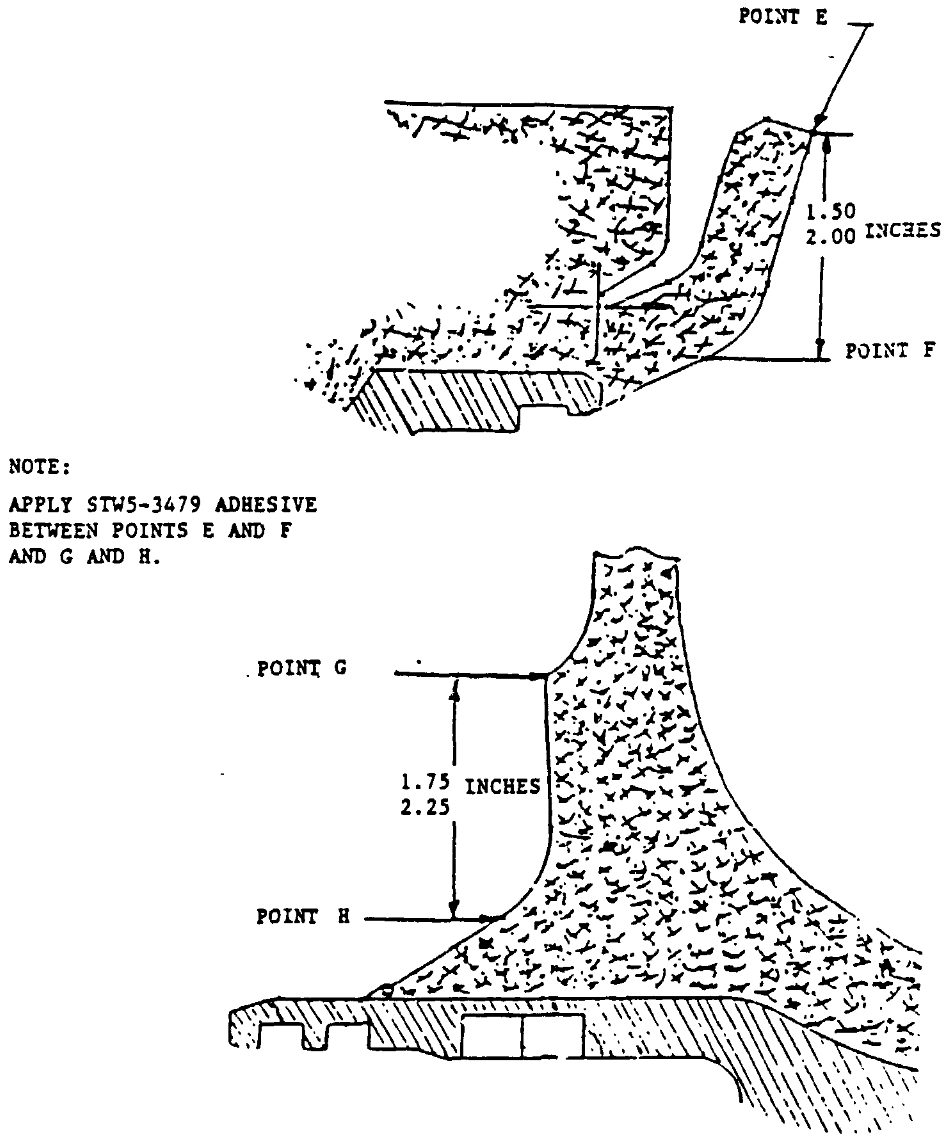

Figure 7-23. J-seal and Insulation Adhesive Application Surfaces

not have affected the joint operation but was repaired by removing the excess adhesive with lint free cloths and trichloroethane to comply with application tolerances.

The final assembly of ATA, using joint pressure sensitive adhesive (wet fit), showed joint contact full circumference at the J-seal ID tip, and at the radius. The adhesive application did not extend around the radius, so the engagement distance was not determined. The adhesive apparently is applied with a thinner, more uniform thickness than the transfer medium and generally shows slightly less contact (radially) than the transfer medium indicated. The reduced radial contact distance may also have been caused by less contact due to insulation set caused by the dry mate.

a. Tang. The adhesive at the ID tip, where initial contact is made at assembly, was increasingly thinner, giving an indication of the contact and scraping action of the tang at assembly (Figure 7-24). The adhesive was not scraped completely off nor was it rolled up. Some indications of adhesive were apparent on the ID facing surface (not the contact surface) of the J-leg where adhesive oozed over the edge at application. No indications were apparent that adhesive plowed up in front of the tang ID edge by the scraping action.

The adhesive failed at the bondline full circumference. No instances were noted where patches of adhesive were pulled up from the NBR.

Contact at the joint ID tip was roughly 0.19 in. radially (typical) and formed a fairly uniform band of contact. Contact ranged from 0.13 in. minimum to 0.34 in. maximum. The minimum and maximum occurrences were for very short arc lengths. The inboard indication of contact, along the band of contact, was very uniform but the outboard edge was ragged intermittently and exhibited a hairline of no contact, in many instances, between the uniform band of contact and the ragged portion of contact.

It is thought that the uniform band defines the original contact point on the clevis joint and the area scraped at assembly. The hairline

MORTON THIOKOL, INC.
Space Operations

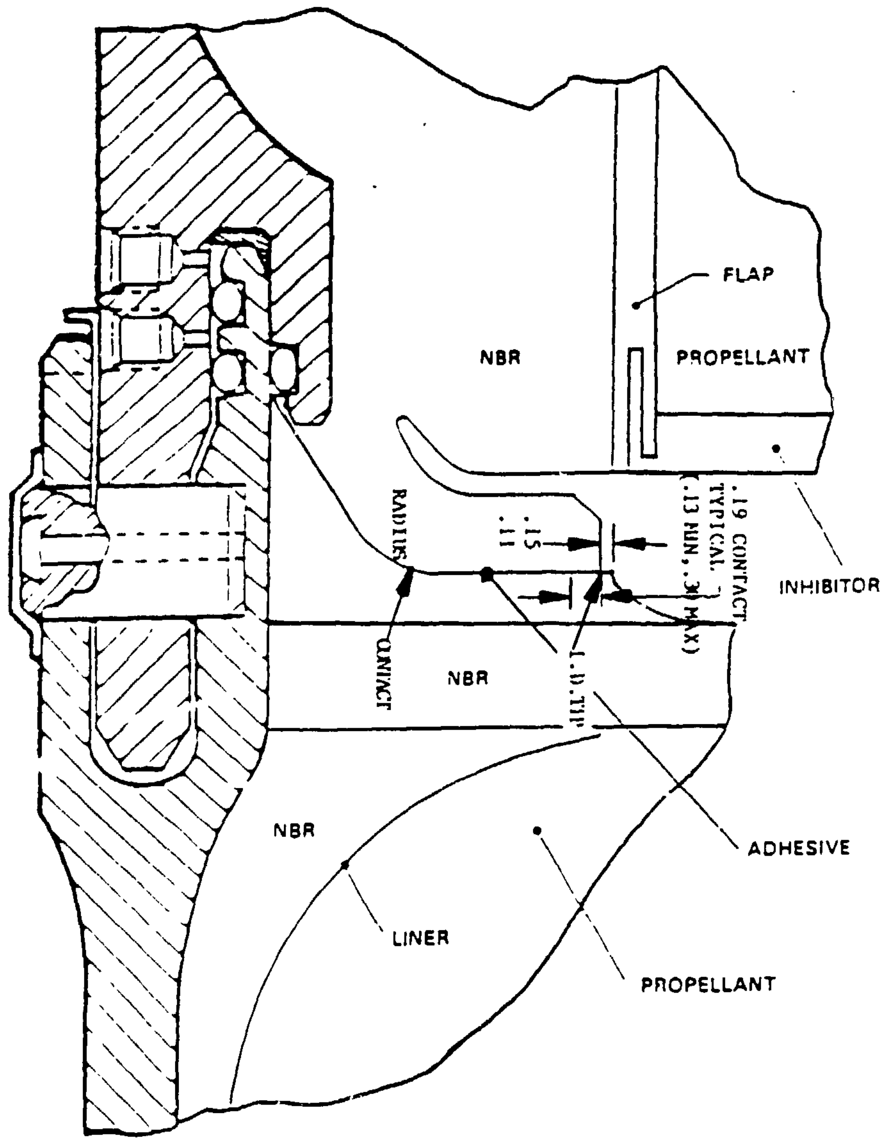

Figure 7-24. Wet Fit Inspection Summary

between the uniform bond and the ragged portions is believed to be the point of original contact and highest pressure at assembly where adhesive was removed or a slight ridge formed and transferred back to the full assembled joint on the tang surface as no contact. The same indications held true for the clevis surface and also suggest the ragged looking contact areas are caused at final assembly and not at initial contact.

Table 7-14, below, presents the definition of the uniform contact distance in the joint and the ragged contact areas each 45 deg.

Table 7 14. Joint Adhesive Inspection J-leg Tip

Location (deg)	Uniform Contact Radial Distance (in.)	Total Contact Incl/Ragged Edge (in.)
0	0.20	0.30
45	0.17	0.23
90	0.20	N/A
135	0.21	N/A
180	0.24	N/A
225	0.14	0.27
270	0.23	N/A
315	0.21	N/A

Data in the above table are typical for the entire tang side of the joint, showing mostly 0.19- to 0.21-in. radial contact. The minimum contact distance was noted at 148 deg and was 0.13 in. for 1.0 in. circumferentially. The largest contact distance was 0.34 in. at 337 deg. A ragged outboard contact edge was evident from 0 to 76 deg and smooths out from 76 to 144 deg. From 144 to 244 deg, a ragged outboard edge was again apparent and exhibited the hairline separation line of no transfer described above. This line was visible most of the way around the joint but was not as evident in this region. The ragged edge decreased significantly from 244 to 360 deg. Spotty indications of ragged edges in this region were visible but not to the extent as found at 0 to 76 deg.

Grease, from the capture feature O-ring installation and joint grease touchup, was noted on the tang joint NBR surface in a uniform, full cover coat approximately 0.3 in. aft of the capture feature where the masking did not extend. It is recommended that the tang joint masking be placed on the tang joint as far aft as possible without introducing a large possibility of degrading the steel joint grease application.

b. Clevis. The clevis surface shows a free, noncontact area at the ID edge as was shown for the transfer medium inspection. The noncontact area is 0.11 to 0.15 in. radial length (Figure 7-5). Contact is shown in a uniform band outboard of this noncontact area with a ragged appearance intermittently just outboard of the uniform band full circumference as was shown for the tang side as described above. The band of contact is typically 0.19 in. radially (0.17 minimum to 0.29 maximum). Contact was representative of that shown on the tang but some areas did not appear to match exactly from tang to clevis. Table 7-15 details some of the inspection dimensions.

Up to 0.29 in. maximum of radial contact at 10 deg was shown for a short arc length. The hairline division between the uniform band of contact and the ragged edge of contact was apparent as described for the tang side of the joint. The contact showing the ragged appearance is heaviest between 0 to 10 deg, 120 to 300 deg, and 334 to 360 deg. At 146 deg the ragged edge shows a total contact variance of 0.15 to 0.23 inch. The joint adhesive also exhibited adhesive failure at the tang adhesive to the clevis adhesive as shown by inspection of the clevis joint surfaces. No areas were noted where joint adhesive had peeled up from the NBR surface and a full cover coat of the joint adhesive remained in place.

No contact of the joint was noted in the adhesive between the contact at the ID of the joint and the radius. Contact is shown full circumference in the radius as well as at the joint ID. The surface distance of contact in the radius was not determined because the adhesive did not extend around the radius. The inboard edge of contact is fairly consistent around the joint circumference and appears to start near the transition point of the radius.

Table 7-15. Joint Adhesive Inspection Clevis Surface

Location (deg)	Noncontact at ID of Surface (in.)	Hard Contact (in.)	Ragged Edge Total Contact (in.)
0	0.11	0.19	N/A
45	N/A	0.19	N/A
90	0.14	0.17	N/A
135	0.13	0.23	N/A
180	0.12	0.20	0.30
225	0.13	0.18	0.30
270	0.15	0.19	0.23
315	0.14	0.20	Spotty

Grease did extend onto the clevis NBR surface but only as far as the initial step at the extreme forward edge of the joint. No beads of grease had been pushed up in front of the capture feature O-ring. Demate inspection of the grease in regard to the insulation was very satisfactory.

Joint

Inspection of the joint surfaces, tang and clevis, did not detect any indications that the joint or insulation structural integrity had been compromised by the mate/demate procedure. There were no visible indications that the J-joint configuration or the insulation material was damaged by the mate or demate process. No fibrous or particulate matter from the insulation was noted. No indications were noted, either, that the J-joint configuration did not maintain structural integrity during the assembly process. Joint inspection did note an unacceptable level of contamination in the joint. Lint, dust, hair, and transfer medium was found in the joint adhesive and in the steel portions of the joint. Recommendations to reduce the contamination are detailed later in the section documenting the joint assembly enclosure.

The results of the wet mate inspection compared favorably with the results of the dry fit inspection. The radial length of engagement at the J-joint ID tip was longer for the dry fit than was noted for the wet mate but the difference can probably be attributed to the difference in the materials and the application thickness and to the effects of material set caused by multiple assemblies. The same regions showed contact for both inspections. The wet mate, therefore, did not compare favorably with the results of the joint profile analysis any better than the dry fit compared with the joint profile analysis.

Contact at the joint ID tip, as noted on the clevis (0.17 minimum to 0.29 maximum), though reduced from the dry fit contact length, is still well within the contact lengths found in Table 7-13 from engineering design analysis.

Photo coverage was not achieved as specified because of restrictions and schedule restraints. Some photos were taken but not with the proper views and not as specified in CTP-0008.

At the completion of the wet mate test the joint adhesive was to be cleaned off prior to closing out the segment. This was to occur for storage and shipment of the segments and to familiarize the technicians with adhesive removal, should it be required for flight motors. Instructions were given that the adhesive should be removed with clean cloths and trichloroethane solvent. The leadman and operations engineer were told that the adhesive does not come off easily and that a lot of work would be required to remove it. They were also told that the adhesive rolls into balls as it comes off and does not dissolve in the solvent. As soon as the work started to remove the adhesive, requests were made to allow the use of alternate solvents and techniques. Power tools are not allowed for use on the joint surface and other solvents have not been used at Morton Thiokol except that methyl ethyl ketone (MEK) was used on a trial basis. MEK does not remove the solvent any more readily than trichloroethane and its flammability is higher and is, therefore, a safety risk. Therefore, the suggested removal method was used to clean the joint. Insulation design recommends that the removal method and acceptance requirements be specified in the appropriate document.

7.3.3.5 Case Unbonds. Case unbond inspection was made of the ATA segments at Morton Thiokol and KSC during fabrication and test operations. Table 7-16 documents the results of the center segment case unbonds noted at Morton Thiokol. Table 7-17 documents case unbonds noted on the same segment at KSC. Table 7-18 documents the case unbonds noted on the aft segment at KSC. Evaluation of the data indicates that detection and documentation of unbonds is highly operator and tool sensitive. The frequency of detected unbonds grows with increased inspection and increased intensity of the inspection as seen by evaluation of the center segment data at Morton Thiokol. Only one set of unbond data is given for the same segment at KSC but the data was gathered from at least two separate inspections, once in the RPSF at receiving and later in the VAB. Data for the aft segment

Table 7-16. Aft Center Segment Clevis Unbonds--Morton Thiokol

--Insulated level inspection at Morton Thiokol, 8 Oct 1987 --Horizonta. --DR 150569		--Loaded level reinspection at Morton Thiokol, 26 Oct 1987 --Horizontal inspection --DR 150569, first MRI		--Loaded level, reinspection per MRI, 27 Oct 1987 --Horizontal inspection --DR 150569, second MRI	
Location (deg/in.)	Axial Length (in.)	Circumferential Location (deg)	Axial Length (in.)	Circumferential Location (deg)	Axial Length (in.)
27/1.050	0.104	27, 1.8	0.104	27, 1.8	0.15
35/0.5	0.075	35, 1.9	0.100	29, 1.3	0.10
39/7.0	0.100	39, 7.0	0.100	30, 0.35	0.10
43/1.5	0.090	43, 1.5	0.090	35, 2.70	0.13
57/0.9	0.C25	57, 0.90	0.025	36-41 ,6.00	0.13
58/0.6	0.010	58, 0.600	0.010	43, 1.5	0.125
62-66	0.006	62-66	0.100	47, 0.50	0.09
174/3.0	0.225	174, 3.0	0.300	57, 1.15	0.008
184/0.4	0.056	184, 060	0.100	58, 0.50	0.06
				64, 1.325	0.125
				68, 0.625	0.110
				70, 1.25	0.110
				76, 1.80	0.125
				101, 0.75	0.10
				110, 0.920	0.10
				114, 1.60	0.10
				172, 3.15	0.13
				184, 0.70	0.125
				326, 0.15	0.10
				328, 0.45	0.15
				329, 0.445	0.25
				332, 3.325	0.15
				348, 0.425	0.165
				359, 1.645	0.125

QA stated that full depth of unbonds were probed. Also, unbonds were noted which were not documented

Note: In DR stated that larger unbonds enlarge while probing

Table 7-17. ATA Aft Center Segment
Clevis Unbonds--KSC

--Receiving inspection at RPSF, 19 Nov 1987
--Horizontal inspection
--PR PV-6-086545

--Inspection with air load tool in VAD not available. Axial unbond distances not taken

Location (deg)	Axial Length (in.)	Circumferential Location (deg)	Axial Length (in.)
0, 0.171 in. circumferential	0.062	104-120, 19.75 in.	0.078
2, 0.187	0.046	121-125, 6.0	0.0932
4.5, 0.656	0.078	173, 2.75	0.343
6, 0.234	0.046	181-182, 1.75	0.155
9, 1.0	0.078	184, 0.50	0.140
18, 0.625	0.046	185, 0.50	0.156
28, 3.812	0.125	187-189, 2.85	0.109
34, 2.125	0.093	191-193, 1.85	0.109
38, 3.718	0.125	195, 0.749	0.093
40, 2,078	0.125	198-210, 15	0.109 average
43, 1.281	0.078	219-226, 8.5	0.109 average
48, 1.5	0.109	230-232, 2.0	0.155
56, 1.625	0.062	237-240, 3.0	0.140
58, 1.343	0.093	244, 1.50	0.124
65, 1.484	0.093	276-292, 20.50	0.109
68, 0.5	0.125	295-338, 4.325 ft	0.124 average
70, 1.0	0.062	338-342, 6.0 in.	0.125
77, 1.0	0.078	353-356, 5.0 in.	0.109
88, 1.0	0.156		
90, 0.75	0.125		
100, 20	0.062		

Table 7-18. Aft Segment Clevis Unbonds--KSC

--Receiving inspection at RPSF 15 Nov 1967 --Horizontal inspection --PR PV-6-086141, Item 1		--Repeat inspection at RPSF 18 Nov 1987 --Horizontal inspection --PR PV-6-086141, Item 1.5		--ATA inspection, full casting segment in VAB, D-level, High Bay 1, 6 Dec 1987 --Vertical inspection --PR PV-6-086141, Item 2	
Circumferential Location (deg/in.)	Axial Length (in.)	Location (deg)	Axial Length (in.)	Location (deg)	Axial Length
76/1/16	0.015	76	0.093	0 to 40	Requested but not determined
120-123/2.5	0.015 at 120 deg, 0.061 at 122 deg	120	0.78	42, 1/4 in. circumferential	
130-133/3.0	0.061 at 130 deg, 0.015 at 132 deg	122	0.046	44, 1/2 in. circumferential	
141-142/1.5	0.046			45 to 54	
219/1.5	0.124			56, 1/4 in. circumferential	
193, 3/8	0.046			60, 1/4 in. circumferential	
198, 1/2	0.015			62, 1/4 in. circumferential	
221-223, 2.0	0.140 at 221 deg, 0.109 at 223 deg			67, 1/2 in. circumferential	
226-230, 4.5	0.124 at 226 deg, 0.109 at 228 deg			72 to 76	
236-252 intermittent	0.061 minimum, 1.140 maximum			77 to 81	
300, 3/8	0.093			82 to 87	
302/1.5	0.109			89 to 91	
307, 1/8	0.078			113 to 120	
306, 1/4	0.078			122 to 148	
309, 1/8	0.078			148 to 156	
				157 to 166	
				167, 1/2 in. circumferential	
				168 to 171	
				172 to 202	
				204 to 224	
				225 to 288	
				290, 1/2 in. circumferential	
				295 to 330	
				332 to 359	
				57	

unbonds at KSC also seems to follow this trend. It was also noted that inspection results from one inspection are not accurately duplicated by the next inspection even on the same DR from inspection to inspection. Unbonds found at Morton Thiokol are not accurately duplicated at KSC either.

Unbond inspection results could be influenced by a number of factors, i.e., temperature (PMBT), horizontal versus vertical segment orientation, tooling, inspection methods and operator sensitivity. Evaluation of the results do not indicate that the unbonds are growing so much as it indicates a need for accurate accepted inspection method which will provide uniform and consistent results.

The air load tool, for inspection of unbonds, was used on the clevis end of the aft segment while the segment was stacked for the dry mate. A detailed inspection was not made but the results were recorded on videotape. Observation of the process noted that large areas of the joint were unbonded. Unbonds extended approximately 0.2 to 0.3 in. maximum axially. Visual inspection noted that the Chemlok® bonding materials were present and that they had all separated from the case wall and were attached to the NBR. The air jet, aimed right at the leading edge of the NBR, opened up the unbonds so that they were readily apparent visually and on the video monitor. The grease had not been cleaned off from the clevis ID surface and it was noted that when the unbonds would open up, the air jet would blow grease into the bondline. It is strongly recommended that future inspection with the air load tool be accomplished only after the grease is thoroughly cleaned off of the clevis ID leg inner face. Repairs may be necessary and would be improved with out grease contamination. Following a pass of the air load tool, it was also noted that the NBR had been forced away from the case, had taken on some material set, and remained open. No data are in hand at this time to determine whether or not the NBR relaxes back into place after a given time.

A later section details that Morton Thiokol has taken action items to evaluate methods of preventing unbonds in the future and to evaluate repair of existing unbonds.

7.3.3.6 Joint Assembly Enclosure. The joint assembly was accomplished in the enclosure which was designed to function as the clean room for joint assemblies. The enclosure consisted, in part, of reinforced plastic draped around the segment being installed and secured several feet above the joint with a strap running around the segment perimeter. This plastic was rolled up and secured to the segment during the lift operation. The remainder of the enclosure consisted of the assembly floor and a structure surrounding the floor which was also draped with reinforced plastic. The assembly floor was approximately 2 ft above the platform level. When the segment being assembled was lifted into place, approximately 1.5 to 2 ft above the previously assembled segment, the plastic was unrolled from the upper segment and pulled out and draped overlapping the enclosure structure of the assembly floor. Entry to the enclosure was made through an opening in the plastic which was essentially a slit fastened with velcro each ft or so. The enclosure, then, consists of plastic which is fastened to a segment with a strap and draped over the assembly floor enclosure. The assembly floor plastic hung below the assembly floor level. None of the enclosure joints was positively sealed but two ducts in the enclosure did direct air into the enclosure to create positive pressure. The enclosure worked partially but must have some improvements as listed below:

a. The platform floor must be cleaned during enclosure setup.

b. Install a floor mat outside the enclosure entrance to clean shoes on.

c. Use full hairnets inside the enclosure which will confine all hair.

d. Air vents in the enclosure should not be aimed directly at the segment. Exit duct filters should be installed and could be used to diffuse the air flow.

e. Modify the entry door to close and seal more easily or to close by itself after entry. The entry did not close and seal easily and was frequently left unfastened.

f. Use Velostat® to cover the forward end of the installed segment during lift operations and enclosure setup to prevent contamination from falling onto the inhibitor and into joint surfaces.

g. The entire inhibitor surface shall be cleaned to remove contaminants prior to final assembly. This is specifically requested if transfer medium was previously applied to joint surfaces.

h. All operators entering the enclosure should wear Tyvek suits to promote environment cleanliness, prevent fibers and lint from coveralls from entering the environment or being introduced to the joint surface by inadvertently getting a coverall sleeve in the joint grease.

i. Improve general house cleaning and remove unnecessary equipment from the floor level.

7.3.3.7 OMI. Specific work accomplished during the test support period included ATA test observation, crew training, and OMI review and comments to the following documents:

a. OMI B5145, ATA Procedures

b. OMI B5308, First Flight Receive and Inspect

c. OMI B5303, First Flight SRM Assembly

Specific attention was given to the ATA procedures, work methods, and inspection. Changes to the OMIs and procedures of ATA were changed, where possible, to follow the sequence and method of procedures defined in TWA-1177 and supported by STW7-2831 (SRM acceptance criteria). The changes in the OMIs were made to improve sequence flow and assembly. The sequences in TWA-1177 were followed for ATA and then additional descriptions, sequence order changes, and comments were added to OMI B5303, for first flight motor segment stacking, based on what was learned and noted during ATA assembly.

The ATA assembly OMI, B4145, had been reviewed prior to the wet fit assembly and a deviation to the OMI was written to arrange the OMI in the order of steps called out in TWR-1177. The order of steps shown in TWR-1177 are based on experience gained assembling test joints and testing joint assemblies at the Space Operations. The resultant chronology of the steps requested by insulation design for flight motor joint assembly is detailed as follows:

--All joint profile measurements, for the joint being assembled, are to be completed with the segment to be stacked still in the transfer aisle.

--Solvent clean all bare metal surfaces.

--Inspect the inhibitors.

--Forward inhibitor shall be cleaned of all residue contamination.

--Solvent clean J-seal contact surfaces.

--Abrade J-seal bonding surfaces with 180- to 220-grit. Include asbestos safety requirements.

--Solvent clean bonding surfaces. Inspect for abrasion residue and remove any contamination found.

--Visually inspect bonding surfaces for cuts, gouges, and protuberances.

--Mask tang and clevis bonding surfaces with aluminum conductive tape and Velostat® per Change TWA-1177. Change the related abrasion figure to show masking closer to the capture feature. Mask as close to capture feature as possible without causing undo possibility of contaminating the metal grease application.

--Regrease if joint assembly will be delayed.

--Place Velostat® over clevis end of lower segment of the assembly and secure.

--Move segment from transfer aisle to position over lower segment of the assembly.

--Remove Velostat® cover.

--Clean all tang and clevis base metal surfaces and pinholes.

--Apply flight coat of grease.

--Inspect and install V-2 fillers.

--Inspect and install all O-rings.

--Place Velostat® over forward joint surfaces of lower segment.

--Remove masking from tang J-seal surfaces.

--Solvent clean tang J-seal surfaces. Air dry 30 min

Note: Refold cleaning cloths regularly to expose clean surfaces each 2 to 4 ft of cleaning.

--Visually inspect tang J-seal surface.

--Ultraviolet light (blacklight) inspect tang J-seal surfaces for grease.

--Apply adhesive to tang joint. (Remove reference to mechanically fastened from the foam brush description.)

--Inspect adhesive application. (Remove reference to bubbles from inspection criteria.)

--Remove Velostat® cover from lower segment.

--Remove masking from clevis J-joint seal surface.

--Solvent clean clevis bonding surface. Air dry 30 minutes.

Note: Refold cleaning cloths regularly to expose clean surfaces each 2 to 4 ft.

--Visually inspect clevis joint.

--Ultraviolet light (blacklight) inspect clevis joint for grease.

--Apply adhesive to clevis J-seal. (Remove reference to mechanically fastened from foam brush description.)

--Inspect clevis J-seal adhesive application. (Remove reference to bubbles from inspection criteria.)

--Perform final inspection of tang and clevis J-seal surfaces for bugs and contamination just prior to mate.

7.3.3.8 Problem Reports (PR) and Action Items. PRs against ATA insulation components have been reviewed and Action Items taken to prevent the same problems in the future. These are documented in memo 1361:FY88:M352.

Additional PR were written and dispositioned which documented defective conditions of the insulation assembly and are noted below.

PR PV6-087668 documents nicks, gouges, and scratches in the tang joint NBR. One of the gouges appeared to have been formed by a piece of tape left on the joint mold tool during vulcanization of the insulation assembly. A slight trapezoidal depression, approximately 0.2 by 0.25 in., was located outboard in the radius area. A couple of smaller depressions were also noted in the tang joint surface. Some small scratches and gouges were noted which could be seen but not felt by touch. The tang molded surface had a few areas which were speckled dark brown. They appeared to be a discoloration in the insulation but did not cause surface discontinuities. A spotty reddish contamination was also noted in several locations which appeared to be in the insulation and did not affect the contour of the joint surface. No repairs were specified for these conditions.

PR PV6-087612 was requested by Insulation Design Engineering to document high spots in the clevis joint insulation surfaces caused by repairing the areas where instrumentation was intended to be placed and later discarded. The adhesive used to repair the instrumentation cutout area had not been finished to match the surrounding contour and was requested to be abraded to meet this condition. The repair was made quickly and with excellent results. The repair at the 0-deg location had a slight low spot along the edge caused by a lack of adhesive during the original adhesive application. However, the repair was at least as good as any accomplished for JES and TPTA test joint repairs. Even so, this was the location noted during the dry fit inspection of the burp track. The burp track was noted only in the radius and did not affect the ID tip contact. Nothing anomalous was noted in this area during the wet mate inspection.

PR PV6-087769 documented grease on the tang joint insulation surface following installation of the capture feature O-ring just before proceeding with the dry mate. The grease was removed by solvent cleaning and the uMI was changed to clean the NBR joint surfaces and mask them off for all future grease application and O-ring installation procedures to preclude contamination.

The ATA wet mate proceeded with the joint surfaces masked as described in a previous section and worked very satisfactorily. There were those persons, and still are, that opposed masking of the joint surfaces for O-ring installation and then working over the joint to apply the joint adhesive. Insulation Design recommends that flight segment joints be prepared following the same sequence of procedures as was accomplished for ATA. If the joint adhesive is applied before O-ring installation, a great risk is taken that the joint and adhesive will become contaminated with grease. This is especially true for the tang joint surfaces.

PR PV6-087593 documents gouges (depressions), foreign materials, and contamination on the aft segment forward inhibitor. The action items for this PR are in the attached memo. It is further recommended that criteria be added to STW7-2831 to establish acceptance criteria for these type of conditions. The black ozone protective coating (Hypalon® paint) was also noted intermittently on the clevis joint sealing surface and was removed. This condition should also be addressed in STW7-2813.

7.3.4 Conclusions

Conclusions made following the ATA test and data evaluation are presented below and are listed by paragraph number referencing the qualification and development objectives of Section 7.3.2 as they are applicable to the insulation components.

a. Conclusions to qualification objectives:

   1. The objective was met. Vertical assembly and disassembly of RSRM segments is possible and incorporate provisions for refurbishment and reuse.

   2. The objective was met in that the design considered tasks to be accomplished by personnel within the objective parameters, however, additional training may be warranted for crew training on transfer medium and adhesive application. This is particularly true of operators not on shift during the demonstrations on the ATA joints.

3. The objective was met. System performance and structural integrity was maintained during the assembly process as verified by post-test visual inspection of the dry fit and the wet fit.

4. The objective was met. The field joint insulation did not shed fibrous or particulate matter.

5. The objective was met. The field joint insulation did permit preflight demate and caused no insulation damage.

b. Conclusions to development objectives:

1. Mate/demate loads were not determined for the insulation components for joint adhesive separation loads, joint bondline stress, insulation to liner/propellant stress or casewall bondline stress because the instrumentation required for this data was deleted from the ATA test by schedule constraints. Laboratory test data for the joint adhesive typically shows 10 pli maximum bond strength which converts to roughly 3,750 lb separation force for the entire joint. Data accumulated for the referee test series shows approximately 7,000 lb separation force for the joint due to the adhesive. The actual separation force is highly dependent on the separation rate and the adhesive temperature, increasing as the temperature drops or the separation rate increases.

2. The objective was met. Inspection of the joint following the dry fit and the wet fit showed contact of the joint surface at the ID contact area to approximate engineering analysis. Contact was also achieved at the joint radius but did not appear to influence the ID tip contact. Profile measurements of the joint prior to assembly tests showed more contact than did the assembly inspections and post-test profile data was not available at this writing.

3. The objective to provide crew training was partially met. One crew watched the transfer spray application but none of them participated in the application. Only one crew was present and assisted with the adhesive application as well. The remaining crews on other shifts

have received no training and have not even seen the operation accomplished. Additional training would probably be warranted in these areas.

4. The objective was met in that the procedures used, including those added to ATA test processing by deviation, were validated by accomplishing them acceptably during the assembly operations, however, there is some rebuttal continuing regarding the sequence of operations involving installation of the O-rings and the adhesive application.

7.3.5 Recommendations

Recommendations are made following ATA test OMI review, assembly and disassembly operations evaluation, and post test inspection evaluation. The recommendations are based on what was learned from ATA and from assembly procedures on test motors at Morton Thiokol which are documented in TWA-1177. Recommendations are as follows:

a. Prior to installing FJAF tooling, perform an inspection for contamination and remove any found.

b. Do not allow tape to be applied to the J-joint critical bonding surfaces. Recommend joint surfaces be masked as defined in TWA-1177.

c. Inspect J-joint surfaces for tape residues and other contaminants and remove them prior to performing the joint abrasion operation.

d. Inspect the J-joint surfaces for protuberances, especially the tang ID tip where the mold tool sprue holes were located, prior to performing the abrasion process. Note the areas where the protuberances were observed and inspect them again after the abrasion process to assure they have been removed.

e. Change the STW7-2831 acceptance criteria for protuberance height from 0.010 in. height maximum to "cannot be felt by touch" and provide an acceptance standard if necessary.

f. Add a caution to the OMI abrasion figure and instructions to use caution not to round the ID corners of the J-joint during the joint abrasion process.

g. Change the figure in TWA-1177 to show masking materials as aluminum conductive tape and Velostat® and not yellow vinyl tape and Kraft paper.

h. Clean all transfer powder off the segment joint and inhibitor surfaces following the dry fit inspection.

i. Following the J-joint abrasion and cleaning processes, carefully inspect the surfaces for minute abrasion products which could contaminate the adhesive and the bondline.

j. Document the STW5-3479 joint adhesive removal process and acceptance criteria should a joint have to be demated and refurbished prior to motor operation.

k. Establish a uniform and accurate case insulation unbond inspection and documentation method.

l. Remove all grease from the clevis leg ID surface prior to performing the unbond inspection using the air load tool to prevent grease deluge of unbond surfaces.

m. Assemble the flight motor joints using the same process sequencing as was accomplished for ATA and included in the OMI by deviations.

n. Add acceptance criteria to STW7-2831 for ozone inhibitor paint (Hypalon® paint) in regard to contamination, gouges, depressions, etc.

o. Make improvements to the joint assembly enclosure as listed in Section 7.3.3.6.

p. Change the note in the OMI instructions and the figure used for joint masking, from "... secure Velostat® with aluminum conductive tape overlapping on each end up to Points A and D" to "... secure Velostat® with aluminum conductive tape overlapping on each end extending to Points A and D." During ATA activities the note was misunderstood to mask anywhere up to Points A and D but it was intended to require masking all the way to Point A and D.

q. The acceptance criteria in STW7-2831 should be expanded to allow no ozone protective paint from the inhibitor application on the J-joint bonding surfaces.

r. Inspect J-joint surfaces with ultraviolet light (blacklight) prior to joint adhesive application and remove all indications of grease.

7.4 PROPELLANT AND ADHESIVE STRUCTURES

7.4.1 Introduction

The principle area of investigation for propellant and adhesive structures during the ATA test was the propellant/insulation dimensions, and the J-seal insulation engagement when the segments were vertically assembled. Dimensional changes induced by vertical slump indicate the propellant modulus. Propellant safety factors are modulus dependent.

7.4.2 Objectives

Development objectives applicable to propellant and adhesive structures were:

a. Determined mate/demate loads on the field joint insulation.

b. Gather data on propellant/insulation dimensions for analytical comparison.

7.4.3 Results and Discussion

Propellant slump measurements were taken before and after segment mating operations. (Due to schedule impact, postmate measurements were not taken on the center segment clevis end.) The dimensional data was converted to axial deflections from the as-cast configuration. Tables 7-19, 7-20 and 7-21 show these deflections. The tables report deflections at every 30 deg and at four radial locations.

Based on VAB hygro-thermograph records the premate PMBT was assumed to be 71°F. The segments had remained motionless long enough for the propellant configurations to be stable when the premate slump measurements were taken. The center segment was under a 4-point lift during tang end slump measurements.

Basically two propellant properties determine the propellant grain deflections: the coefficient of thermal expansion (CTE) and modulus. Finite element analysis was used to determine the linear relationships between these parameters and the axial deflections. Thiokol Automated Stress System (TASS) was the finite element program used. By considering the premate deflections at both center segment ends, the CTE and modulus were determined.

The calculated CTE for the ATA segments was 5.9E-5 in./in./°F, which is in the range of previous lab testing (which is 4.7E-5 to 6.5E-5 in./in./°F). For modulus calculations the CTE was assumed to be constant. However, the modulus is known to be time and temperature dependent. The calculated ATA moduli are shown below.

Segment	Pre or Postmate	Modulus (psi)
Center	Pre	310
Center	Post	340
Aft	Pre	270
Aft	Post	210

The average of the four moduli is 280 psi. It is not fully understood why the aft center segment modulus increased with time, while the aft segment modulus decreased. The deflections, however, indicate this is what occurred.

All propellant modulus estimates are based on a 71°F PMBT. If this assumption is incorrect it would cause errors and could explain the above inconsistency in the modulus predictions. Although the analysis assumes equilibrium conditions, time-dependent behavior such as creep (deformation during a constant load) or modulus relaxation, could be more significant than expected. Propellant modulus is also believed to vary within each segment, due to mix-to-mix variation. This is another complication factor in modulus predictions.

Comparable CDR analyses used a 130 psi propellant modulus, which is based on uniaxial lab data. This modulus is about half what the ATA test data indicates. It is not surprising that this uniaxial modulus is too low to simulate loaded segment behavior, as past experience has also indicated this. For example, previous analysis has used 265 psi to characterize forward segment fin slump (Reference TWR-13040, page. 141).

The ATA center segment deflection analysis, which used the 130-psi modulus, predicted 0.26 in. down axial deflection near the bore on the tang end. The corresponding measured value on ATA, however, was 0.7 in. up. Clevis end predicted and actual values were closer, being 1.8 and 1.4 in. down, respectively. (Reference TWR-17052, Table III for analysis). The 130 psi modulus analysis also predicted that the center segment propellant stress relief flap gap would close, which also disagreed with actual measurements.

Clearly, the CDR analyses using the 130 psi modulus are not correctly predicting the propellant structural behavior. Using a higher propellant modulus, derived from ATA, will cause a reduction in stress-based safety factors. Some safety factors for worse-case storage conditions would be below the 2.0 requirement. For five year horizontal storage and at 32°F, the center segment stress relief flap bulb would have a 1.4 safety factor

Tables 7-19, 7-20 and 7-21 also show an asymmetric pattern with maximum deflection near 90 deg and minimum deflection near 270 deg. This pattern probably occurred due to a slight post-casting-pit propellant cure when the segments were stored horizontally with the 90-deg location up. The asymmetry did not noticeably affect insulation contact at the field joint.

The estimated disassembly load after wet mate was 20,000 lb. This matches experience from the Joint Assembly Demonstration (JAD-2) test. JAD-2 also showed that 7,000 lb is required to break the adhesive bond on

Table 7-19. ATA Aft Segment, Clevis End Downward Slump Deflections

Premate

	Radial Location			
Angle (deg)	68.3 (in.)	56.3 (in.)	44.3 (in.)	32.3 (in.)
2	0.236	0.718	1.072	1.304
32	0.246	0.783	1.142	1.360
62	0.266	0.841	1.194	1.406
92	0.256	0.827	1.176	1.385
122	0.253	0.790	1.117	1.329
152	0.266	0.757	1.067	1.277
182	0.200	0.723	1.059	1.234
212	0.211	0.691	1.019	1.205
242	0.209	0.665	0.980	1.166
272	0.211	0.682	0.983	1.166
302	0.209	0.697	1.029	1.209
332	0.216	0.687	1.039	1.230
Average	0.228	0.738	1.073	1,273

Postmate

	Radial Location			
Angle (deg)	68.3 (in.)	56.3 (in.)	44.3 (in.)	32.3 (in.)
2	0.228	0.791	1.183	1.399
32	0.233	0.854	1.249	1.473
62	0.256	0.914	1.300	1.513
92	0.245	0.897	1.280	1.493
122	0.245	0.864	1.221	1.436
152	0.230	0.840	1.180	1.388
182	0.221	0.807	1.186	1.391
212	0.233	0.780	1.147	1.365
242	0.235	0.755	1.110	1.325
272	0.243	0.780	1.121	1.335
302	0.239	0.796	1.172	1.384
332	0.243	0.778	1.174	1.400
Average	0.238	0.821	1.194	1.409

Table 7-20. ATA Center Segment, Tang End Upward Slump Deflections

Premate

	Radial Location			
Angle (deg)	68.3 (in.)	56.3 (in.)	44.3 (in.)	32.3 (in.)
2	0.096	0.399	0.557	0.679
32	0.052	0.408	0.624	0.774
62	0.099	0.482	0.685	0.870
92	0.064	0.396	0.644	0.941
122	0.103	0.484	0.703	0.942
152	0.069	0.313	0.534	0.684
182	0.050	0.222	0.397	0.578
212	0.083	0.219	0.343	0.499
242	0.085	0.299	0.467	0.635
272	0.035	0.251	0.432	0.638
302	0.015	0.191	0.335	0.512
332	0.052	0.220	0.360	0.518
Average	0.067	0.324	0.507	0.689

Postmate

	Radial Location			
Angle (deg)	68.3 (in.)	56.3 (in.)	44.3 (in.)	32.3 (in.)
2	0.053	0.389	0.597	0.786
32	0.021	0.372	0.639	0.850
62	0.095	0.457	0.676	0.858
92	0.008	0.367	0.627	0.886
122	0.139	0.442	0.691	0.910
152	0.037	0.319	0.595	0.839
182	0.045	0.237	0.462	0.581
212	0.085	0.253	0.434	0.598
242	0.087	0.296	0.518	0.598
272	0.041	0.257	0.475	0.562
302	0.012	0.201	0.411	0.579
332	0.032	0.251	0.456	0.597
Average	0.055	0.320	0.548	0.722

Table 7-21. ATA Center Segment, Clevis End Downward Slump Deflections

Premate

	Radial Location			
Angle (deg)	68.3 (in.)	56.3 (in.)	44.3 (in.)	32.3 (in.)
2	0.221	0.760	1.184	1.438
32	0.241	0.809	1.243	1.496
62	0.250	0.825	1.313	1.527
92	0.257	0.836	1.267	1.527
122	0.262	0.800	1.195	1.500
152	0.249	0.763	1.178	1.452
182	0.233	0.734	1.135	1.377
212	0.213	0.691	1.092	1.353
242	0.193	0.649	1.047	1.310
272	0.192	0.625	1.014	1.282
302	0.197	0.634	1.029	1.298
332	0.215	0.703	1.107	1.358
Average	0.227	0.736	1.150	1.420

the J-seal insulation. This 7,000 lb load is lower than the adhesive tensile strength and indicates peel as the dominant failure mode. A conservative analysis, assuming adhesive tensile failure, showed that demate induced insulation stresses were less than 36 psi. This is well within the 390 psi insulation tensile stress capability. Buried insulation stress transducers in JES-3A confirm that these induced stresses are very low.

7.4.4 Conclusions and Recommendations

The ATA test provided useful data for analysis verification. Propellant grain slump deflection predictions were unsatisfactory and indicated a problem with the lab-derived modulus. The ATA test showed that the propellant modulus is roughly 280 psi, which is more than double what has been assumed in CDR analyses. Redoing the analyses with the higher modulus would reduce the propellant grain structural safety factors.

Plans have been made to rectify the modulus discrepancy. A propellant long-term effective modulus is being determined which can be used in finite element analysis and then experimentally be verified with analogs. TWR-17720 proposes this required lab testing, including use of analogs called structural test vehicles (STVs).

Mate and demate operations were successfully completed without structural damage to the field joint insulation. Insulation structural analysis verifies that a 2 minimum safety factor will be maintained during segment assembly and disassembly operations.

In order to broaden the data base and further refine the analysis model, it is recommended that the slump measuring tool be used to collect more data from loaded segments.

8

APPLICABLE DOCUMENTS

The latest revision of the following list of documents are applicable to the extent specified herein.

Morton Thiokol

Drawings	Title
7U75781	Instrumentation Installation Kit
1U52636	Stiffener T-rings
1U75427	Segment, RSRM Loaded, Center
1U50502	Aft Dome, Insulated
7U52919	Field Joint Separation Tool
8U75676	Field Joint Separation Tool
8U75677	Hydraulic Control Console - Field Joint Separation Fixture
8U75686	Assembly Fixture, SRM Field Joint - Assembly and Details
7U75777	Assy, Aft Segment, ATA
7U75782	Joint Installation, Field and Skirt Kit
7U75869	Assy, Fixed Housing and Plate

Documents	Title
CPW1-3600A	Prime Equipment Contract End Item (CEI) Detail Specification - including Addendum H.
TWR-18140	ATA Insulation Design Final Report
TWR-17947	ATA Structural Application Final Report
TWR-17052	ATA Propellant Structural Analysis Final Report
TWR-17720	RSRM TP-H1178 Propellant Characterization
TWA-791	Receive, Stack, Destack and Ship Assembly Test Article (ATA) Operation and Maintenance Documentation
TWR-15723	Redesign D&V Plan, TGX-10.0

TWR-16010	RSRM NDE Plan
TWR-16802	Hazard Analysis for RSRM ATA Test Article
TWR-16081	Prototype Sine Bar Measuring Device, Operations and Maintenance
TWR-16503	Field Joint Separation Fixture, Assembly and Operating Procedure
TWR-16544	Operating Procedure, Field Joint Assembly Fixture
TWR-16927	Operating Procedure Vertical Field Joint Separation Fixture. Installation, Operation and Removal
TWR-17110	Vertical RSRM Operation Procedure For the 8U75686 Field Joint Assembly Fixture, Installation and Removal
OMRSD	Solid Rocket Booster, Operations and Maintenance Requirements Specification - File V, Vol. 1.

Other Documents

Documents	Title
MIL-STD-45562	Calibration Systems Requirements

DISTRIBUTION

Recipient	Mail Stop	No. of Copies
J. Elwell	E06	1
A. McDonald	L00	1
L. Bailey	L10	1
B. McBeth	L10	1
D. Roth	L10	1
P. Petty	L10	1
J. Keller	E12	1
B. Tydeck	E06	1
H. Reed	M33	1
J. Sutton	L10	1
B. McQuivey	L10	1
M. Allison	L10	1
G. LeBaron	L10	1
J. Kapp	L20	1
G. Anderson	L20	1
S. Stein	L22D	1
J. Furgeson	L22D	1
K. Parsons	L22D	1
K. Eckhardt	L21	1
F. Baugh	L21	1
A. R. Thompson	L22	1
B. Lowe	L22D	1
D. Ferney	L22D	1
T. R. Hoffman	L22	1
L. Abrahamson	L22	1
M. Cox	L30	1
C. Johnson	L31	1
D. Sauvageau	L36	1
M. Williams	L36	1
G. Ricks	L36	5
R. J. Bell	L36	1
H. Gittins	815	1
K. Sanofsky	815	1
F. Call	E05	80
G. Shick	L33	1
D. Stone	C10	1
Data Management	L23E	6
Print Crib	L23E	5